## *A study of mineralisation in the Jew limestone, Rookhope borehole.*

R. A. S. Cayzer

# A STUDY OF MINERALISATION IN THE JEW LIMESTONE, ROOKHOPE BOREHOLE.

R. A. S. Cayzer, B.Sc. (Sydney).

Thesis submitted for the degree of Master of Science,

University of Durham.

November, 1972.

CONTENTS

## TABLES

## ABSTRACT

The nature and distribution of sulphide and non-sulphide epigenetic mineralisation in a section of the Jew Limestone, Rookhope Borehole, are discussed. The pre-mineralisation textural nature and mineralogical and elemental composition of the host rock and the modification of such under the influence of the hydrothermal activity are considered as well as the trace element distribution pattern in the host rock, geothermometric aspects of the mineral assemblage, and the attitude of the mineralisation.

Certain aspects of the physical chemistry of the system are discussed and limits imposed on the composition of the depositing fluid at various stages during the mineralising process.

Unusual features of the sphalerite and the epigenetic carbonates as revealed by electron microprobe analysis are emphasised.

Several of the results of the study are not in agreement with previously-published data on the Jew Limestone in particular and the Northern Pennine mineralisation in general.

ACKNOWLEDGEMENTS

My thanks are due to many people, both staff (technical and academic) and research students alike, most of whom at some stage during the work, provided guidance or advice on various specialist aspects of the investigation. It is not possible to name all here, but I should like in particular to thank Ronald Hardy and Kevan Ashworth for the way in which they willingly gave of their time on all requests for assistance. Assistance of a different nature was provided by room-mates Les Knight, Bryan Leach, Andy Chambers, and during the early part of the year, Robin Gill.

I should also like to thank Professors M.H.P. Bott and G.M. Brown for providing the facilities for the study, and especially my supervisor Mr. R. Phillips for his guidance and helpful suggestions during the investigation and for his detailed constructive criticism of the final manuscript.

# INTRODUCTION

The following dissertation has resulted from an investigation into a section of mineralisation comprising a portion of the Rookhope Borehole (see later), in the Northern Pennine Orefield.

## 1. Aims

The primary aim of the study was to carry out an investigation into a small portion of mineralisation rather than a general study of a larger area, with a view to determining detailed small scale aspects of mineralisation in the Jew Limestone in particular and to determine how these could be related in a more general sense to mineralisation in the Northern Pennines.

## 2. Location and History of Borehole

The Rookhope Borehole is located in the Northern Pennine Orefield, Northern England (fig. 1), a field which at various times during its history has been a recognised producer of lead, zinc and fluorite. More specifically, the borehole was sited at Nat. Grid NY.938428 near the crossing of the Boltsburn vein (ENE-WSW) and the Red vein (ESE-WNW), both of which dip towards it (fig. 2), near the village of Rookhope, approximately 35 kms. west of Durham.

The Rookhope Borehole Project was initiated in 1960 under the auspices of the Department of Scientific and Industrial Research for the prime purpose of testing theories relating to the existence

of a granite body in depth formulated from the study of gravity anomalies which were plotted from the results of a geophysical survey over the area. The site selected was chosen as the lowest topographic elevation consistent with proximity to the minimum of the Bouguer anomaly. A more detailed account of the history of the borehole is provided by Dunham et al (1965). En route to the basement granite the borehole intersected mineralised sections of various limestones in the Yoredale sedimentary sequence. It is one of these sections, the Jew Limestone (678'10" - 703'8") that has been chosen for the present study. Unfortunately, the information provided by the borehole is all that is available concerning the particular mineralised sections, i.e. the relationship to the remainder of the orefield is not proven, nor even the relationship to nearest known mineralisation and the attitude of the vein cannot be determined. As a result of these unknown factors, severe limitations are placed on the amount of information which can be obtained. It is this same situation however, which is likely to be encountered in practice during exploration or development of properties, where a maximum amount of information is to be extracted from the minimum of available material.

## 3. Selection of Material

The actual section studied was the 24'10" from 678'10" to 703'8" of the Rookhope Borehole and consisted of a wedge of material split from the original core. The latter was approximately 8 inches in diameter at the depth considered, the triangular wedge having height and base of 2 inches and 1 inch respectively.

In this section the borehole intersects relatively fresh Jew limestone, replaced limestone wallrock and cavity filling mineralisation, enabling the maximum amount of information to be extracted

by a study of all three types of material. Of the total 24'10" from the top of the Jew limestone (which grades into a mudstone band) to the base (showing a relatively sharp contact with a highly baked pale grey calcareous sandstone), approximately 7'11" is unaltered wallrock, 7'9" replaced wallrock and cavity-filling mineralisation and a total of 9'2" cavities (Johnson, personal communication), no core being recovered in the latter case. The baking of the basal sandstone is caused by the intrusion of the Great Whin Sill prior to the hydrothermal activity.

The section selected for study was chosen for several reasons:

a). both the hypogene mineralisation and the host rock comprise minerals which are environmentally sensitive.

b). The results of a considerable amount of experimental work on many of the phases present are available.

c). The borehole provides a continuous cross section across a vein, a feature rarely available from mine cores.

d). The mineralisation is typical of that mined at various periods in the Northern Pennines and thus the deductions made are likely to have more far-reaching applications.

## 4. Previous Work

Although in the past a considerable amount of work has been carried out on most aspects of mineralisation in the Northern Pennines, work of a similar nature to that discussed herein has not been previously attempted. The most comprehensive literature on the Northern Pennines in general has been provided by Dunham (1948), in which most material published on the general area up to that date has been collated. Apart from this, since the completion of the Rookhope Borehole a considerable volume of literature has

been published on certain aspects of the borehole itself, mostly on features other than the mineralisation. The present investigation is, among other things, an attempt to fill that gap. The published material is mentioned where relevant and acknowledged in the text.

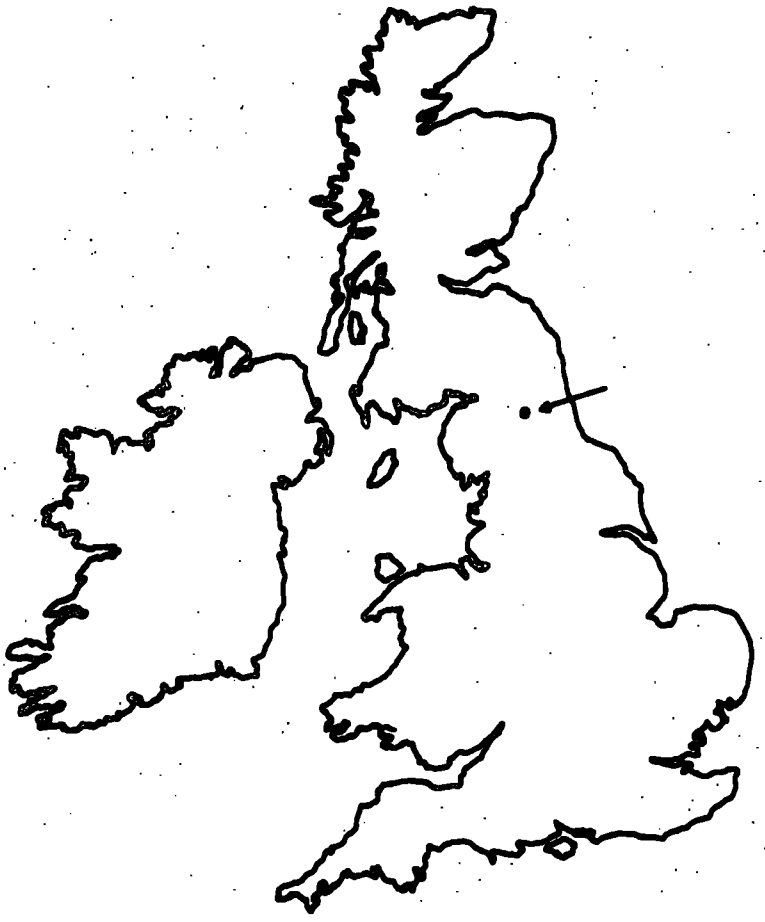

FIG. 1. Location of area detailed in fig. 2.

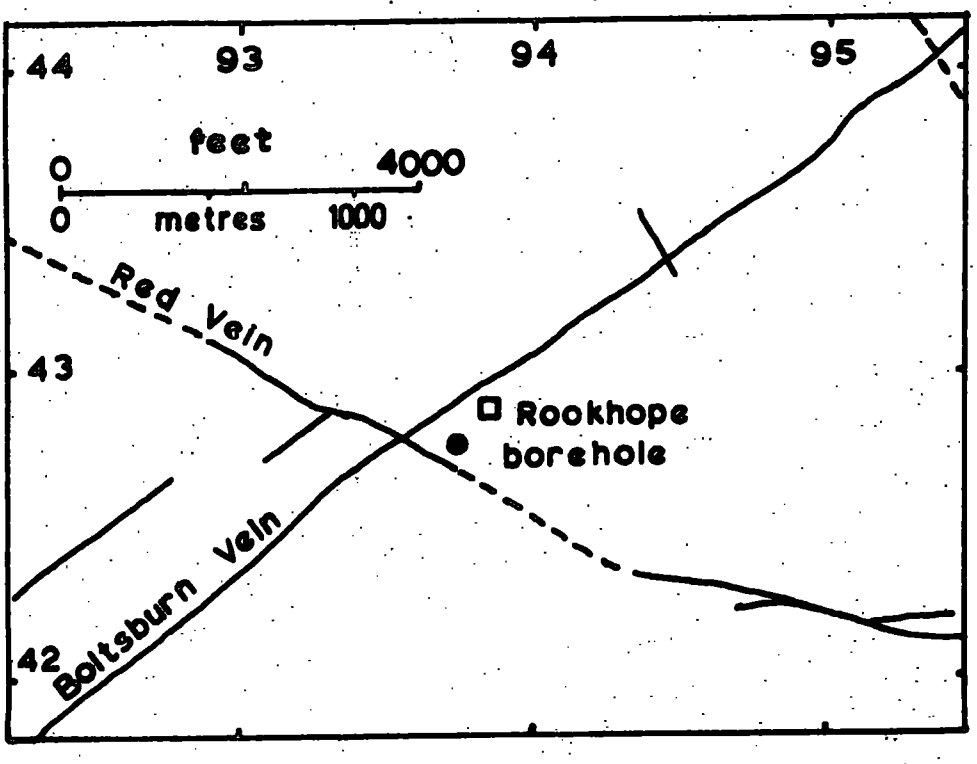


FIG. 2. Detailed location of Rookhope borehole.

# CHAPTER 1

## ANALYTICAL TECHNIQUES AND RESULTS

In the course of the following chapter, analytical techniques used in the present investigation are described. Where relevant, a summary of sample preparation procedures and manner of presentation to the instrument is given, together with comments on sources of interference and how these were minimised, sources of errors, the accuracy and precision to be expected from the method and the reasons why the particular method was chosen. The results of such analyses are then given at the end of each section.

In most cases physical methods of analysis were preferred to the classical chemical methods as greater speed and precision are normally obtainable with comparable accuracy.

## 1.1 MICROSCOPY

In the following section and in all subsequent discussions, the unaltered limestone is referred to as "host rock" and the replaced material as "wallrock".

### 1.1.1. Polished Sections

Polished specimens were used for preliminary identification of the opaque minerals present, and to examine textural relationships among the minerals with a view to determining the paragenesis and certain aspects of the geochemistry of the system. Before examination under the reflecting microscope, larger-scale textural relationships were studied by means of a binocular microscope. The procedure was also used as a prelude to electron microprobe analysis in order to select portions from which maximum information could be obtained.

A total of 8 polished sections were made from one-inch diameter cores taken from locations considered to represent a variety of significant features by means of a Meddings diamond drill. A Vickers ore microscope was then used for a study of these sections under reflected light.

A brief description of each specimen and an indication of the depths from which the specimens were taken, follows:

689' - PS2 Cavity-filling colloform sphalerite and disseminated sphalerite in replaced wallrock.

691'2" - PS3 " " " " "

691'6" - PS1 Chalcopyrite/pyrite crystal aggregate projecting into open space.

694'2" -- PS6 Galena/sphalerite contact plus replaced wallrock.

694'3½" - PS5 Galena/quartz/fluorite vein transecting boundary between barren replaced wallrock, and wallrock with disseminated sphalerite.

694'4" - PS4 Disseminated sphalerite and barren wallrock beyond limit of disseminations.

696'5" - PS7 Quartz and fluorite replacing colloform sphalerite with some wallrock.

700' - PS8 Colloform and disseminated sphalerite.

Detailed descriptions:

PS1

The section is cut from one of several similar predominantly chalcopyrite aggregates which project into open space from a quartz lining which supports the loosely-attached chalcopyrite, and associated minerals.

Pyrite is irregularly concentrated around the borders of, and is replaced along grain boundaries by chalcopyrite (fig. 3) which also surrounds and replaces the few large crystals of marcasite. The marcasite grades imperceptibly through narrow necks into pyrite. Multiply-twinned and untwinned crystals are found in the same crystal aggregate.

Sphalerite/chalcopyrite boundaries were not intersected in the section examined, but under the binocular microscope euhedral sphalerite crystals can be seen protruding from the chalcopyrite. Crystal forms and twin-plane intersections are well developed on the free sides of the chalcopyrite. Under slightly uncrossed nicols and after etching growth twin lamellae are clearly visible.

Small amounts of unidentified gangue (quartz?) concentrate at pyrite/chalcopyrite interfaces and within the body of the chalcopyrite.

The several broad areas into which pyrite is concentrated extinguish as a whole at different angular positions on rotating the stage under slightly uncrossed nicols. This suggests that the aggregate consisted originally of an aggregate of large crystals of pyrite, each of which has been replaced along grain boundaries and cleavages by the later chalcopyrite. Anisotropy in pyrite has been explained as being produced during polishing of the specimen (Gibbons, 1967), the extinction position depending on the orientation of a particular crystal.

Evidence of a later generation of sphalerite and quartz replacing the chalcopyrite and pyrite was noted.

PS2

Minerals present in order of abundance: Quartz, sphalerite, fluorite, carbonate, orthoclase feldspar, pyrite, chalcopyrite, graphite.

The specimen was selected so as to include portions of both the colloform and disseminated sphalerite. On detailed examination, it can be divided into distinct areas. On a traverse at right-angles to the wallrock - an area containing disseminated sphalerite, a strip of barren wallrock (replaced by silica but still containing carbon), a strip of pure quartz, and an area of colloform sphalerite.

The colloform sphalerite contains inclusions of both quartz and fluorite but these were proven to be the two-dimensional expression of extensions from veinlets of these minerals.

Fluorite is disseminated in irregular masses in the wallrock.

Galena occurs as euhedral but normally anhedral, crystals in the silicified wallrock. One euhedral, doubly-terminated rod of galena is embedded in sphalerite but quartz and fluorite are normally the surrounding and replacing minerals.

One small chalcopyrite grain borders sphalerite.

Small amounts of carbonate are present with obscure paragenetic relationships to other minerals. The carbonate could be distinguished by its reflectivity, bireflectance and anisotropy from quartz and fluorite, but the electron microprobe was resorted to for actual composition determinations.

Minute fluid inclusions are present in all transparent minerals except vein quartz.

Feldspar and graphite remain apparently unaffected by the mineralising processes, as they occur in the proportions and form noted in the unaltered host rock.

Carbon rims individual grains of wallrock - replacing cryptocrystalline quartz.

PS3

Minerals present in order of abundance: Quartz, sphalerite, fluorite, carbonate, galena, orthoclase,feldspar, pyrite, graphite.

The specimen includes both colloform and disseminated sphalerite.

Fluorite fills fractures in sphalerite and quartz without replacement. Irregular patches of carbonate appear to be partially replaced by fluorite but relationships between these two minerals are generally uncertain. Carbonate residuals are enclosed within quartz which also replaces sphalerite. Generally sphalerite surrounds scattered grains of galena.

Chalcopyrite is irregularly scattered in small ovoid grains through sphalerite but also occurs surrounded by quartz.

Carbon, graphite and feldspar occur as noted in specimen PS2.

PS4

Minerals present in order of abundance: Quartz, sphalerite, fluorite, pyrite, orthoclase feldspar.

The section comprises sulphide-free silicified limestone abutting a portion of identical material containing disseminated sphalerite.

Wallrock quartz replaces the sphalerite.

Carbon rims the cryptocrystalline wallrock quartz and fluorite and is particularly concentrated near the borders of the sphalerite disseminations.

Fluorite is disseminated in the barren wallrock and is equigranular with the cryptocrystalline quartz.

Rare crystals of euhedral pyrite are present, sometimes enclosing carbon and usually surrounded by sphalerite.

Fine-grained potassium feldspar is distributed throughout the specimen.

PS5

Minerals present in order of abundance: Quartz, sphalerite, fluorite, galena, feldspar, pyrite, graphite, chalcopyrite.

The specimen of silicified wallrock is bisected by a vein containing quartz, fluorite, and galena.

Sphalerite is disseminated through one half of the specimen while the remainder is sulphide-free apart from an area (approx. 2 mms. X 4 mms.) consisting of quartz, fluorite and sphalerite.

Textural indications are that quartz replaces sphalerite and galena.

Several crystals of euhedral pyrite are surrounded by sphalerite and quartz. Grains of galena and quartz are seen in one case to be enclosed within a pyrite crystal.

Galena shows a strong affinity for sphalerite, many of the anhedral grains abutting the latter mineral and sometimes being enclosed by it.

Chalcopyrite grains are rare and are present mainly within the sphalerite.

Carbon is irregularly distributed throughout the specimen. Several graphite flakes are also present.

Large crystals of othoclase feldspar occur, but small grains are distributed throughout the specimen.

PS6

Minerals present in order of abundance: Galena, sphalerite, quartz, fluorite, carbonate, orthoclase feldspar, chalcopyrite.

The specimen comprises a group of sphalerite and galena crystals and includes a small portion of replaced wallrock abutting the sphalerite.

Textural criteria suggest that the sphalerite replaces galena and is replaced by quartz. The sphalerite/galena contact is in some sections serrated under high magnification. In one case a portion of a galena crystal is pseudomorphed by sphalerite.

A stringer of exsolved chalcopyrite was noted in the sphalerite close to the galena contact. Chalcopyrite also occurs as small spheroids in other portions of the sphalerite and surrounded by other gangue minerals.

The carbonate shows complex inter-relationships with quartz, galena and sphalerite with conflicting evidence concerning replacement relationships. Euhedral rhombs of carbonate are scattered

through most other associated minerals.

Fine grained feldspar is distributed throughout.

PS7

Minerals present in order of abundance: Sphalerite, quartz, fluorite, galena, carbonate, pyrite, feldspar.

The specimen comprises colloform sphalerite, partly replaced by quartz and fluorite, and a portion of replaced wallrock with disseminated sphalerite.

Small portions of sphalerite are surrounded by a large galena crystal suggesting replacement by the latter. Quartz embays galena, also suggestive of replacement of the latter mineral by quartz.

Euhedral pyrite crystals cut across grain boundaries of most other minerals.

The quartz contains fluid inclusions of varying sizes.

Fine-grained feldspar is evenly distributed throughout the replaced wallrock.

Fluorite replaces sphalerite and galena and is replaced by quartz.

Patches of residual carbonate are distributed through the quartz.

PS8

Minerals present in order of abundance: Sphalerite, quartz, fluorite, carbonate, galena, feldspar, pyrite, chalcopyrite, graphite.

Colloform, open-cavity filling sphalerite abuts replaced wallrock with disseminated sphalerite.

Sphalerite is replaced by quartz, as is evidenced by the cross-cutting of composition zones by the quartz, and is relatively strongly fractured. Under crossed nicols the sphalerite shows a variety of colours from yellow to dark brown but these are irregular and difficult to trace.

Galena is surrounded by sphalerite and is replaced by quartz.

Segmented veinlets as described by Kutina and Sedlackova (1961) are filled with fluorite and quartz. As concluded by these authors the components of the veinlets appear to be of different ages. Some textures indicate that quartz replaces fluorite but the quartz/carbonate relationship is uncertain. Carbonates are usually surrounded by quartz.

Fluorite partly replaces carbonate in one case.

Spots of chalcopyrite occur at the border of some sphalerite grains, but are otherwise surrounded by fluorite.

Fluorite is practically free of fluid inclusions but in quartz these are abundant.

Several rod-shaped forms replaced by quartz and lined with carbon are probably fossil relics.

Fine-grained feldspar is distributed throughout the replaced wallrock. Graphite flakes are also present.

X4

Polished section of host rock, from a depth of 679'6".

The section contains several large recrystallised fossil shell fragments set in a fine-grained groundmass of carbonate, clays and

carbon. Pyrite is finely disseminated throughout the specimen and is especially abundant, and disseminated through, the fossil remains.

Orthoclase feldspar is also abundant and is disseminated in uneven-sized grains throughout the slide.

Several large flakes of graphite are present.

Etching

Sphalerite was etched with chlorine fumes as other techniques suggested by Ramdhor (1969) were found to be ineffective. These included the use of concentrated and dilute $HNO_3$, $KMnO_4 + H_2SO_4$, and concentrated and dilute HCl. After etching, grain boundaries, twin lamellae and composition zones are clearly defined thus providing a large amount of information with regard to the pattern of growth of the sphalerite and its paragenetic relationship to associated minerals.

Techniques suggested by the above author for the etching of galena and pyrite were also attempted, but no etch could be produced..

Chalcopyrite was etched with $KMnO_4$ + KOH to outline twin and grain boundaries.

In summary, the results suggest the following paragenetic sequence for the assemblage: pyrite/sphalerite, galena, fluorite/carbonate, quartz, fluorite, quartz, galena/pyrite/marcasite, chalcopyrite, sphalerite/quartz, carbonate.

1.1.2. Thin Sections

Thin sections were cut of portions of the reject material from which polished sections were taken, in order that features which are not visible under reflected light but which are clearly discernable

in transmitted light might be studied. These included (a) the distribution and relationship of the organic carbon to other minerals (b) the composition zoning in the sphalerite (c) the qualitative nature of the silicates (d) the distribution and form of individual quartz crystals (e) the cause of cloudiness in the quartz.

In some sections organic carbon showed regular patterns of distribution, always rimming cryptocrystalline quartz grains (fig. 10) having been forced to the borders during replacement of the remainder of the rock. The relationship of the carbon to other minerals is difficult to establish. In general there appears to be a distinct paucity of C in the immediate vicinity of the sphalerite but in several cases it was seen to be included in the outer rims of the sphalerite grains. The carbon also rims replaced fossil relics.

The composition zoning in the sphalerite and arrangement of the zones was clearly brought out in the thin sections. These were seen to consist of light and dark zones arranged concentrically in the disseminated sphalerite in the wallrock. Normally only one dark zone was noted, but in several grains a dark core was also present. This may indicate that all grains possess a dark core, but depending on the level of intersection of the section with the grain, this core might not be shown. Quartz was seen to penetrate the zones (fig. 11) in many cases.

The silicate noted in the polished sections was identified as a feldspar.

Under crossed nicols, the detailed arrangement of individual quartz crystals in the wallrock, and particularly in the small veins

was clearly discernable. An arrangement of well-formed interlocking quartz crystals projects from each wall of the veins to fill the existing open space. Ingress of later solutions was still possible, as is evidenced by the stringers of galena deposited between the apices of the projecting crystals.

Under high magnification, the cloudiness of the wallrock quartz is seen to be due to minute fluid inclusions. The vein quartz in the sections is free of these, except in a zone close to the walls of the veins.

X3 Host Rock Sections

Consists predominantly of a mass of cemented calcareous fossils of various sizes and shapes, the larger grains being recrystallised to a certain extent. Large euhedral pyrite crystals are present with no apparent relationship to other constituents. Pyrite also outlines the form of many of the fossils below an outer layer of carbonate. The specimen is taken from a depth of 679'3".

The cloudiness of the specimen is probably due to contaminating clays and to organic carbon.

X19

This specimen is taken from material indicated by XRF and XRD analyses to be so rich in clays as to warrant classification as a calcareous shale, at a depth of 683'3".

Several relatively large fossil fragments are present together with sparsely distributed smaller sized fragments.

Large grains of anhedral, elipsoid-shaped grains of pyrite parallel the bedding. The borders of these bodies are serrated.

The clay minerals are cemented by fine-grained calcite. Carbon which is finely distributed throughout the section, is occasionally concentrated into bands.

Several narrow calcite veins transect the specimen.

X26

Similar to specimen X3 but with small, irregularly-distributed euhedral crystals of pyrite.

The observed composition supports the results determined from XRF and XRD analyses.

Location of specimen - 684'9".

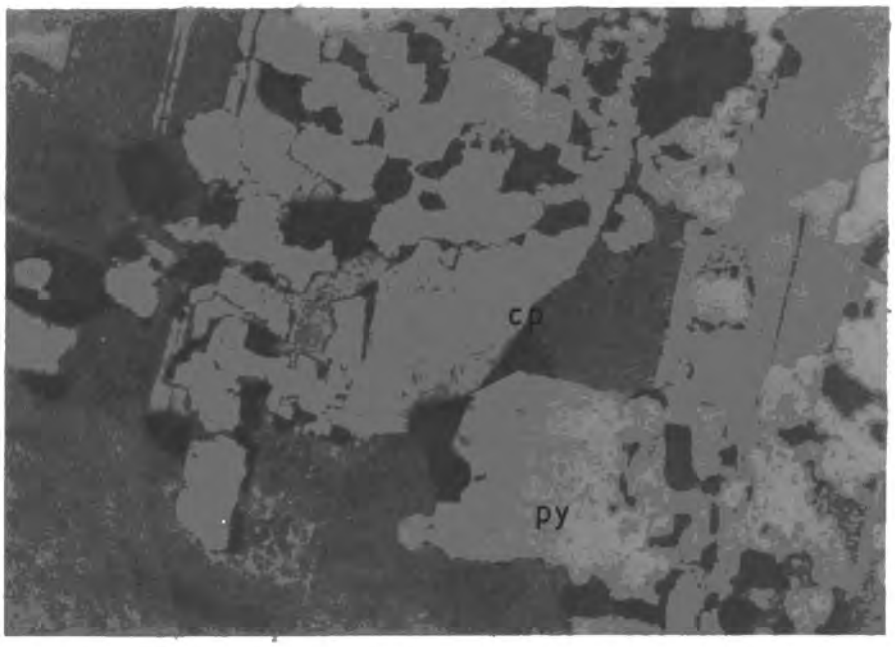


Fig. 3. Chalcopyrite (cp) replacing pyrite (py) along grain boundaries and cleavage planes. Chalcopyrite etched with $KMnO_4$ + Kl to bring out twin boundaries. Not all the chalcopyrite has been affected by the etching solution.

Reflected light. X 100. Specimen PS1.

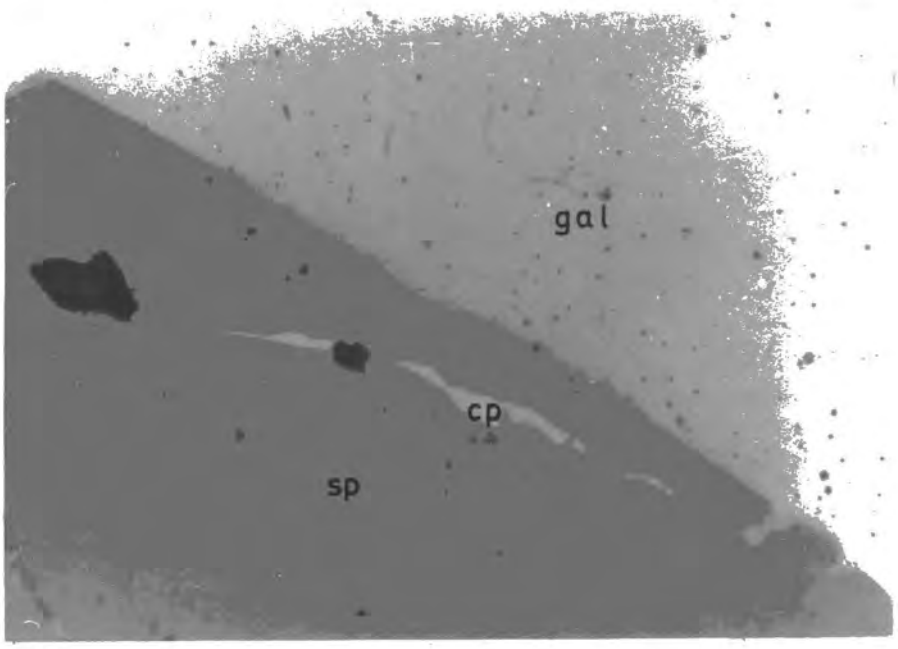


Fig. 4. Stringer of exsolved chalcopyrite (cp) in sphalerite (sp) abutted by galena (gal).

Reflected light. X 600. Specimen PS6.

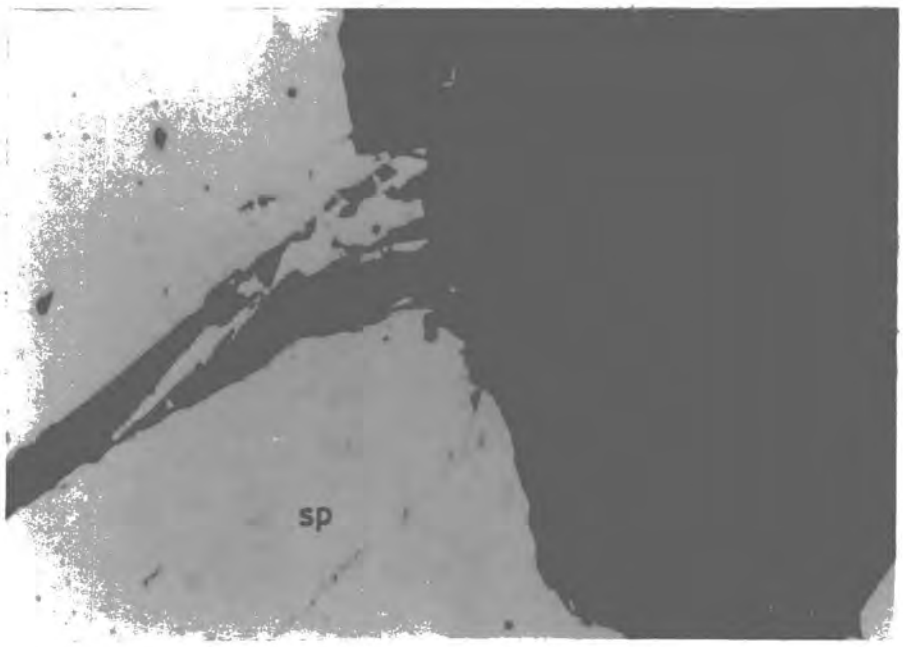


Fig. 5. Fluorite II (flt) filling fractures in sphalerite (sp) and quartz (q). Reflected light. X 500. Specimen PS3.


Fig. 6. Sphalerite (sp) etched with $Cl_2$ fumes to bring out composition zoning and twinning. Wallrock quartz (q) clearly cuts across zones and twin planes.
Reflected light. X 400. Specimen PS5.

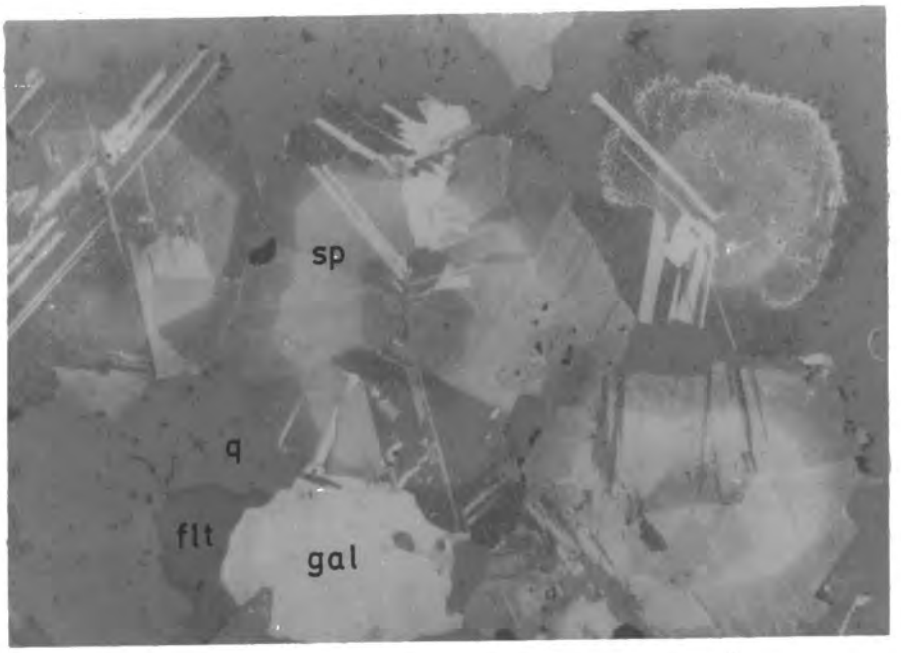


Fig. 7. Sphalerite (sp) "pisolites" in the wall rock, etched with $Cl_2$ fumes to show twin patterns and composition zones. Quartz (q), the latest mineral in the paragenetic sequence is seen to replace the sphalerite, galena (gal) and fluorite (flt). Reflected light. X 400. Specimen PS5.

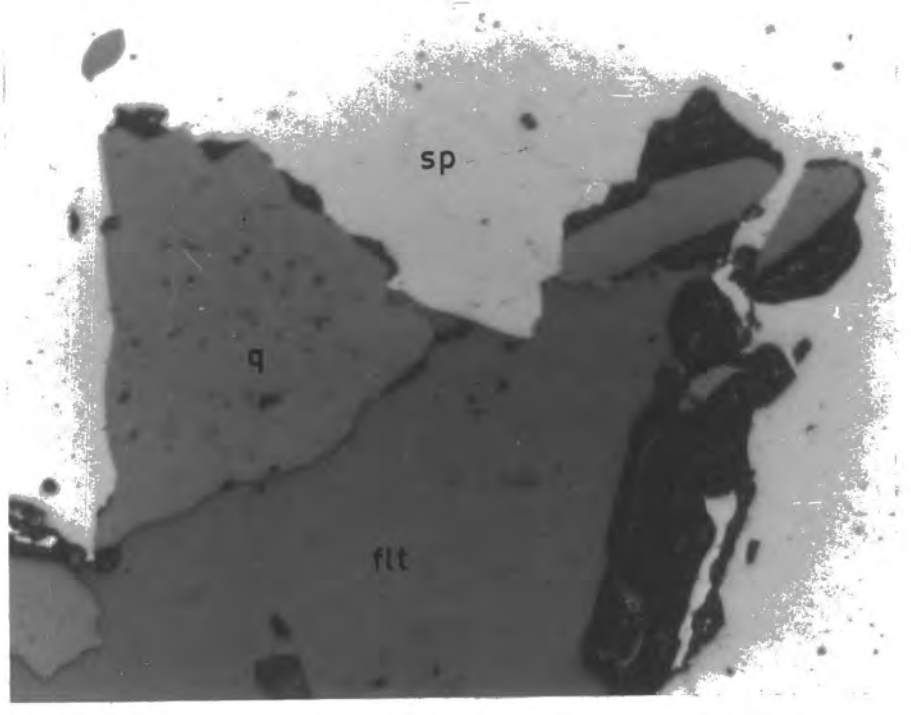


Fig. 8. Conflicting evidence of replacement relationships among sphalerite (sp), quartz (q), and fluorite (flt.). Reflected light. X 200. Specimen PS2.

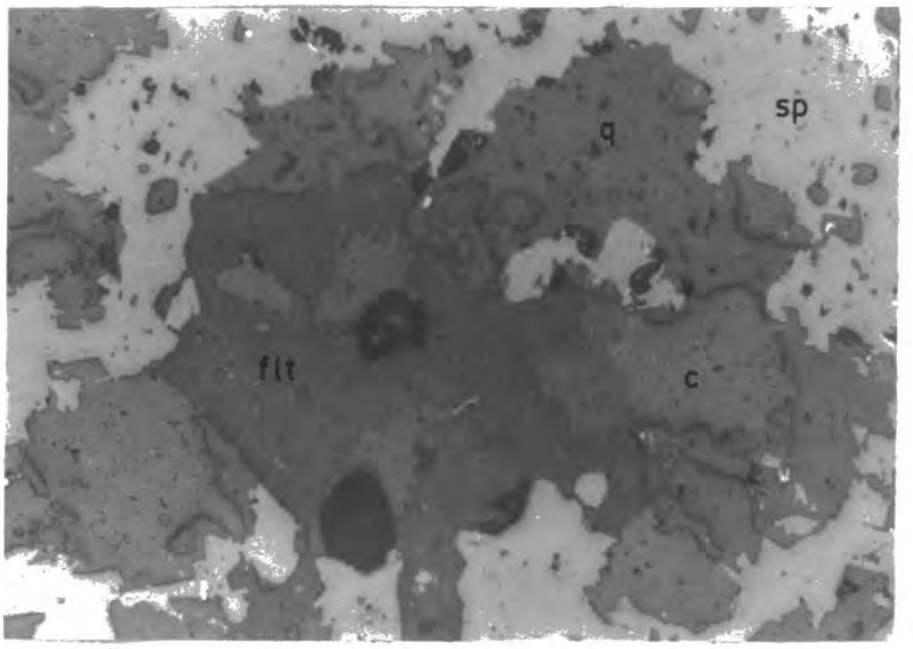


Fig. 9. Showing complex textural relationships among sphalerite (sp), quartz (q), fluorite (flt) and carbonates (c).
Reflected light. X 300. Specimen PS6.

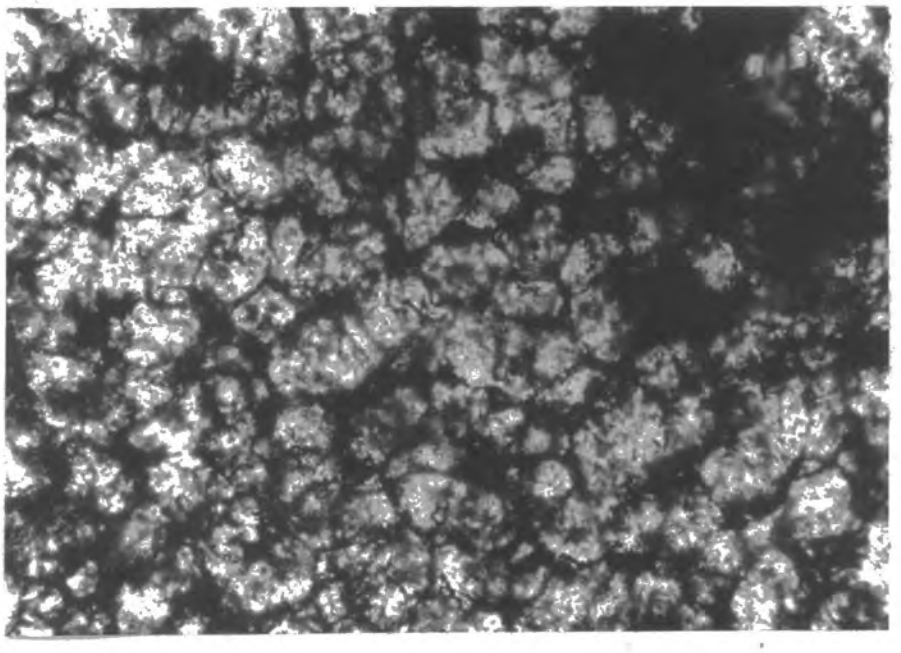

Fig. 10. Showing localisation of carbon (black) around quartz grain boundaries in replaced wallrock.
Transmitted light. X 400. Specimen PS5.

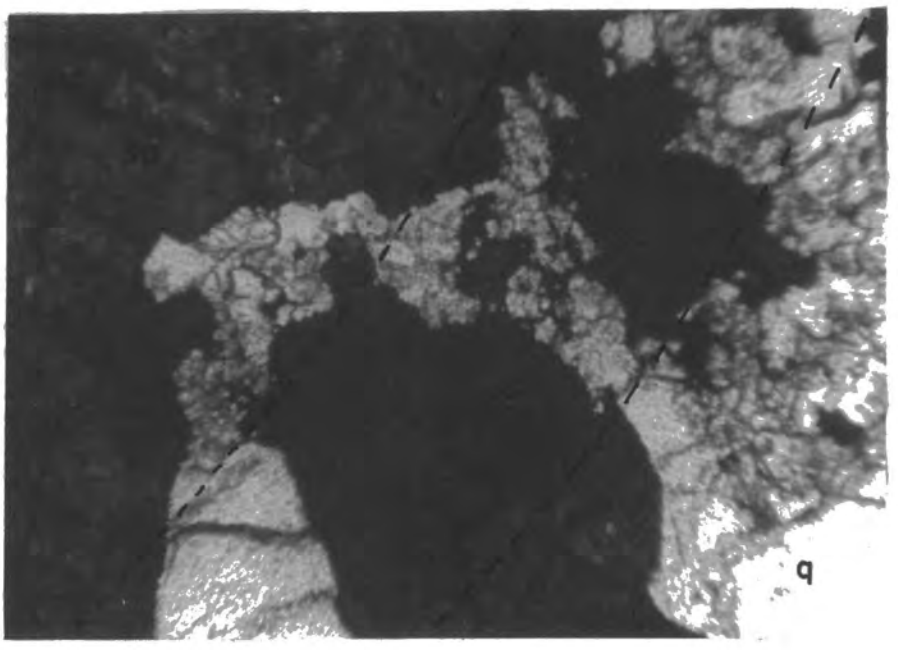


Fig. 11. Quartz (q) clearly replaces a sphalerite (sp) "pisolite" cutting across composition zones. The zone boundaries are outlined as they are not immediately apparent.

Transmitted light. X 200. Specimen TS5 (thin section of PS5),

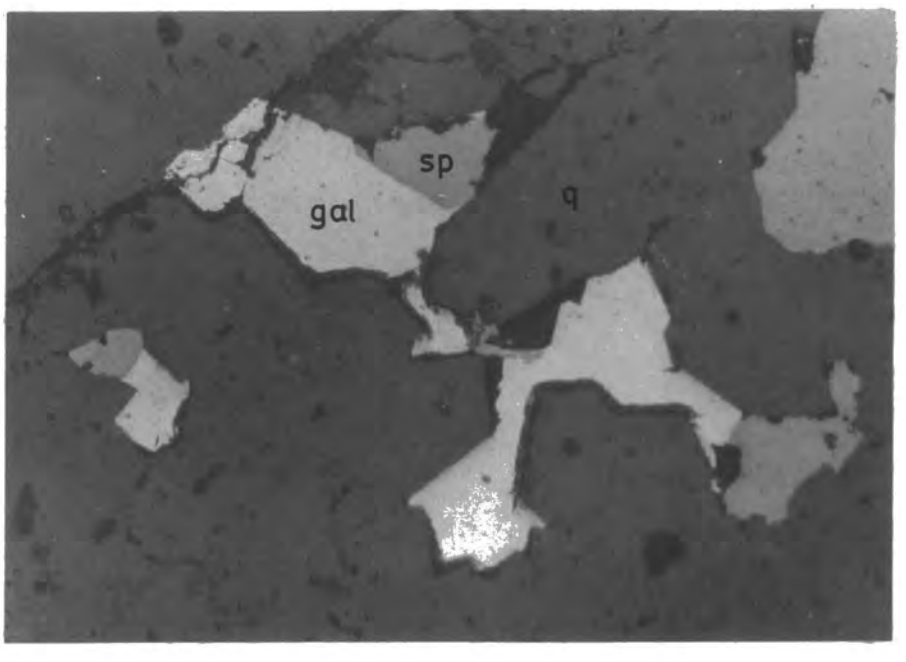


Fig. 12. Quartz (q) metacrysts penetrating galena (gal) and sphalerite (sp).

Reflected light. X 200. Specimen PS8.

## 1.2. X-RAY FLUORESCENCE

An X-ray fluorescence technique was employed for the determination of all trace elements and most major elements in both the host rock and wallrock. Elements outside the range of the instrument were determined by other means.

The instrument used for the investigation was a Philips PW1212 Automatic Spectrograph with attached Pye-Unicam automatic sample loader and IBM computer card print-out.

### 1.2.1. Selection and Preparation of Samples

Samples for analysis consisted of composites taken from three-inch intervals from the top of the Jew limestone to the top of the mineralised section, a length of approximately 8 feet. The three-inch sections of material were split by a mechanical splitter from the core. Representative samples from the altered wallrock proved more difficult to obtain due to the variable nature of the material. Samples from these sections were taken in the form of one-inch diameter cores by means of a Meddings diamond drill from the portions which, on visual inspection, appeared to be as close as possible to an "average" composition of the material in the vicinity.

Both sets of material were then crushed to approximately -300 mesh in a Tema Disc Mill, due precautions being taken against the oxidation of iron (Fitton & Gill, 1970), and stored in polythene sample bags.

Samples for presentation to the x-ray spectrometer were pelletised at a pressure of 5 tons per square inch, and, where

considered desirable, bound with mowiol or backed with boric acid, when only small amounts of material were available.

1.2.2. Major Elements

The same pellets were used for the major and trace element determinations. For all major elements a chromium x-ray tube was used (except Mn for which the tungsten tube was retained), and the instrument operated in the absolute - ratio mode under the conditions set out in the table 1. Background counts were taken on those elements which were expected to be present in small concentrations, otherwise peak heights alone were measured. In order to obtain maximum response it was necessary to vary the conditions as may be seen in the table, for most channels.

A monitor was used for all major element analyses, and thus the time taken to accumulate the fixed number of counts on the monitor was used as the counting time on both the peak and background positions of the samples.

A great difficulty encountered in the major element analyses was in the selection of standards for the determinations. Only Argillaceous Limestone 1a in the series of internationally recognised standards had a composition approximating the material considered and thus was used as one of the standards in the analyses. In order to overcome this difficulty all samples were first run on the spectrograph from which the individual count-rates were recorded on printed tape. From these results a series of six samples were chosen as sufficiently covering the full range of counts recorded on each element. All samples gave

different count-rates on different elements so only a minimum of samples, which, taken as a group, covered the widest range of count-rates, were selected. A complete elemental (major element) analysis was then undertaken on these samples by Atomic Absorption Spectroscopy, Spectrophotometry, and Flame Photometry (each of which are described in detail in succeeding sections). The samples thus chosen were X3, X7, X25, X26, X33 and X54. These were then considered as the standards, against the count-rates and concentrations of which all other samples were compared.

Due to the difficulty in determining S by other instrumental methods, and the small amount present compared with other major elements, a series of additional standards were constructed with Analar calcium carbonate containing 10,000 ppm., 5,000 ppm., 2,500 ppm., 1,000 ppm., 500 ppm., 50 ppm., of Analar S. The concentrations in the samples were then determined by the same method used for trace elements.

Three computer programmes were called upon to produce the final print-out of major element oxide concentrations in the samples. The raw counts on both peak and background positions printed out on tape from the Mn and other major element analyses were processed by programmes PKBD and TAPE respectively, the functions of which were simply to subtract background from peak readings where taken, and to tabulate the resulting counts in columns for each particular element. Cards containing the combined information from the print-out of these two programmes, together with the results of C, $CO_2$ and $H_2O$ analyses were then repunched to constitute part of the data for inclusion in programme XRFR for final processing. Other data required by the programme

included:

1). a block containing published values (Heinrich, 1966) of atomic absorption coefficients of a particular oxide with respect to each element in turn.

2). a block containing the full analyses of each standard, together with the count-rate corresponding to each element in the standards.

After correction of all count-rates for mass absorption effects, and calibration using the standards by the method of Holland and Brindle (1966), XRFR computes the individual oxide percentages to give a 100% total.

Print-out from the programme included:

1). a repeat of the information presented as data in the standard block, but with the addition of the computed mass absorption coefficient for each oxide and the corrected counts.

2). a summary of the essential features of the computed linear regression equations for each element, i.e. the correlation coefficient, slope, and intercept.

3). the range of the calibration for each element, i.e. the range between the highest and lowest values of the standards.

4). the final normalised individual oxide percentages for each sample.

During the computation, the $CO_2$, C and $H_2O$ values were manipulated with the other values, and thus the results printed out contained values different from those originally presented to the computer. As these amounts were determined absolutely by independent methods, the original values were resubstituted and the oxides renormalised manually to give a 100% total.

The results of the major element analyses are presented in the Appendix, table 1.

### 1.2.3. Trace Elements

For trace element analyses standards were constructed by using a composite of portions of each of the unknowns as base material in order to obtain a matrix of good average composition and thus eliminate, or at least minimise, the effects of matrix variation on the analyses. Matrix effects and instrumental drift were practically eliminated by using in addition scattered x-rays as variable internal standards (Andermann & Kemp, 1958) during the calculations of absolute concentrations of the elements. The calculated amount of the compound containing the element to to be measured was added to the base material in a concentration greater than that to be expected in the unknowns, and thoroughly mixed in a Spex Mill/Mixer for one hour. Calculated portions of this were then diluted and mixed with the original base material to produce a set of standards with a range of concentrations between the limits of which the unknowns were expected to fall. In order to keep the matrix as close as possible to the original composition, it was deemed necessary to limit the number of elements added to any one series of standards.

Thus two series were constructed, comprising the following elements and related concentrations:

Series 1 ;

Elements :- Ba, Nb, Zr, Y, Sr, Rb.

Concentrations :- 5 ppm., 10 ppm., 20 ppm., 50 ppm., 100 ppm., 200 ppm., 300 ppm., 750 ppm., 1,000 ppm., 2,000 ppm.

Series 2;;

Elements :- Cu, Ni, Zn.

Concentrations :- 10 ppm., 50 ppm., 100 ppm., 200 ppm., 300 ppm., 500 ppm., 750 ppm., 1,000 ppm., 2,000 ppm.

The operating conditions for trace element analysis are shown in table 2.

On obtaining the count rates on the respective peak and background 2θ positions, these were converted to peak minus background/background ratios by a preliminary computer programme. These ratios were then plotted against concentration of the standard for each particular element, and on determining the line of best fit, the slope, x-axis intercept and correlation coefficients by linear regression analysis on an Olivetti - Underwood electronic desk-top computer, Programma 101, the calibration factor (slope) was presented to the IBM computer as additional data. Other data included a correction to be applied for the amount of tube contamination (determined from the relevant count-rates obtained on a blank sample of specpure calcium carbonate), interference factors, where applicable (Nb was assigned a value of 0.0195 due to Y $K\beta$, Zr 0.0469 due to Sr $K\beta$, and Y 0.1450 due to Rb $K\beta$), the 2θ goniometer position on which readings were taken (both peak and background)

and the limits of applicability of the method in ppm.. The lower limit was taken as the detection limit calculated from accumulated background values and the upper limit that value at which the standard calibration curve was found to deviate from linearity, above which, therefore, the calibration factor was not applicable. On occasions, samples did fall outside this range, notably the sulphur and zinc concentrations in several sphalerite - containing wallrock samples. The concentrations given for these particular samples must be considered as only very approximate.

The print-out from the computer after input of all the above data consisted of the sample number with the corresponding peak-background/background ratios and the calculated concentration for each particular element in ppm., together with detection limits.

As a means of determining the precision of the analyses, one group of samples (Cu, Ni and Zn) were run with a counting time of 40 secs. and a recycle on each set of samples. The count rates obtained were then run through a preliminary computer programme (COMPARE) the function of which was to compare the corresponding count-rates from each cycle on a particular specimen and to indicate when the count-rates differed more widely than that which could be attributed to normal statistical fluctuations in the counting process. The maximum amount by which divergence of count rates could be tolerated was defined by the programme to be five times the standard deviation. In only three cases was this tolerance limit exceeded. This was interpreted as being due to spurious pulses through the machine causing the higher count-rate. Both sets of count-rates within the acceptable limits were

summed during the computation. For those samples producing spurious count-rates the lower value was taken to be nearest to the true count-rate and the final value found by doubling this. The values thus obtained were then fed into the original programme, TRATIO, to produce the actual elemental concentrations in ppm..

The results of the trace element analyses are presented in the Appendix, Table 2, together with the detection limits applicable to each element. Graphical representations of the variation of each element with depth are shown in figs. 24, 25 and 26. The possible significance of the elemental distributions will be discussed in a succeeding chapter.

Due to the fact that an excessively high calibration factor was obtained from the Ba analyses it was inferred that the constructed standards used were of insufficient thickness for the determination of this element, allowing the primary x-ray beam to penetrate to the borax backing while being still capable of producing useful Ba K$\alpha$ quanta. This was remedied by re-running both samples and standards with the 2$\theta$ positions set on the Ba L$\beta_1$ line. Satisfactory results were then obtained.

## TABLE I PW 1212 OPERATING CONDITIONS FOR MAJOR ELEMENT ANALYSES.

| Element | Si | Al | Fe | Mgp | Mgb | Ca | Nap | Nab | K | Ti | Sp | Sb | Pp | Pb | Mnp | Mnb |
|---|---|---|---|---|---|---|---|---|---|---|---|---|---|---|---|---|
| Collimator | C | C | C | C | C | C | C | C | C | C | C | C | F* | F* | C | C |
| Crystal | PET | PET | LIF(100) | KAP | KAP | LIF(100) | KAP | KAP | LIF(100) | LIF(100) | PET | PET | PET | PET | LIF(110) | LIF(110) |
| Counter | F | F | F+S | F | F | F | F | F | F | F | F | F | F | F | F+S | F+S |
| Time | FC | FC | FC | FC | FC | FC | FC | FC | FC | FC | FC | FC | FC | FC | FC | FC |
| Counts | $10^5$ | $10^5$ | $10^5$ | $3x10^4$ | $3x10^4$ | $3x10^5$ | $3x10^4$ | $3x10^4$ | $10^5$ | $10^5$ | $10^4$ | $10^4$ | $10^4$ | $10^4$ | $10^5$ | $10^5$ |
| MA | 8 | 40 | 8 | 40 | 40 | 8 | 40 | 40 | 8 | 8 | 40 | 40 | 40 | 40 | 40 | 40 |
| KV | 60 | 50 | 20 | 50 | 50 | 20 | 50 | 50 | 40 | 40 | 50 | 50 | 50 | 50 | 50 | 50 |
| Angle 2θ | 109.15° | 145.13° | 57.50° | 43.40° | 41.40° | 113.09° | 53.12° | 55.12° | 136.65° | 86.15° | 75.65° | 73.50° | 89.45° | 87.50° | 95.25° | 97.00° |

where
p = peak
b = background
C = coarse
F = flow counter
S = scintillation counter
FC = fixed counts

Mode : Absolute-ratio

* To remove Ca interference.

Crystal 1 - LiF (100)
Crystal 2 - PET
Crystal 3 - KAP
All Cr Tube, except Mn-W Tube.
$K_\alpha$ line used on all elements.
All crystals 1st order.
Spectrometer Chamber Evacuated.

TABLE 2. PW1212 OPERATING CONDITIONS FOR TRACE ELEMENT ANALYSES

| | | |
|---|---|---|
| Tube | : | W |
| Crystal | : | LiF (110) |
| Collimator | : | Coarse |
| Counter | : | Scintillation |
| Fixed Time | : | 100 secs. Cu, Ni, Zn two cycles of 40 secs. each. |
| MA | : | 32 |
| KV | : | 60 |
| Mode | : | Automatic |
| Line | : | $K_{\alpha}$ except Ba - $L_{\beta_1}$. |

Spectrometer Chamber Evacuated.

2θ Angles

| | | | | | |
|---|---|---|---|---|---|
| | Bkgd | 16.55° | Zn | Pk | 60.55° |
| Nb | PK | 30.39° | | Bkgd | 59.33° |
| | BKgd | 30.88° | | BKgd | 61.53° |
| Zr | PK | 32.08° | Cu | PK | 65.51° |
| | BKgd | 32.93° | | BKgd | 66.43° |
| Y | PK | 33.88° | Ni | PK | 71.24° |
| | BKgd | 34.78° | | BKgd | 69.92° |
| Sr | PK | 35.81° | | BKgd | 73.13° |
| | BKgd | 36.78° | Ba | PK | 79.18° |
| Rb | PK | 37.97° | | BKg. | 80.48° |
| | BKgd | 39.63° | | | |

## 1.3. ATOMIC ABSORPTION SPECTROSCOPY

As mentioned previously, atomic absorption spectroscopy was the method chosen for the determination of the bulk of the major element concentrations in the samples selected as covering the range of count-rates obtained from x-ray fluorescence analysis. The method was chosen as being the most rapid, potentially accurate, precise, sensitive and relatively free from interference. When interference is suspected, this can be relatively easily eliminated or minimised. Several disadvantages, however, pertain to the method:

(a) Samples must be presented to the instrument in solution.

(b) Due to the sensitivity and low concentrations producing full scale expansion, for most elements it was found necessary to dilute the unknowns by several orders of magnitude in order to bring the concentrations within the range of standards.

(c) The viscosity and surface tension of the solutions, directly affecting the aspiration rate of the solution to the burner (Dean 1960), must be identical in each solution and the standards. Steps taken to minimise inter-solution differences included the preparation of standards containing each of the elements to be analysed in the same solution, and the addition of acids to the standards in amounts similar to those used during sample preparation.

(d) It was not possible to analyse for phosphorous, potassium, and sulphur, on the instrument available, and thus recourse was made to other techniques for the determination of these elements. In theory, potassium is within the range of the instrument, but as the resonance.....

wavelength is close to the long wavelength limit of the instrument, very poor response was obtained.

The instrument employed was a Hilger & Watts "Atomspek".

1.3.1. Preparation of Samples.

Standards were prepared by making up a stock solution in which compounds of the elements to be determined were dissolved in amounts corresponding to the concentration recommended as producing full scale deflection of the absorbance meter on the instrument. Portions of this stock solution were then diluted down to produce a series of four standards consisting of the stock solution, and three solutions respectively 3/4, 1/2, and 1/4 of the concentration of this. It was ensured that the compounds used for the standards were mutually soluble, and did not precipitate out on the addition of either $H_2SO_4$ or HCl acids.

Standards used for the determinations of Si and Ti were commercially prepared BDH solutions of silicon and titanium sulphate. Portions of these solutions were added to the stock and other standard solutions in known amounts to produce an additional series of standards.

Unknowns were prepared for analysis by fusing a known amount of the ground powder with sodium hydroxide in a nickel crucible for ten minutes, dissolving the product in 1 c.c. of $H_2SO_4$ and 2 c.c. of HCl (heating when necessary) and diluting the resultant solution to 200ml. with distilled water. Fusing was deemed necessary as other methods of dissolution involve hydrofluoric acid, by which method silicon, one of the elements to be determined, is removed in a volatile phase as $SiF_4$.

An attempt was made to determine Na in the samples, but as this element had been added in large amounts during the preparation of the samples, so many dilutions were required to bring the concentration within the range of the standards, thereby greatly increasing the possibility of error, that another method had to be found for the procedure.

For this determination portions of the original samples were re-fused in KOH and dissolved as previously, The total sodium was determined and the actual Na concentration in each sample found as the difference between this figure and that calculated for the impurity present in the KOH, from the analysis of a KOH blank solution.

1.3.2. Operation

Samples and unknowns were aspirated directly into the flame in alternation with distilled water which was defined during each determination, as having zero absorbance - that is the absorbance of distilled water for each element constituted the reference base line against which all other samples were compared.

A permanent record of each of the determinations was obtained on a Servoscribe chart recorder attached to the instrument. Samples were aspirated for at least 30 secs. to ensure stability of the absorbance peak. Likewise the distilled water was aspirated for a time sufficient to ensure removal of all traces of the previous sample from the instrument tubes. Duplicate analyses of both standards and unknowns were run and the average absorbance reading taken as the final figure. In most cases the two readings were identical, testifying to the high precision of the method.

Elements analysed were Si, Al, Mg, Ca, Na, Ti, and Mn. Occasionally the conditions recommended by the manufacturer were used, but it was found necessary in several cases to alter these in order to obtain maximum response from the equipment (table 3). In most cases the concentration specified for each element as being equivalent to full scale deflection of the absorbance meter did not conform with the results obtained, which were invariably higher than the specified values. It is inferred that the discrepancy is due to the different aspiration rates of the solutions used, the instrument being calibrated at 2.5 ml/ min. for a simple compound of the element in distilled water. The properties of the solutions being investigated are different to those of the calibrating solution, but as previously mentioned, any errors introduced are minimised by using standards of similar properties.

Due to the complexing action of Si, Al and the phosphate and sulphate radicals with Ca, initially no response could be obtained on the instrument for this element. The calcium was released from the complex and subsequently successfully determined by adding known amounts of a concentrated lanthanum choride solution to both samples and unknowns (Volborth, 1969).

As was the case with Ca, chemical interference from Al, Si, P and $SO_4^{2-}$ is present in the determination of Mg (Angino & Billings, 1967). This was eliminated by the addition of the lanthanum buffer to both samples and standards in equal amounts.

Billings (1965) has shown that molecular absorption by Ca, and possibly by Mg and Na occurs on the Fe ( 2,483Å) line using an air/

acetylene flame. The interfering absorption was measured on the non-absorbing Fe line (2,510.8Å) and its value subtracted from the total result obtained on the absorbing line.

Silica interferes with the determination of Mn, presumably by the formation of complex ions or colloidal silicates (Platte & Marcy, 1965). It is considered, however, that the Ca concentration in the samples is sufficient to eliminate this effect.

1.3.3. Treatment of Data

For each element, a plot of absorbance vs. concentration was made for each of the standards, enabling the sample concentration to be read directly from the graph by comparing the absorbance of the unknowns. From the values thus obtained the actual concentrations in the original sample were recalculated. These were then incorporated in the data previously obtained from x-ray fluorescence analysis, spectrophotometry, flame photometry, and the $CO_2$ absorption train to allow the computation of total major element concentrations in all samples.

| ELEMENT | WAVE-LENGTH | LAMP CURRENT | SLIT WIDTH | FUEL | | OXIDANT | | | BURNER TOP | BURNER HEIGHT | RANGE | SENSITIVITY |
|---|---|---|---|---|---|---|---|---|---|---|---|---|
| | Å | mA | | MATL. | IND. FLOW | MATL. | IND. N | FLOW S | | MM BELOW AXIS | p.p.m. | p.p.m. |
| Al | 3093 | 10 | 30 | $C_2H_2$ | 9.1 | $N_2O$ | 12.5 | 3 | H.1163 | 15.0 | 0-200 | 1.0 |
| Ca | 4227 | 5 | 30 | " | 2.4 | AIR | 14.0 | 6 | H.1164 | 1.0 | 0-10 | 0.05 |
| Fe | 2483 | 20 | 20 | " | 2.3 | AIR | 14.0 | 6 | H.1164 | 1.5 | 0-20 | 0.08 |
| Mg | 2852 | 4 | 20 | " | 2.1 | AIR | 14.0 | 6 | H.1164 | 3.0 | 0-1 | 0.006 |
| Mn | 2795 | 15 | 20 | " | 2.2 | AIR | 14.0 | 3.6 | H.1164 | 5.0 | 0-10 | 0.06 |
| Si | 2516 | 27.5 | 30 | " | 10.5 | $N_2O$ | 12.5 | 3 | H.1163 | 14.0 | 0-500 | 2.0 |
| Na | 5846 | 8 | 20 | " | 2.5 | AIR | 14.0 | 4 | H.1164 | 2.0 | 0-3 | 0.04 |
| Ti | 3643 | 15 | 30 | " | 11.2 | $N_2O$ | 12.5 | 5.1 | H.1163 | 14.0 | 0-500 | 2.5 |

TABLE 3. OPERATING CONDITIONS FOR ATOMIC ABSORPTION SPECTROSCOPY

## 1.4. FLAME PHOTOMETRY.

Flame photometry was used for the analysis of Na and K in the samples chosen as standards for XRF analyses, the former element being analysed as a check on the results obtained by atomic absorption spectroscopy. The latter could not be determined on the AAS equipment available, the absorption spectra being outside the wavelength limit of the machine.

The instrument employed was an "Eel" flame photometer operated with a natural gas/air mixture, with an air pressure of 10 lb./sq.in. The gas pressure was held constant by means of an inbuilt stabiliser, and the flame maintained at a constant height by adjusting the gas supply such that the blue cone produced in the flame could be split into separate cones defined by the fuel entrance slits in the burner head, on a small adjustment to the gas supply. This allowed for reproducible conditions of operation for successive determinations.

After aspirating all standards for a given element, the potentiometer was adjusted to the position of minimum sensitivity and the required unknown aspirated into the flame. By subsequently adjusting the potentiometer to produce a full scale deflection (5 ppm for Na and 4 ppm for K, at full sensitivity) the approximate amount of dilution necessary to bring the sample within the range of the standards was determined. After dilution, the unknowns were again aspirated at full sensitivity, and the results obtained compared with the standard calibration curve. The concentration of each element in the original sample could then be obtained by calculation.

For the determination of sodium, those samples fused with KOH were aspirated using a Na filter. For the determination of K, samples fused with NaOH were run with a K filter.

The results of the K analyses were incorporated with those obtained from atomic absorption analysis and the particular samples used as standards for x-ray fluorescence analysis as previously described. The results of the Na determinations were compared with those obtained from the corresponding samples by AAS, both sets of which compared favourably within the limits of experimental error.

In order to ensure that contamination of K was not effected by possible impurities in the Analar NaOH used for the preparation of the original samples, a blank sample containing NaOH in solution was analysed. The K concentration in the NaOH was found to be negligible (compare Na impurities in KOH).

Spectral interferences occurring with the instrument employed are minimal, due to the insertion of a heat-absorbing glass and K and Na filters in the light path, and the relatively low temperature flame employed. Other types of interference, however, do occur, and can serve to either enhance or depress true concentrations. In the present case, interference could result from the presence of Ba, Ca, Fe, Mg, Mn, (Dean 1960) and Na (Poluektov et al, 1958). The effects are small, however, at the concentrations considered, and in addition, assuming that the effects of the interferences are algebraically additive, these would approximately cancel out, due to the preponderance of Na over the other elements, this element alone causing enhancement.

Afurther source of possible interference is a negative error produced by acids (Dean, op.cit.). The severity of the interference is a function of the elemental concentration, flame temperature, and

nature and concentration of the acid. In this case the acids possibly causing interference are HCl and $H_2SO_4$. However, due to a favourable combination of circumstances, viz. the low concentration of K and Na, relatively low flame temperatures, and low acid concentrations, particularly after dilution of the samples to bring them within the range of the instrument, the interference due to this source can be neglected. The extend of interference also depends on the fuel used (Cooper, 1963).

Due precautions with regard to viscosity and surface tension differences between samples and standards were taken by adding proportionate amounts of the acids used in the dissolution of the sample to the standards.

## 1.5. SPECTROPHOTOMETRY

Spectrophotometric methods were employed to determine phosphorus on the solutions analysed by atomic absorption spectroscopy, as the resonance wavelength of this element is beyond the range of the latter instrument.

The phosphorous was determined as the yellow molybdivanadophosphoric acid complex formed by the addition of molybdivanadate solution (ammonium metavanadate, ammonium molybdate, conc. nitric acid and distilled water) to each sample and a blank. Standards were constructed from a solution of potassium dihydrogen phosphate.

The optical density of each solution was measured at a wavelength of 430mμ, after calibration of the instrument with a didymium crystal, on a Unicam spectrophotometer. The values obtained were compared with those of the standards and calculated back to $\%P_2O_5$ in the samples. These values were then taken to represent the concentrations corresponding to the respective count rates obtained from x-ray fluorescence analysis. The concentrations of $P_2O_5$ in all other samples were determined by computer using the spectrophotometrically analysed samples as standards.

On the instrument used, it was found that although the readings obtained from the standards with reference to the blank remained constant, those obtained from the actual unknowns tended to increase with time. It was deduced that this was due to a sluggish reaction of the complexing agent with the phosphorous in the sample. The series of samples was analysed several times under identical conditions over a period of days until the readings were found to remain essentially constant. A further suggestion of the slow

action of the complexing agent was noted as the colour of each of the unknown solutions was observed to deepen over the period of the runs.

The results of the analyses after calibration and computation are presented in the appendix, table 1.

Replicate analyses were carried out on all samples, and the instrument found to be sufficiently precise. The method is said to be accurate to 0.005 % P (Snell and Snell, 1936).

## 1.6. THERMOGRAVIMETRY AND $CO_2$ ABSORBTION TRAIN

As a Stanton Thermobalance was available an attempt was made to determine C and $CO_2$ using the technique suggested by Waugh and Hill (1960). Although many variations on the basic procedure were tried (carrying out runs both in air and in nitrogen), variable results were obtained on replicate runs, and interpretation of the curves suggested considerable overlap of the weight-loss from different reactions. The method was therefore abandoned in favour of the absorbtion train technique as described by Groves (1951).

This method consists essentially of boiling the sample in orthophosphoric acid and determining the increase in weight due to the absorbtion of $CO_2$ by two U-tubes filled with soda-lime, after passing the gas through water and $H_2S$ traps. C is subsequently determined by oxidation on boiling with chromium trioxide, absorbtion as $CO_2$, and calculation back to original C. Blank values were subtracted from the above.

The results of the analyses are presented in the Appendix, table 1, and again graphically in figs. 31 and 32.

## 1.7 WATER DETERMINATIONS

Essential or combined water ($H_2O+$) and hygroscopic water ($H_2O-$) were determined, the former by the classical Penfield Tube method (Penfield, 1894) and the latter by determining the loss in weight of oven-dried (110°C) material.

The essential features of the Penfield Tube method are as follows. A small quantity of sample (approx. 1 gm.) was poured through a long-stemmed filter funnel to the base of a pre-weighed 30 cm. pyrex tube which was then reweighed to determine the sample weight. Tube and sample were placed overnight in a 110°C oven and the loss in weight reported as $H_2O-$. The tube was then clamped in a horizontal position and two strips of water - soaked filter paper wrapped around the tube at least 10 cm. from the sample in order to condense expelled water. The sample was heated for a period of 15 mins. by means of an oxygen/air blowtorch to ensure that all water had been expelled and removed from the main body of the tube by fusing to a neck immediately in front of the sample which was subsequently detached from the main body of the tube. The tube was then weighed, dried and reweighed, to give the reported value of $H_2O+$.

The samples investigated were portions of the powdered material used for other assaying techniques. The results of the analyses are presented in table 4, where it may be seen that the amounts of both $H_2O+$ and $H_2O-$ fluctuate markedly up the section. Replicate determinations were made on 5 samples. The results indicated an acceptable level of precision for the method the maximum difference in readings being 0.06%.

TABLE 4. RESULTS OF WATER DETERMINATIONS

| Sample No. | $H_2O^-$ | $H_2O^+$ |
|---|---|---|
| X1 | 0.41% | 2.24% |
| 2 | 0.75% | 1.41% |
| 3 | 0.38% | 1.46% |
| 4 | 1.11% | 2.71% |
| 5 | 1.17% | 1.70% |
| 6 | 2.01% | 3.35% |
| 7 | 0.82% | 2.71% |
| 8 | 0.79% | 2.47% |
| 9 | 0.99% | 3.15% |
| 10 | 0.86% | 1.82% |
| 11 | 1.29% | 2.07% |
| 12 | 1.21% | 2.77% |
| 13 | 0.52% | 1.12% |
| 14 | 0.59% | 1.47% |
| 15 | 0.28% | 0.63% |
| 16 | 1.06% | 0.97% |
| 17 | 0.82% | 2.45% |
| 18 | 0.68% | 3.09% |
| 19 | 0.27% | 3.55% |
| 20 | 0.61% | 2.33% |
| 21 | 0.68% | 2.37% |
| 22 | 0.93% | 2.04% |
| 23 | 2.29% | 0.51% |
| 24 | 0.93% | 0.93% |
| 25 | 0.38% | 2.02% |
| 26 | 0.70% | 0.20% |
| 27 | 0.32% | 0.56% |
| 28 | 0.61% | 1.22% |
| 29 | 0.59% | 0.72% |
| 30 | 0.68% | 0.68% |
| 31 | 0.30% | 0.35% |
| 32 | 0.54% | 0.36% |

| Sample No. | $H_2O^-$ | $H_2O^+$ |
|---|---|---|
| X33 | 0.57% | 1.94% |
| 46 | 1.65% | 3.63% |
| 47 | 0.11% | 1.32% |
| 48 | 0.56% | 0.56% |
| 49 | 0.27% | 1.00% |
| 50 | 0.59% | 0.68% |
| 51 | 0.82% | 1.37% |
| 52 | 0.09% | 0.54% |
| 53 | 0.57% | 0.23% |
| 54 | 0.56% | 0.90% |
| 55 | 0.50% | 1.10% |
| 56 | 0.62% | 0.16% |

## 1.8 1 ELECTRON MICROPROBE ANALYSIS

For electron microprobe analysis a Cambridge Instrument Co. Geoscan was used for the following purposes:

(a) To confirm the identification of phases made by microscopy.

(b) To determine the major element composition of carbonates.

(c) To determine the major element composition of sphalerite.

(d) To determine the trace element contents of chalcopyrite, galena, carbonates and sphalerite.

(e) To obtain an indication of the degree of variation and pattern of distribution of major elements through sphalerites and carbonates.

Each of these points is further discussed hereunder:

Prior to analysis, each of the specimens (the polished sections used for microscopic studies), was coated with carbon to produce a conductive layer 100Å in thickness.

The composition of phases, which, under ordinary microscopic methods were too small to identify accurately, or about which doubt existed as to their identification, (such as marcasite which showed optical properties close to those of arsenopyrite), were analysed by means of the probe. This applied not only to ore minerals but to the gangue minerals whose reflectivities differ by small amounts and thus whose boundaries are difficult to resolve. A problematic silicate noted in thin sections was confirmed as potassium feldspar by this method, one analysis being returned as 27.31% , $Al_2O_3$, 58.76%, $SiO_2$ and 9.18% $K_2O$ for a total of 95.25%.

The carbonates show considerable variation in composition both in an intergranular and intragranular sense. Quantitative determi-

nations of the compositions of the carbonates were made by taking spot analyses for Ca, Mg, Fe and Mn. Due to the possibility of decomposition of the specimen under the beam during analysis it was found necessary to utilise a defocused spot on both specimen and standards.

Analyses were made on several grains in each of the polished sections, usually at several points within each particular grain. The results of some of these analyses are shown in table 6 and plotted on a triangular diagramme in fig. 13.

The highly irregular variation in composition of individual specimens even on a micron scale, and the relationship of individual element concentrations to each other, can be seen in fig. 14. This shows how Fe and Mn vary sympathetically and Mg varies antithetically to both of these on a traverse across a specimen. Fig. 16 is a raster image of Mg $K_{\alpha}$ across a portion of the same specimen, showing the completely irregular distribution of the phases and demonstrating the limited value of making point analyses to determine compositions of individual carbonates.

No correlation could be discerned between the composition of the carbonates and their location or form with respect to other minerals in the assemblage.

Zinc, sulphur, iron and manganese analyses were attempted of sphalerite, under the conditions shown in table 5.

In the disseminated sphalerite grains point analyses were made at regular intervals in traverses across individual grains. These results are presented in table 7. The results clearly are at variance with those quoted by Sawkins (1966) in which 0.9% Fe is implied as being representative of the Jew Limestone sphalerite, and also with those of Sawkins et al (1964) for sphalerite taken from lower stratigraphic levels. Both sets of analyses were by wet chemical means.

It has been previously mentioned that colour banding in the sphalerite is clearly visible with the naked eye. Several of these bands were marked for analysis on the section where possible (as they are not distinguishable on the polished surface) and point analysed. Although the bands may not be homogeneous on a sub-micron scale (Roedder, 1968) the probe gives an average concentration in the bands which consist predominantly of either the dark or light colours observed.

A direct correlation was found between colour of the sphalerite and ironnconcentration, the darker bands being richer in iron. Fig. 15 shows a raster image of Fe K$\alpha$ taken over a small colour - zoned sphalerite grain in the wallrock. Superimposed over this is an x-ray scanning image of Fe K$\alpha$ showing the degree of variation represented by the various concentrations produced by the raster.

Roedder and Dwornik (1968) have shown that in at least one case, the iron content of sphalerite could not be correlated with colour banding, although many other investigators have produced evidence to the contrary.

Selected trace element analyses were attempted on several of the specimens of galena (Cd, Se, Mn), chalcopyrite (Se) sphalerite (Cd, Cu, Se, Mn), and carbonates. It had been hoped to be able to utilise trace element fractionation data between the sulphides as indicators of the environment of deposition (Bethke & Barton, 1959). The concentrations were found in most cases, however, to be below the limits of detection of the methods used. Only Mn was occasionally detected in low concentrations in sphalerite.

The ability to determine the nature and extent of variation of elements within individual crystals is a distinct advantage of this method of analysis over other instrumental techniques, as discussed by Williams (1965).

Several methods were used in such a study of both sphalerites and carbonates. The first of these involved mechanical scanning by the beam at a rate of 30 μ/min. across the specimen with continuous simultaneous recording of the levels of concentration of 2 elements on a chart recorder with a calibrated full scale deflection. Absolute values for various points on the graph could then be assigned by calculating the true concentration of the particular element at several points on the trace, and extrapolating between those points.

The second method produced a scanning image of a chosen element on a cathode ray tube. After setting up the instrument on each element in turn, the electron beam was made to scan across a chosen line. The form of the resulting trace on several of the specimens was recorded manually (fig.14) and photographic records obtained where relationships were particularly well displayed (fig. 15).

Adler (1963) asserts that on occasions analyses may be performed accurate to 1% of the amount present, but that more frequently the results are good to within 5 to 10%. With present day instrumentation, however, it is likely that the 1 to 2% suggested by Barton and Skinner (op.cit.)is more reasonable.

As is pointed out by Wittry (1963), the accuracy of

obtaining the true primary intensities of the characteristic x - radiation is only partly limited by the accuracy of the corrections to the data. Statistical errors or drifts in the analysis conditions occur, but more important in this case is considered to be the assumption that the specimen is homogeneous throughout the region analysed. Both the sphalerite and particularly the carbonates have been shown to be inhomogeneous even on a very small scale. This is important in considering fluorescence effects and other applied corrections, and may account in many instances for deviations of the totals from 100%.

Wittry lists the corrections which must be taken into account to obtain the true primary x-ray intensities from the observed intensities as

(1) a shift in the wavelength of the characteristic x-ray lines due to valence state.

(2) contamination of the specimen during analysis.

(3) finite resolving time of the detector.

(4) background due to the continuum.

(5) absorption of the x-rays by the specimen.

(6) fluorescence excitation by line radiation.

(7) fluorescence excitation by the continuum.

The first of these is not considered in the present case as the peak is determined for the particular analysis and the valence state in both the specimen and the standard of the element analysed are identical. Little or no contamination was noted. To the list of remaining corrections is added an adjustment for the atomic number effect - the difference in average atomic number between the specimen and standard.

The raw count-rates printed out by the machine were converted into apparent percentages after adding dead time and subtracting background readings, by reference to the count rates obtained on the standards. Corrections for atomic number effects, absorption and fluorescence were made by computer, using the method of Sweatman & Long (1969) in preference to that of Williams (1967), and the true percentages thus obtained.

For the sulphides and silicates, print-out from the computer constituted the final results, but for the carbonates, additional adjustments were necessary. Apart from the apparent percentages for the analysed elements, a dummy carbon figure (11%) was included in the data, as it is an integral part of the correction procedures. The corrected true percentages for the original analysed elements were then each converted manually to carbonate percentages and the sum of these taken as the analytical total.

TABBE 5. OPERATING CONDITIONS FOR ELECTRON MICROPROBE

| ELEMENT | KV | CRYSTAL | COUNTER | LINE | $^{o}2\theta$ PEAK | STANDARD |
|---|---|---|---|---|---|---|
| Ca | 15 | Qtz. | Flow | CaK $\alpha$ | $60^{o}18'$ | $CaSiO_3$ |
| Mg | 15 | KAP | Flow | MgK $\alpha$ | $42^{o}40'$ | MgO |
| Fe | 15 | LiF | Flow | FeK $\alpha$ | $57^{o}28'$ | Fe |
| Zn | 15 | LiF | Sealed | ZnK $\alpha$ | $41^{o}41'$ | Zn |
| S | 15 | Qtz. | Flow | SK $\alpha$ | $106^{o}56'$ | $FeS_2$ |
| As | 20 | KAP | Flow | AsL $\alpha$ | $42^{o}40$ | As |
| Mn | 20 | LiF | Flow | MnK $\alpha$ | $63^{o}56'$ | Mn |
| Se | 20 | KAP | Flow | SeL $\alpha$ | $39^{o}32'$ | CdSe |
| Cd | 20 | Qtz. | Flow | CdL $\alpha$ | $72^{o}33'$ | CdS |
| K | 15 | Qtz. | Flow | KK $\alpha$ | $67^{o}58'$ | $KAl_2Si_3O_8$ |
| Al | 15 | KAP | Flow | AlK $\alpha$ | $36^{o}16'$ | $Al_2O_3$ |
| Si | 15 | KAP | Flow | SiK $\alpha$ | $30^{o}57'$ | $CaSiO_3$ |
| Na | 15 | KAP | Flow | NaK $\alpha$ | $52^{o}57'$ | $NaAlSi_2O_6$ |
| Cu | 20 | LiF | Sealed | CuK $\alpha$ | $44^{o}59'$ | Cu |

Spot Size 1µ
Take Off Angle $75^{o}$
Fixed Time 10 secs.
Specimen Current 4 µm A.

Mn 15kv in carbonates
Counter Voltage approx. 1.6 kv.
Cosec $\theta$ = 1.0353.

Beam Defocused during analysis of carbonates.
Beam normal to sample surface.

TABLE 6. RESULTS OF ELECTRON MICROPROBE ANALYSIS

SPHALERITE

WEIGHT %

| Zn | S | Fe | Mn | Total | Mol.%.FeS |
|---|---|---|---|---|---|
| 62.90 | 32.90 | 3.54 | n.d. | 99.34 | 6.17 |
| 62.00 | 33.63 | 4.62 | n.d. | 100.25 | 8.02 |
| 63.93 | 33.00 | 3.52 | n.d. | 100.45 | 6.06 |
| 66.25 | 32.31 | 1.46 | 0.20 | 100.22 | 2.51 |
| 66.05 | 31.93 | 1.67 | 0.06 | 99.71 | 2.86 |
| 66.04 | 32.48 | 0.94 | n.d. | 99.46 | 1.63 |
| 65.42 | 32.29 | 1.57 | 0.04 | 99.32 | 2.73 |
| 65.52 | 32.68 | 2.40 | n.d. | 100.60 | 4.10 |
| 64.07 | 32.83 | 2.71 | 0.06 | 99.67 | 4.71 |
| 65.10 | 32.53 | 2.43 | 0.06 | 100.12 | 3.97 |
| 63.89 | 32.02 | 3.20 | 0.04 | 99.15 | 5.54 |
| 65.60 | 32.86 | 2.08 | n.d. | 100.54 | 3.58 |
| 65.45 | 32.53 | 1.87 | n.d. | 99.85 | 3.23 |
| 64.50 | 32.62 | 2.81 | 0.05 | 99.98 | 4.85 |
| 60.10 | 32.29 | 6.04 | 0.09 | 98.52 | 10.51 |
| 66.77 | 32.24 | 1.46 | n.d. | 100.47 | 2.49 |
| 63.04 | 33.19 | 4.46 | 0.07 | 100.76 | 7.64 |
| 66.30 | 32.86 | 1.48 | 0.05 | 100.69 | 2.50 |
| 63.70 | 33.53 | 3.37 | n.d. | 100.60 | 5.83 |
| 63.51 | 32.82 | 4.25 | 0.09 | 100.67 | 7.25 |
| 56.32 | 32.01 | 10.66 | 0.02 | 99.01 | 18.13 |
| 56.10 | 32.30 | 10.99 | 0.09 | 99.48 | 18.63 |
| 60.19 | 32.96 | 7.16 | 0.06 | 100.37 | 12.20 |
| 63.51 | 32.83 | 4.25 | 0.09 | 100.68 | 7.25 |
| 57.60 | 31.14 | 10.86 | 0.04 | 99.64 | 18.07 |

n.d. - not detected

TABLE 7. RESULTS OF ELECTRON MICROPROBE ANALYSIS

CARBONATES

WEIGHT %

| Ca | Mg | Fe | Mn | Total | Specimen No. |
|---|---|---|---|---|---|
| 21.35 | 4.93 | 9.96 | 3.22 | 100.06 | PS3 |
| 20.36 | 3.72 | 12.52 | 4.67 | 99.48 | PS3 |
| 20.46 | 4.93 | 11.22 | 3.62 | 99.05 | PS8 |
| 19.76 | 2.54 | 13.88 | 4.89 | 100.14 | PS8 |
| 20.07 | 1.60 | 16.51 | 4.44 | 99.19 | PS8 |
| 20.30 | 4.72 | 11.39 | 4.32 | 99.74 | PS8 |
| 27.99 | 1.38 | 9.69 | 2.93 | 100.94 | PS8 |
| 20.03 | 3.65 | 13.14 | 4.53 | 99.39 | PS8 |
| 19.79 | 3.97 | 11.64 | 4.66 | 97.05 | PS8 |
| 20.30 | 2.88 | 14.06 | 4.41 | 99.06 | PS8 |
| 20.91 | 9.96 | 4.10 | 1.92 | 99.09 | PS8 |
| 21.67 | 11.76 | 1.81 | 0.72 | 100.20 | PS3 |
| 21.92 | 11.61 | 1.76 | 0.46 | 99.59 | PS3 |
| 21.79 | 11.94 | 1.02 | 0.30 | 98.56 | PS3 |
| 22.06 | 11.77 | 1.16 | 0.39 | 99.15 | PS6 |
| 21.80 | 11.98 | 1.01 | 0.36 | 98.18 | PS6 |
| 21.62 | 11.43 | 1.92 | 0.66 | 99.00 | PS6 |
| 20.83 | 10.28 | 4.45 | 1.32 | 99.67 | PS6 |
| 21.45 | 10.50 | 3.45 | 1.40 | 100.05 | PS6 |
| 23.09 | 11.68 | 0.39 | 0.15 | 99.34 | PS6 |

| Mol. % | $CaCO_3$ | $MgCO_3$ | $FeCO_3$ | $MnCO_3$ |
|---|---|---|---|---|
| | 54.67 | 20.83 | 18.30 | 6.20 |
| | 52.47 | 15.65 | 23.12 | 8.76 |
| | 52.09 | 20.70 | 20.50 | 6.71 |
| | 52.72 | 11.19 | 26.58 | 9.51 |
| | 51.51 | 19.74 | 20.75 | 7.99 |
| | 71.11 | 5.80 | 17.67 | 5.43 |
| | 51.64 | 15.51 | 24.32 | 8.53 |
| | 51.96 | 17.18 | 21.93 | 8.93 |
| | 52.92 | 12.39 | 26.30 | 8.38 |
| | 50.30 | 39.25 | 7.08 | 3.37 |
| | 50.53 | 45.21 | 3.03 | 1.23 |
| | 51.38 | 44.87 | 2.97 | 0.79 |
| | 51.38 | 46.40 | 1.71 | 0.51 |
| | 51.81 | 45.57 | 1.96 | 0.66 |
| | 51.25 | 46.44 | 1.70 | 0.60 |
| | 51.07 | 44.53 | 3.25 | 1.14 |
| | 49.69 | 40.41 | 7.61 | 2.29 |
| | 50.76 | 40.95 | 5.87 | 2.42 |
| | 54.03 | 45.07 | 0.65 | 0.25 |
| | 53.11 | 6.97 | 31.35 | 8.58 |

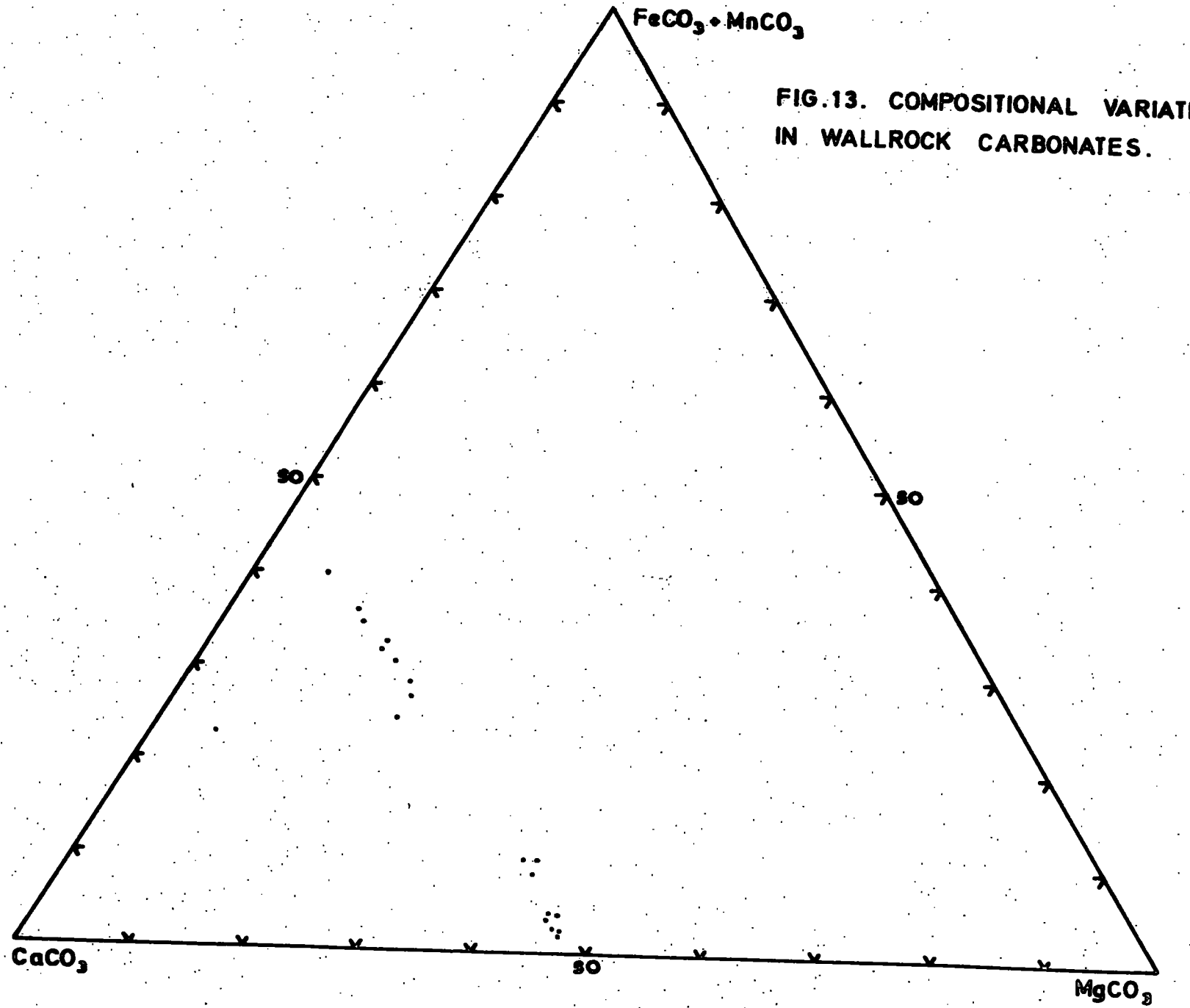


FIG.13. COMPOSITIONAL VARIATION IN WALLROCK CARBONATES.

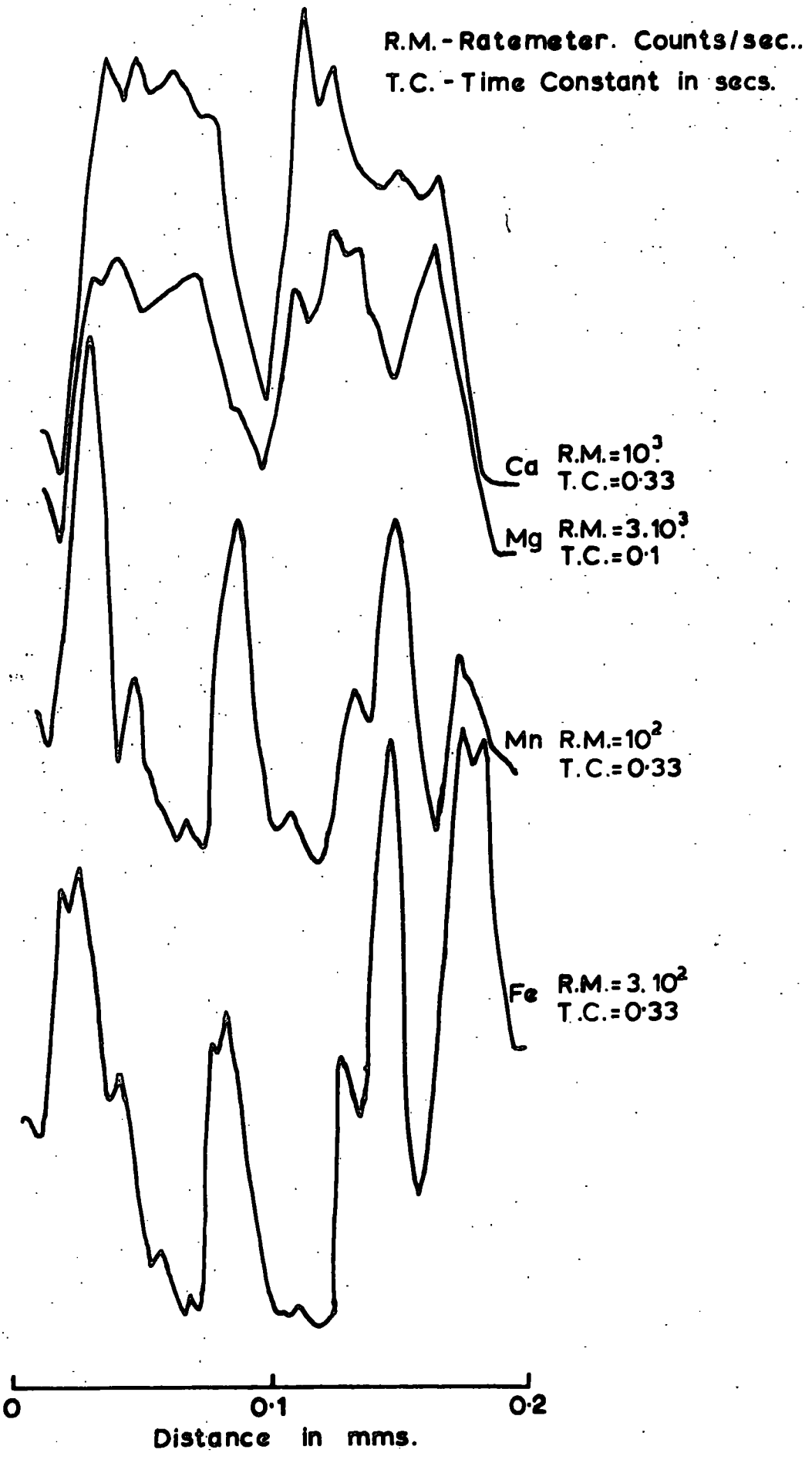


FIG.14. X-RAY (Kα) SCANNING IMAGES OF CARBONATE GRAIN.

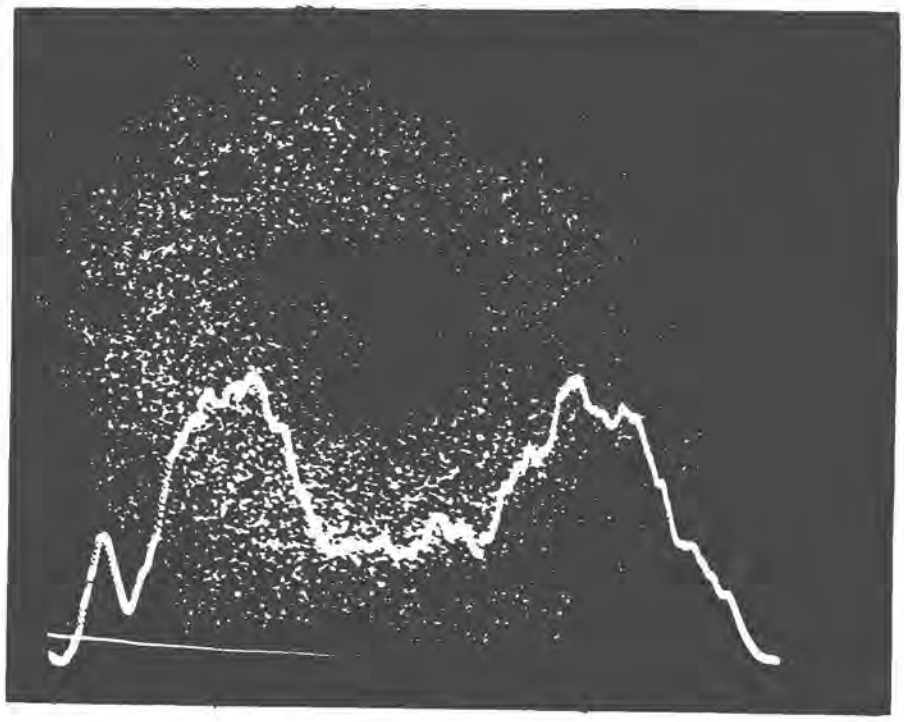

Fig. 15. X-ray (Fe K$\alpha$) raster and scanning images across a sphalerite "pisolite" demonstrating correlation of Fe concentration with colour zoning. Small peak to left of scan is due to interference from fluorite inclusion to left centre of grain. Embayments in top right of grain are due to quartz replacement across zones. Magnification X 600. Peaks on scan represent approx. 18 mole % Fes.

Fig. 16. X-ray (Mg K$\alpha$) raster across portion of a carbonate grain showing irregular distribution of phases even on a small scale. Magnification X 600.

## 1.9 X-RAY DIFFRACTION

X-ray diffraction procedures were used in order to determine quantitatively the mineralogy of each of the samples used for x-ray fluorescence analysis.

The machine employed was a Philips 1010 Diffractometer with attached Philips chart recorder operated under the conditions set out in table 8.

A selection of samples covering the full range of mineralogy to be expected was run initially to determine optimum settings, and these were maintained throughout the remainder of the analyses. Replicate runs were made on six samples and results obtained indicated the high precision of the method. Several samples were scanned from 2θ angles of $3^{o}$ to $90^{o}$, but after identification of all peaks by reference to the Fink Index and ASTM file it was found that peaks included between the limits of the 2θ angles of $20^{o}$ to $45^{o}$ were sufficiently diagnostic. Three samples were treated with ethylene glycol as a means of positively identifying montmorillonite on causing an increase from $15^{o}$A to $18^{o}$A of the (001) d-spacing of the mineral.

Samples were prepared by smearing a small amount of the powder, after regrinding in an agate, on a glass slide with acetone, taking care to minimise any tendency towards preferential orientation of any of the constituent minerals.

Under the best of conditions, even with minerals showing strong reflections, such as quartz, concentrations below 1% are not detected, and thus phases other than those displayed on the chart may be present. For example, although pyrite is known to be present, it was not detected without prior treatment of the samples.

In order to improve the limits of detection with respect to the original sample, to improve the quality of the peaks, and to remove some interfering peaks, calcium carbonate was removed by treating the sample with acetic acid (so as not to damage clay structures) thus concentrating the remaining fraction. It was found that pyrite could then be detected, and other phases previously identified displayed more prominently. However no new phases were detected and thus it was considered sufficient to process the remainder of the samples without prior treatment.

Although XRD was recommended by Kaye et al (1968) as the most accurate method of quantitative analysis from the results of an investigation of samples of fairly simple mineralogy, the mineralogy in this case was found to be too complex to attempt a similar study.

The results of each of the runs, giving the minerals identified, together with comments on important features and uncertainties in the interpretation of the record are presented in table 9. An example of a trace as returned on the XRD chart recorder is reproduced in fig. 17.

X-ray diffraction traces were also run as a control on the results of staining techniques as discussed in section 1.13.

## OPERATING CONDITIONS OF PW1010 X-RAY DIFFRACTOMETER

## TABLE 8.

MOUNT: SMEAR
TARGET: Co
TUBE RATING: 2 KW
KV: 60
MA: 25
GONIOMETER SCAN SPEED: $1^{o}$/MIN.
CHART SPEED: 10 mm/min.
DIVERGENCE SLIT: $1^{o}$
RECEIVING SLIT: $0.1^{o}$
SCATTER SLIT: $1^{o}$
COUNTER: GEIGER
RATE METER: $2 \times 10^{2}$.
TIME CONSTANT: 4
ATTENUATION: 1
LOWER LEVEL: 8.30
WINDOW: 1.65.

### PEAK POSITIONS ($^{o}2\theta$) USED FOR MINERAL IDENTIFICATION

| | | |
|---|---|---|
| Quartz | $31.09^{o}$ | (101) |
| Calcite | $34.25^{o}$ | (104) |
| Ankerite | $35.96^{o}$ | (104) |
| Pyrite | $38.57^{o}$ | (200) |
| Orthoclase | $32.26^{o}$ | (040), (002) |
| Illite | $22.90^{o}$ | (020), (110) |
| Montmorillonite | $22.80^{o}$ | (020), (110) |
| Fluorite | $33.02^{o}$ | (111) |
| Sphalerite | $33.34^{o}$ | (111) |
| Dolomite | $36.14^{o}$ | (104) |
| Kaolinite | $23.53^{o}$ | ($1\bar{1}0$) |
| Saponite | $27.95^{o}$ | (004) |
| Galena | $34.54^{o}$ | (200) |
| Siderite | $37.42^{o}$ | (104) |

## TABLE 9. RESULTS OF X-RAY DIFFRACTION ANALYSIS

| SAMPLE NO. | MINERALS IDENTIFIED | | | | | | | | | | | COMMENTS |
|---|---|---|---|---|---|---|---|---|---|---|---|---|
| | Quartz | Calcite | Ankerite | Siderite | Orthoclase | Dolomite | Fluorite | Montmor. | Sphal. | Kaolinite | Illite | Saponite | |
| x1 | x | x | | | | | | | | x | | | Unidentified peak at 38.6° 2θ (d.2.708) |
| x2 | x | x | | | | | | x | | x | x | x | High cal. Other peaks low. |
| x3 | x | x | | | x | | | | | x | x | | " " " |
| x4 | x | x | | | x | | | | | | | | " " " |
| x5 | x | x | | | x | | | x | | x | x | x | " " " |
| x6 | x | x | | | x | | | x | | x | x | x | " " " |
| x7 | x | x | | | x | | | x | | x | x | x | " " " |
| x8 | x | x | | | x | | | x | | x | x | x | " " " |
| x9 | x | x | | | x | | | x | | x | x | x | " " " |
| x10 | x | x | | | x | | | x | | x | x | x | Unidentified peak at 38.6° 2θ |
| x11 | x | x | | | x | | | x | | x | x | x | High or. peak |
| x12 | x | x | | | x | | | x | | x | x | x | High cal. peak |
| x13 | x | x | | | x | | | x | | | | | Cal. very high, other peaks low. |
| x14 | | x | | | | | | | | | | | " " " |
| x15 | x | x | | | | | | | | | | | " " " |
| x16 | x | x | | | | | | | | | | | " " " |
| x17 | x | x | | | x | | | | | | x | | High or. peak |
| x18 | x | x | | | x | | | | | | x | | " " |
| x19 | x | x | | | x | | | x | | x | x | x | " " |
| x20 | x | x | | | x | | | | | x | x | | High cal. peak |
| x21 | x | x | | | x | | | | | x | x | | " " " |
| x22 | x | x | | | | | | | | | | | " " " |

| SAMPLE NO. | MINERALS IDENTIFIED | | | | | | | | | | | | COMMENTS |
|---|---|---|---|---|---|---|---|---|---|---|---|---|---|
| | Quartz | Calcite | Ankerite | Siderite | Orthoclase | Dolomite | Fluorite | Montmor. | Sphal. | Kaolinite | Illite | Saponite | |
| x 23 | x | x | | | | | | | | | | | High cal. peak |
| x 24 | x | x | | | | | | | | | | | " " " |
| x 25 | | x | | | | | | | | | | | " " " |
| x 26 | | x | | | | | | | | | | | Unidentified peak at 38.6°2θ High cal. peak |
| x 27 | x | x | | | | | | | | | | | High cal. peak |
| x 28 | x | x | | | | | | | | | | | " " " |
| x 29 | x | x | | | | | | | | | | | " " " |
| x 30 | x | x | | | x | | | | | x | | | " " " |
| x 31 | x | x | | | | | | | | | | | Unidentified peak at 38.6°2θ High cal. peak. |
| x 32 | x | x | | | | | | | | | | | High cal. peak. |
| x 33 | x | | | | x | x | | x | | | | | Unidentified peaks at 32.1°2θ (d3.238) and 26.12θ (d3.964) |
| x 46 | x | | | | | | | x | x | | | | High quartz peak |
| x 47 | x | | | | | x | x | | x | | | | " " " |
| x 48 | x | | | x | | x | | | x | | | | High qtz. & Sp. peaks. |
| x 49 | x | | | | | x | | | x | | | | " " " |
| x 50 | x | | x | | | x | | | x | | | | " " " |
| x 51 | x | | | x | | x | | | x | | | | Unidentified peak at 35.7° (d2.920). |

TABLE 9. (Continued)

| SAMPLE NO. | MINERALS IDENTIFIED | | | | | | | | | | | COMMENTS |
|---|---|---|---|---|---|---|---|---|---|---|---|---|
| | Quartz | Calcite | Ankerite | Siderite | Orthoclase | Dolomite | Fluorite | Montmor. | Sphal. | Kaolinite | Illite | Saponite | |
| x 52 | x | | | | | | | | x | | | | Unidentified peak at 21.95° (d4.702) |
| x 53 | x | | | | | x | | | x | | | | High Qtz. and Sp. peaks |
| x 54 | x | | | x | | x | x | | x | | | | Unidentified peak at 21.95° |
| x 55 | x | | | | | x | x | | x | | | | High qtz. peak, unidentified peak at 20.75° (d4.970) |
| x 56 | x | x | | | | | | | | | | | Unidentified peak at 38.6° |

FIG. 17. X-RAY DIFFRACTION RECORD OF SAMPLE X 19.

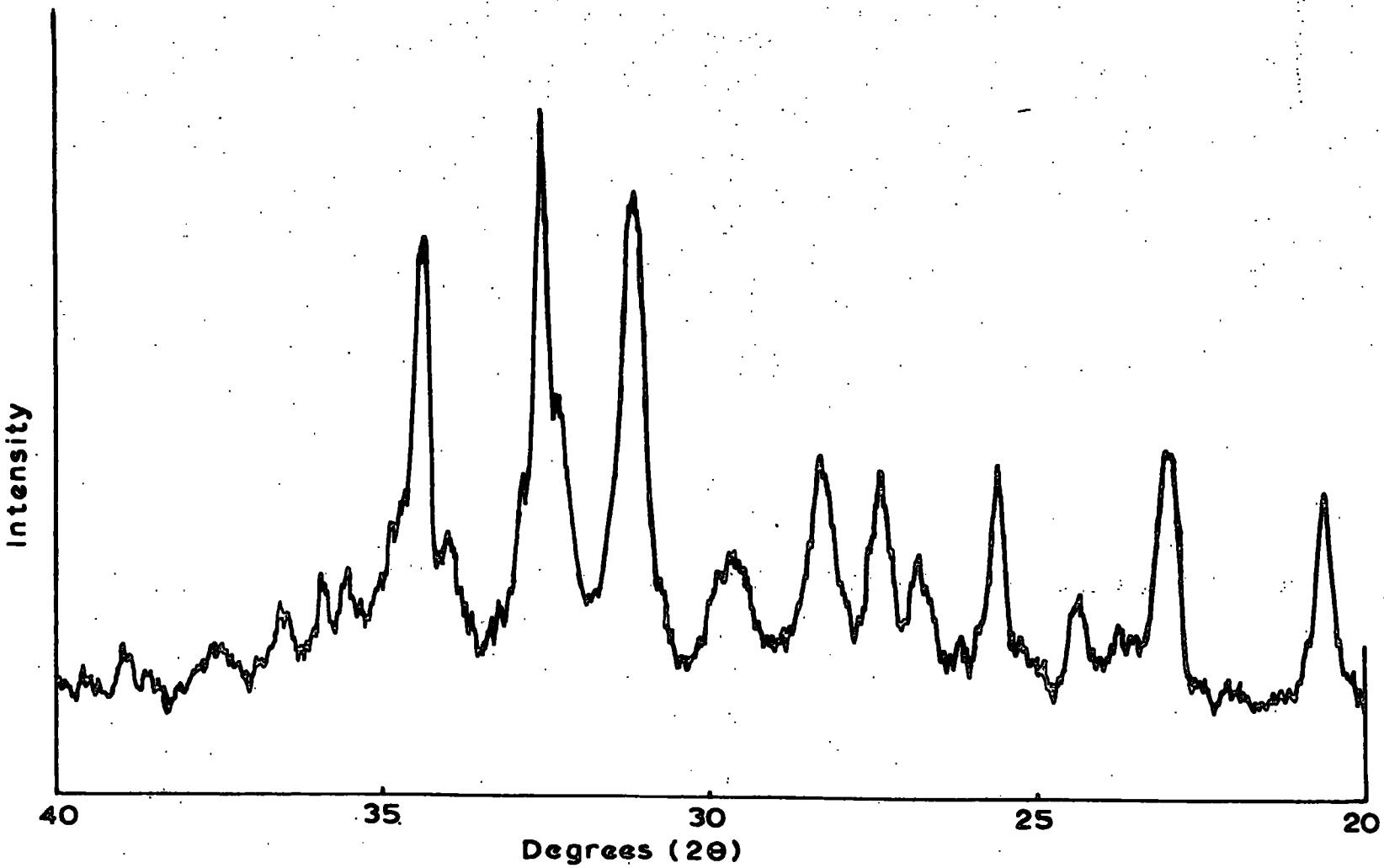

## 1.10 DIFFERENTIAL THERMAL ANALYSIS

Differential Thermal Analysis was carried out on selected samples for several reasons:

(a) to confirm the identification made by x-ray diffraction methods of the clay minerals present.

(b) to determine, if possible, the phase changes occurring during the application of thermogravimetric analysis, thus enabling identification of interferences.

(c) to detect and identify any minor phases which may be present in concentrations below the limits of detection of x-ray diffraction methods, where these phases possess properties which render them detectable by DTA methods, i.e. phases which undergo either endothermic or exothermic changes, or both, on heating.

(d) to determine, of those minerals which had been previously identified, any peculiar properties which may subsequently allow for more comprehensive interpretations concerning the environment of mineralisation.

The apparatus used for the investigation was a Stanton Instruments "Standata" 5 - 50 Differential Thermal Analysis apparatus incorporating interchangeable furnaces and sample holders, a West controller with photoelectric cell arrangement to give the reference sample temperature, and a mechanically driven cam with attached pointer indicating the furnace temperature. The furnace is fitted with cooling coils which serve the dual purpose of promoting rapid cooling and maintaining a regular temperature increase. A platinum - rhodium thermocouple is employed to measure the differential temperature between the sample and the reference material (aluminium oxide). The signal produced is amplified and fed to a chart recorder where the reference absolute temperature

and differential temperature are continuously displayed during a heating run. The amplification of the signal can be varied depending on the sensitivity desired.

In the present investigation a single wound, platinum-rhodium furnace was used, being capable of accomodating temperatures of up to 1,500°C. The sample and reference material holders consisted of small 6.5 mm. diameter and 8 mm. length platinium cylinders, open at the top, and with hollow, platinum-enclosed projections from the bottom in which were inserted the thermocouple terminals. Care was taken to ensure that the volume of sample and reference material and the degree of packing of each were as similar as possible for each run and for each series of runs. By running several portions of the same sample, it was found that most satisfactory results were obtained with a chart speed of 6 in./hr. and a sensitivity of 50, that is full scale deflection of the chart representing 50 mv.. The most satisfactory zero setting, so as to permit both exothermic and endothermic changes to remain on the chart was determined as 40 scale divisions, the base-line trimmer being set at 1. When $\Delta T$ changes fell outside the range of the chart, the sensitivity setting was increased to 100 until the particular change was completed and then returned to a value of 50.

The temperature of the furnace was raised at a constant rate of approximately 13°C/min. and could be read directly from the West Controller. The temperature of the reference material was obtained from the recording chart, on which a temperature-injection mechanism, activated every 10 mins., indicated an MV. reading which was then compared with a

calibration graph of mV. vs. T. to give the actual temperature of the reference material. This temperature - injection mechanism could be activated manually whever so desired, to allow accurate measurement of endotherm or exotherm peak temperatures, or suppressed so as not to obscure a particular change.

An example of a chart recorded during a run is shown in fig. 18.

All samples of wallrock were analysed by this technique but only selected samples of host rock, as these are fairly similar in mineralogical composition.

A considerable amount of difficulty was encountered in attempting to identify the causes of the various peaks despite the fact that several standards were run. The standards consisted of mixtures of relatively pure components of the unknown samples, so as to approximate the compositions of the unknowns. In this way some of the reactions could be identified.

The temperatures of occurrence of the various reactions were carefully noted. It was found that particular reactions took place within a range of values of T, and the areas of the exo - and endothermic peaks varied considerably. A peak of particular interest is that of the quartz inversion temperature (true value - 573°C), for this varied from approx. 560°C to 580°C with a large variation in the peak area. However, as has been discussed by MacKenzie and Mitchell (1962) these are dependent on the degree of packing, amount of material in the sample and rate of heating. Insufficient time was available to isolate these causes of variation and discover whether a variation in inversion temperature really exists.

During the runs, at temperatures in excess of approx. 900°C base line drift became uncontrollable towards the endothermic side of the chart. This was due to sintering of the sample which during the process fused, and detached from the walls of the sample holder. Thus it was not possible to obtain information above 1000°C, a region of interest in the identification of clay minerals. Base line displacement has also been attributed to poor matching of the packing of the sample and the reference material (Garn, 1965).

Steps taken to improve the quality of the trace and the sensitivity of the method included the removal of calcium carbonate by treatment with acetic acid, and treatment with hydrogen peroxide to remove carbon. After drying, these samples were run under the same conditions as previously. It was found that little advantage was gained by this pretreatment. Carbon oxidation and calcium carbonate dissociation appeared to interfere little with overlapping peaks and thus remaining samples were run without prior treatment.

Replicate analyses of several powders were made, the results corresponding within acceptable limits.

The essential features of the traces produced are summarised in table 10. Shown are the sample number, the thermal nature of the peak, the temperature at which each peak occurs, the relative peak width, the relative peak height, and the significance attached to a particular peak. In the table the series of changes attributed to pyrite are those proposed by Garn (op.cit.)

Although some characteristic heat effects were detected in the clay minerals, most were overprinted by larger peaks from other sources, such as the oxidation of C and the series of changes related to pyrite.

Thus the D.T.A. work served only to confirm a part of the results obtained by X.R.D. and gave no additional information.

TABLE 10. RESULTS OF DIFFERENTIAL THERMAL ANALYSIS.

| SAMPLE NO. | Δ T PEAK TEMP °C | | CHARACTERISTICS OF PEAK | | INTERPRETATION |
|---|---|---|---|---|---|
| | EXOTHERM | ENDOTHERM | PEAK HALF WIDTH | PEAK HEIGHT | |
| X4 | | 100° | 1 | 20 | Oxidation of iron from pyrite. |
| | 390° | | 2 | 12 | Decomposition of pyrite to oxysulphide and sulphur. |
| | 460° | | 1 | 5 | " " " " " |
| | 570° | | 5 | 8 | Quartz inversion |
| | | 820° | 2 | 15 | Dissociation of calcite. |
| | | 810° | 1 | 3 | Transformation of iron oxide to haematite. |
| | 920° | | 4 | 6 | Dehydroxilation of kaolinite. |
| X49 | | 100° | 3 | 10 | Oxidation of iron in pyrite. |
| | 450° | | 1 | 6 | Decomposition of pyrite to oxysulphide and sulphur. |
| | 530° | | 2 | 30 | Quartz inversion. |
| | 620° | | 5 | 40+ | FeO oxidation from carbonate decomposition. |
| | 850° | | 15 | 7 | Transformation of iron oxide to haematite. |
| X50 | | 80° | 3 | 6 | Oxidation of iron in pyrite. |
| | 570° | | 19 | 55 | Quartz inversion |
| | 830° | | 5 | 6 | Transformation of iron oxide to haematite. |
| X51 | 570° | | 20 | 60+ | Quartz inversion. |
| | | 1000° | 5 | 60 | Decomposition of calcite from dolomite decomposition. |

(Table continued)

| SAMPLE NO. | ΔT TEMP. °C | | CHARACTERISTICS OF PEAK | | INTERPRETATION |
|---|---|---|---|---|---|
| | EXOTHERM | ENDOTHERM | PEAK HALF WIDTH | PEAK HEIGHT | |
| X52 | 320° | | 18 | 7 | Decomposition of pyrite to oxysulphide and sulphur. |
| | 510° | | 1 | 2 | " " " " " |
| | 570° | | 9 | 60+ | Quartz inversion. |
| X53 | | 100° | 1 | 36 | Oxidation of iron in pyrite. |
| | 460° | | 2 | 1 | Pyrite oxidation to oxysulphide and sulphur. |
| | 620° | | 12 | 60+ | Overlap of quartz inversion and oxidation of FeO in siderite. |
| | | 810° | 5 | 7 | Decomposition of dolomite structure. |
| | | 950° | 4 | 4 | Decomposition of residual $CaCO_3$ from dolomite decomposition. |
| X54 | | 80° | 3 | 5 | Oxidation of iron in pyrite. |
| | 480° | | ½ | 11 | Decomposition of pyrite to oxysulphide and sulphur. |
| | 560° | | 2 | 54 | Quartz inversion. |
| | 630° | | 3 | 4 | Possibly FeO oxidation from siderite decomposition. |
| | 780° | | 3 | 3 | Transformation of iron oxide to haematite. |
| X55 | | 130° | 2 | 42 | Oxidation of iron in pyrite. |
| | 520° | | 1 | 45 | Decomposition of pyrite to oxysulphide and sulphur. |
| | | 570° | 2 | 5 | Evolution of $CO_2$ from siderite. |

(Table continued)

| SAMPLE NO. | AT TEMP. °C | | CHARACTERISTICS OF PEAK | | INTERPRETATION |
|---|---|---|---|---|---|
| | EXOTHERM | ENDOTHERM | PEAK HALF WIDTH | PEAK HEIGHT | |
| | 620° | | 4 | 36 | Oxidation of FeO from siderate decomposition. |
| | | 640° | 3 | 4 | Decomposition of iron oxysulphide (from pyrite) to oxide. |
| X56 | 540° | | 3 | 60+ | Quartz inversion. |
| | 620° | | 5 | 6 | Oxidation of FeO from carb. decomposition. |
| X57 | 580°+ | | 60+ | 60+ | Quartz inversion overprints other peaks. |

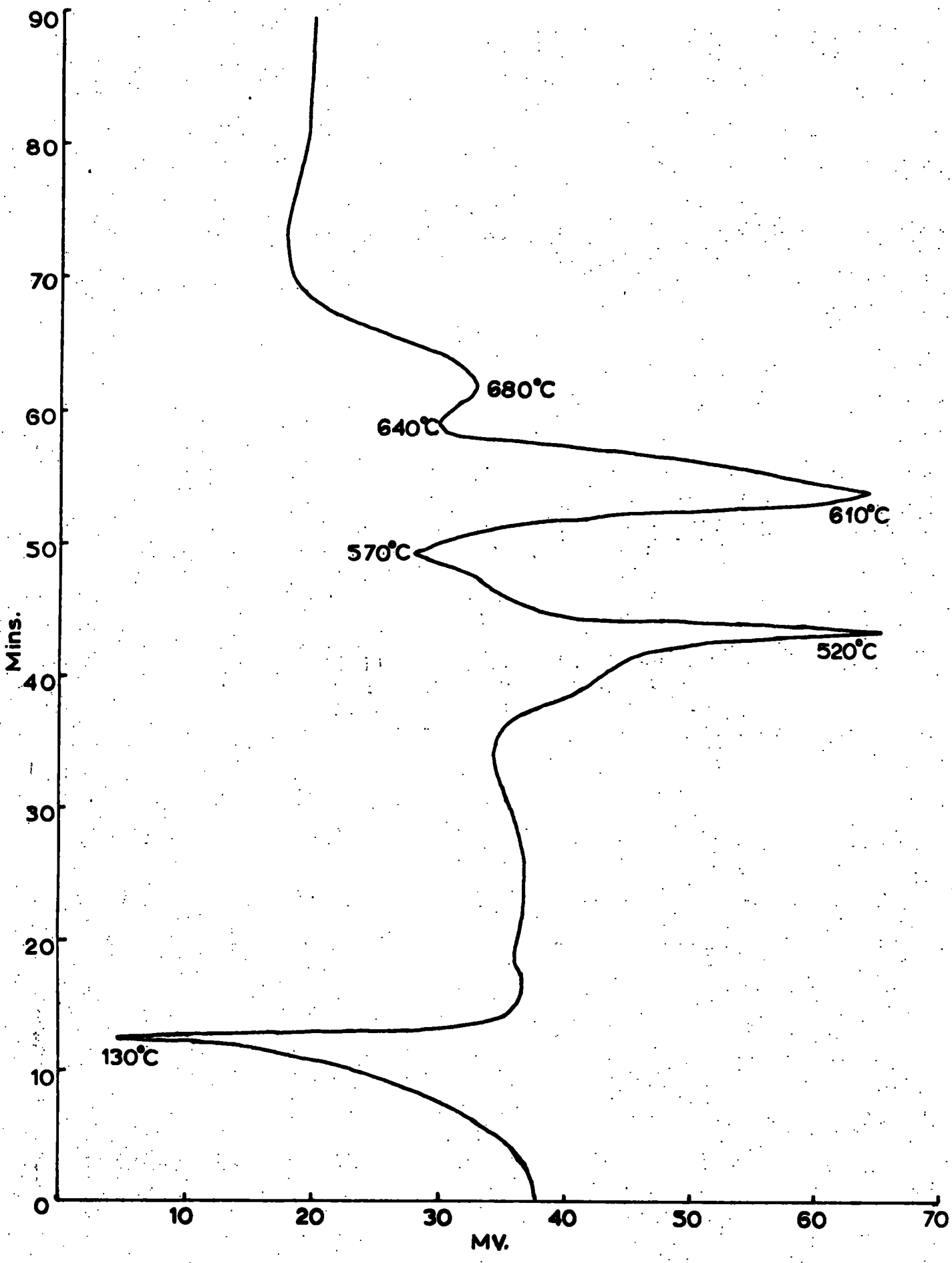


FIG.18. D.T.A. RECORD OF SAMPLE X55.

## 1.11 FLUID INCLUSIONS

In an effort to define further parameters controlling the physico-chemical environment of deposition, detailed studies were undertaken of the fluid inclusions distributed in a representative suite of cleavage flakes taken from the main body of the mineralisation at irregular intervals throughout the length of the section. Of necessity this was limited to an examination of the fluorite, as the other minerals on which it was hoped to conduct a similar investigation, sphalerite, quartz and carbonates were not, in general, amenable to such a study. These were found to be either remarkably uniform and free from inclusions, or to contain inclusions of sizes below the limit of resolution of the microscope used.

Of prime importance in the study of fluid inclusions is the necessity to be able to distinguish between primary, pseudo-secondary and secondary inclusions, each being defined as follows:-

(a) Primary inclusions - those which have become trapped during the growth of a crystal and thus bear a relation to the fluid immediately depositing the surrounding host minerals.

(b) Secondary inclusions - those inclusions which have been formed after the crystallisation of the host mineral is complete and probably result from fracturing of the host mineral followed by the ingress of a later solution causing recrystallisation of the host around the fracture.

(c) Pseudosecondary - the term applied when fracturing and ingress of solutions takes place before crystallisation is complete and thus bridges the gap between primary and secondary inclusions.

These give information on the solutions depositing minerals in the same environment but not on those which deposited the immediate enclosing mineral.

Hall and Friedman (1963) suggest that cleavages filled by pseudosecondary inclusions may be evidence of stress operating within the crystal due to a post-crystallisation rise in temperature. These authors also found in many analyses that stages of sulphide deposition, particularly sphalerite and galena, are characterised by high Ca/Na ratios in the depositing fluid.

The accuracy of the information to be gained from a study of inclusions depends to a large extent on the ability to distinguish between the three types. In many cases this is not possible by direct observation, and the status of an inclusion may have to be inferred from the results obtained from homogenisation temperature measurements.

For the measurement of these temperatures, a relatively simple arrangement involving a heating stage coupled with a Leitz microscope fitted with a UM 20/0.33 objective and a X10 ocular was used. A chromel - alumel thermocouple was connected via a cold junction to a Philips chart recorder and the thermocouple calibrated by observing the chart deflection produced at the known melting point of several organic compounds sealed into thin capilliary tubes. A calibration curve could then be prepared by plotting chart deflection against temperature. A heating rate of approximately $10^{o}$/min. was used until the inclusions began to homogenise, when the rate was decreased.

A large number of specimens were examined but of these only 33 were found to be amenable to measurement. Those specimens rejected were found to be unsuitable for one or more of the following reasons:

(a) The inclusions were so small that accurate measurements would be impossible.

(b) The inclusions were obviously all of secondary origin and therefore of limited significance.

(c) No inclusions were found.

(d) The inclusions leaked on heating.

The fragment to be studied was placed on the heating stage and focused through the microscope. A portion was chosen in which several relatively large inclusions occurred within the field of view or at least which could be easily and quickly focused by racking up or down on the microscope when it was desired to study inclusions on different planes during the same heating run.

In addition to the temperature at which homogenisation took place, the following features were noted:

(a) The relative abundance of inclusions in a given specimen.

(b) The distribution of inclusions through the specimen.

(c) The absolute and relative sizes of the inclusions and the spatial variation in size distribution.

(d) The bubble: inclusion size ratio and its variation.

(e) Inclusion shapes and variations within specimens and between specimens.

A total of 200 inclusions (190 fluorite, 10 quartz) were measured from the 33 specimens (only one of which was quartz) taken

from various locations throughout the length of the section.

The frequency of occurrence of particular filling temperatures of inclusions was plotted against temperature (fig. 19 ). The temperature distributions are seen to be irregular, but distinct peaks occur at temperatures of approximately 140°C, 128°C, 116°C and 101°C. That at 128°C is predominantly due to the quartz and thus this is considered to be the depositional temperature (uncorrected for pressure) of the particular generation of quartz. 140°C is taken to be the maximum depositional temperature (uncorrected for pressure) of the fluorite. The remaining peak temperatures may be interpreted as either being due to later lower-temperature stages of deposition, or the inclusions measured were actually pseudo-secondary or secondary inclusions.

Four inclusions having temperatures far in excess of 140°C were measured - 157°, 162°, 169° and 176° . These are considered to be spurious temperatures, most likely the result of leakage after deposition, or during heating. These readings are omitted from the frequency distribution curve.

No daughter minerals, nor oil bubbles were observed in the two-phase inclusions studied.

Inclusions were found to vary widely in size both within a particular specimen, and among other specimens. However, those inclusions localised along a particular plane were generally of uniform size.

The bubble: inclusion size ratio appeared to be fairly uniform, suggesting that the depositing fluid was itself internally

homogeneous. In cases in which bubbles seemed to be unusually large in relation to the remainder of the inclusion, this could usually be attributed to the larger size of the inclusion in the third dimension.

The shapes of the inclusions varied widely, particularly in the larger sizes. Some of the smaller inclusions distributed among the larger sizes appear to be the product of necking down of the larger inclusion. This may account for some of the erratic temperatures noted.

Schmidt (1962) found systematic decreases in temperature measurements from the centre of crystals to the margins in certain generations but distinct individual crystals could not be so investigated in the present study.

Many possible sources of error in the filling temperature measurements are present, such as the difficulty in observing the exact instant at which the bubble disappears and the obscuring of the bubble by the cavity walls before disappearance. Leakage from inclusions along fractures can take place, giving higher filling temperatures. Each inclusion was checked after a run, however, to ensure that the bubble reappeared on cooling.

The use of liquid inclusions as a geothermometer is based on a series of assumptions, each of which is a source of error if it can be shown to be invalid. These assumptions are as follows (Bailey and Cameron, 1951).

(1) The fluid completely filled its cavity at the time of crystallisation of the enclosing mineral.

(2) Primary fluid inclusions can be distinguished from secondary inclusions.

(3) The included fluid is a dilute aqueous solution containing no carbon dioxide or other gas in great amounts.

(4) The pressure on the liquid at the time of inclusion was small, or its magnitude can be estimated.

(5) There has been no significant change in volume of the cavity due to the effects of pressure, solution or precipitation.

(6) There has been no addition of liquid to the cavity or loss of liquid from the cavity.

(7) Representative samples are used for temperature determinations.

The compressibility and solubility of fluorite is so low as to make volume changes during heating of negligible importance.

Repetition of several measurements showed that they could be reproduced to within about $2^{o}C$ of the original determination.

In order to obtain the actual temperature of formation from the filling temperature, an adjustment for the difference between the vapour pressure of the solution and the total pressure must be made. The pressure correction also depends on the salinity of the hydrothermal fluid. It is considered that in the present case the pressure on the fluids was predominantly hydrostatic as is indicated by the apparent ability of the fluids to move freely through the conduits. As the average density decreases with increasing temperature and increases with content of dissolved salts, a value of 1 gm./c.c. is taken as a reasonable figure, giving a hydrostatic pressure of approx. 120 atm. at the depth envisaged. As the actual deviation

from true hydrostatic pressure towards lithostatic pressure (360 atm.) is unknown, the value has been set at 200 atm.

For a 20 equiv. wt. % NaCl solution, a maximum pressure correction of the filling temperatures is 20°C (Sawkins, 1966). As it is doubtful as to the magnitude of the difference between the vapour pressure of the solutions and the total pressure, half the maximum value plus 2°C for instrumental uncertainty has been used and an uncertainty of this amount placed on all derived temperatures. The true temperature of deposition of the primary inclusions is thus given as 151°C±11°C. The pressure is greater than the vapour pressure of saturated NaCl solutions at this temperature (Holland, 1967) and it is therefore unlikely that the solutions will boil in this environment. The distribution of the inclusions and regularity of the bubble volume: inclusion volume ratios in the fluorite support this conclusion. Changes in the salinity of the fluid may take place (Roedder et al, 1968) but even fairly large fluctuations would not affect the discussion. Boiling will take place when the confining pressure on the solutions is less than the vapour pressure of the solution.

Apparent temperature fluctuations could reflect changes in the difference between total pressure and the vapour pressure of the solutions, the effects of erratic dilution with ground water or true temperature fluctuations with time due to effects at the source, as suggested by Roedder (1960). Freas (1961) has suggested that temperature fluctuations observed may be due to exothermic reactions on deposition of fluorite during replacement of limestone. The inclusions measured, however, are taken from open-space filling fluorite, and thus the argument is not valid in this case.

The fluorite from which the inclusions were measured was deposited late in the paragenetic sequence and thus, if it can be assumed that the temperature during mineralisation was falling (Miller, 1969), this places a lower limit on the temperature of deposition of earlier minerals.

TABLE 11. FLUID INCLUSION HOMOGENISATION TEMPERATURES

(uncorrected for pressure)

| Inclusion No. | Temperature °C | Inclusion No. | Temp. °C |
|---|---|---|---|
| 1.1 | 106 | 6.3 | 103 |
| 1.2 | 120 | 7.1 | 106 |
| 1.3 | 142 | 7.2 | 101 |
| 1.4 | 137 | 7.3 | 106 |
| 1.5 | 101 | 7.4 | 108 |
| 1.6 | 118 | 7.5 | 108 |
| 2.1 | 162 | 7.6 | 135 |
| 2.2 | 176 | 7.7 | 130 |
| 2.3 | 137 | 7.8 | 132 |
| 2.4 | 120 | 7.9 | 130 |
| 3.1 | 91 | 8.1 | 118 |
| 4.1 | 120 | 8.2 | 118 |
| 4.2 | 145 | 8.3 | 120 |
| 5.1 | 130 | 8.4 | 120 |
| 5.2 | 125 | 8.5 | 120 |
| 5.3 | 126 | 9.1 | 137 |
| 5.4 | 128 | 9.2 | 142 |
| 5.5 | 125 | 9.3 | 142 |
| 5.6 | 130 | 9.4 | 140 |
| 5.7 | 130 | 9.5 | 145 |
| 5.8 | 111 | 9.6 | 140 |
| 5.9 | 135 | 10.1 | 106 |
| 5.10 | 128 | 10.2 | 103 |
| 6.1 | 101 | 10.3 | 140 |
| 6.2 | 103 | 10.4 | 108 |

| Inclusion No. | Temperature °C | Inclusion No. | Temp. °C |
|---|---|---|---|
| 10.5 | 106 | 15.4 | 140 |
| 11.1 | 128 | 15.5 | 140 |
| 11.2 | 128 | 16.1 | 140 |
| 11.3 | 125 | 16.2 | 99 |
| 11.4 | 128 | 16.3 | 106 |
| 11.5 | 123 | 16.4 | 101 |
| 11.6 | 99 | 16.5 | 101 |
| 11.7 | 99 | 16.6 | 103 |
| 11.8 | 118 | 16.7 | 103 |
| 11.9 | 123 | 17.1 | 101 |
| 12.1 | 118 | 17.2 | 118 |
| 12.2 | 120 | 17.3 | 120 |
| 12.3 | 118 | 17.4 | 103 |
| 13.1 | 157 | 17.5 | 99 |
| 13.2 | 142 | 17.6 | 101 |
| 13.3 | 140 | 17.7 | 96 |
| 13.4 | 142 | 18.1 | 118 |
| 14.1 | 142 | 18.2 | 116 |
| 14.2 | 140 | 18.3 | 116 |
| 14.3 | 140 | 18.4 | 120 |
| 14.4 | 140 | 18.5 | 118 |
| 14.5 | 142 | 19.1 | 101 |
| 14.6 | 137 | 19.2 | 96 |
| 15.1 | 145 | 19.3 | 96 |
| 15.2 | 140 | 19.4 | 103 |
| 15.3 | 140 | 19.5 | 99 |

| Inclusion No. | Temp. °C | Inclusion No. | Temp. °C |
|---|---|---|---|
| 19.6 | 99 | 23.1 | 116 |
| 19.7 | 101 | 23.2 | 116 |
| 19.8 | 101 | 23.3 | 120 |
| 19.9 | 111 | 23.4 | 118 |
| 19.10 | 103 | 23.4 | 120 |
| 20.1 | 120 | 23.5 | 125 |
| 20.2 | 116 | 23.6 | 118 |
| 20.3 | 116 | 24.1 | 103 |
| 20.4 | 116 | 24.2 | 99 |
| 20.5 | 118 | 24.3 | 101 |
| 20.6 | 120 | 24.4 | 99 |
| 20.7 | 169 | 24.5 | 101 |
| 20.8 | 118 | 25.1 | 125 |
| 21.1 | 135 | 25.2 | 125 |
| 21.2 | 135 | 25.3 | 128 |
| 21.3 | 130 | 25.4 | 125 |
| 21.4 | 132 | 25.5 | 130 |
| 21.5 | 132 | 25.6 | 123 |
| 21.6 | 135 | 25.7 | 128 |
| 21.7 | 135 | 25.8 | 128 |
| 21.8 | 130 | 25.9 | 125 |
| 21.9 | 132 | 25.10 | 128 |
| 22.1 | 135 | 26.1 | 128 |
| 22.2 | 132 | 26.2 | 125 |
| 22.3 | 142 | 26.3 | 125 |
| 22.4 | 137 | 26.4 | 130 |
| 22.5 | 137 | 26.5 | 128 |

| Inclusion No. | Temp. °C | Inclusion No. | Temp. °C |
|---|---|---|---|
| 26.6 | 128 | 31.4 | 103 |
| 27.1 | 99 | 31.5 | 101 |
| 27.2 | 99 | 31.6 | 116 |
| 27.3 | 101 | 31.7 | 103 |
| 27.4 | 101 | 31.8 | 101 |
| 27.5 | 128 | 32.1 | 103 |
| 28.1 | 101 | 32.2 | 103 |
| 28.2 | 125 | 32.3 | 103 |
| 28.3 | 125 | 32.4 | 108 |
| 28.4 | 118 | 32.5 | 101 |
| 29.1 | 113 | 32.6 | 103 |
| 29.2 | 116 | 33.1 | 113 |
| 29.3 | 113 | 33.2 | 116 |
| 29.4 | 116 | 33.3 | 101 |
| 29.5 | 113 | 33.4 | 116 |
| 29.6 | 116 | 33.5 | 120 |
| 30.1 | 101 | 33.6 | 116 |
| 30.2 | 103 | 33.7 | 113 |
| 30.3 | 116 | 33.8 | 108 |
| 30.4 | 113 | | |
| 30.5 | 116 | | |
| 30.6 | 113 | | |
| 31.1 | 113 | | |
| 31.2 | 103 | | |
| 31.3 | 103 | | |

FIG. 19. FLUID INCLUSION HOMOGENISATION TEMPERATURES.
FREQUENCY DISTRIBUTION CURVE.

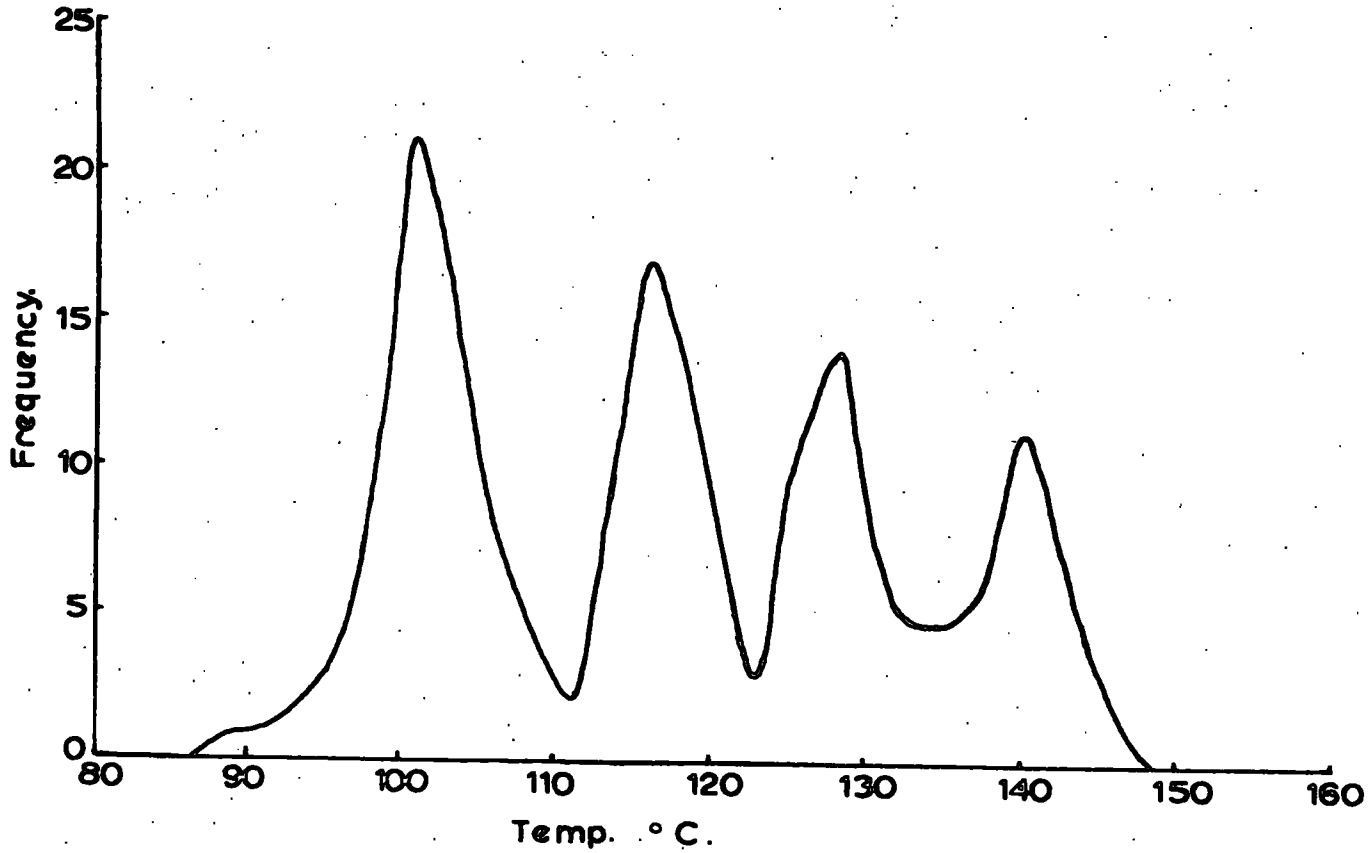

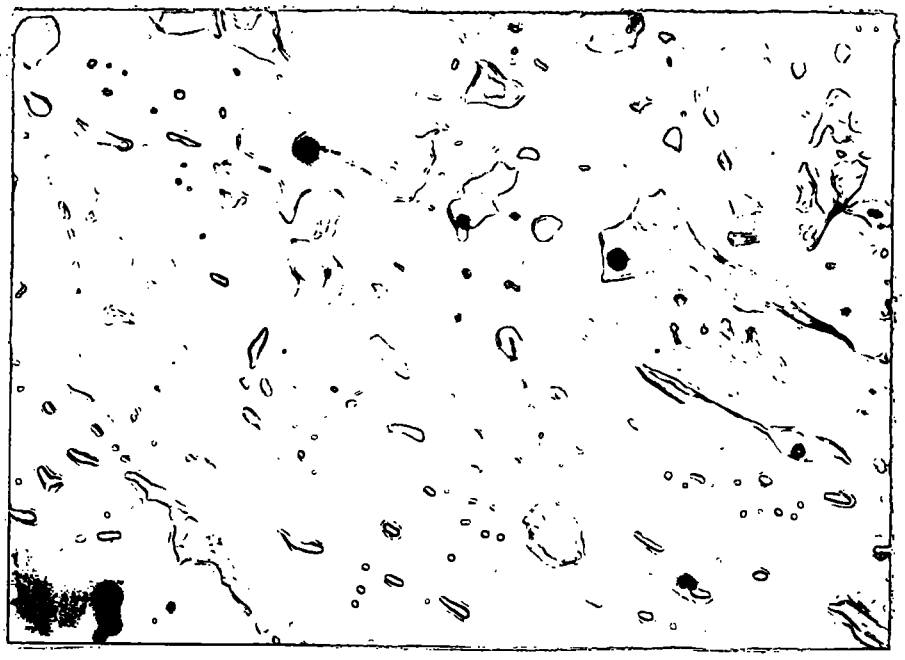

Fig. 20. Fluid inclusions in fluorite, showing variation in size and shape. Several inclusions appear to be in the process of "necking down".
Transmitted light. X 300.

Fig. 21. Fluid inclusions in fluorite, showing large possible primary inclusions with small, even-sized pseudosecondary inclusions on a different cleavage plane.
Transmitted light. X 500.

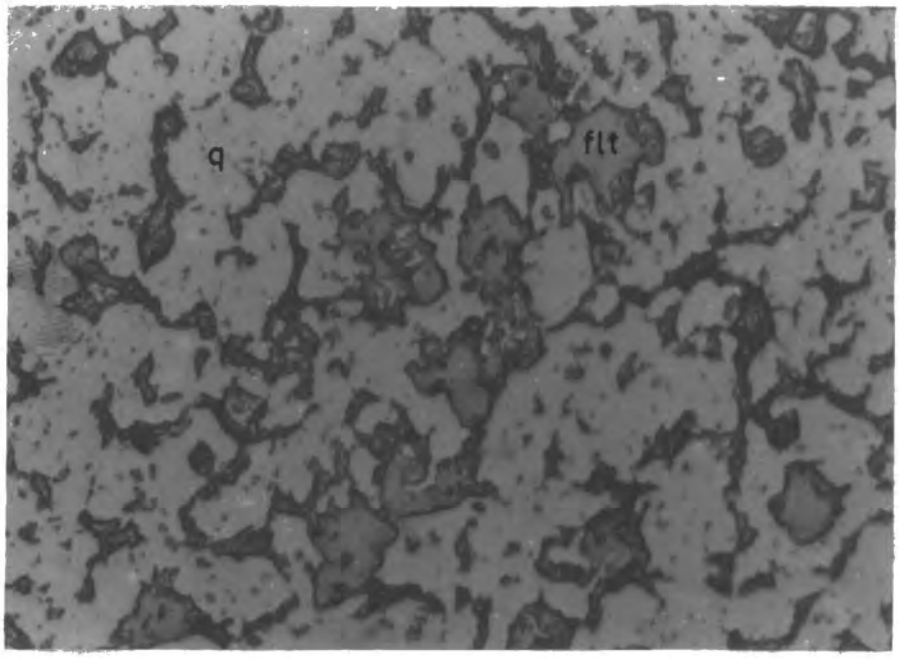


Fig. 22. Wallrock quartz (q) and fluorite (flt) surrounded by carbon. Unlike the quartz, fluorite is normally free from inclusions in this situation.
Reflected light. X 400.

## 1.12 POWDER PHOTOGRAPHY

Powder photographic techniques were used in the measurement of the cell edges of sphalerite, and to confirm the identification of some minerals.

Portions of banded sphalerite were removed from several sections of the original specimen and crushed as coarsely as possible with a mortar and pestle. The crushed material was then examined under a binolcular microscope and separated into three groups - light, medium and dark coloured. Each of these three groups from each specimen was then separately crushed to a fine powder, mounted on a silica spindle with a binder of collodion, and loaded into a 11.46 cm. Debye-Scherrer camera. Several test runs were carried out on the initial mounts in order to determine the optimum collimation and exposure times necessary to produce maximum intensity with good line resolution. The conditions subsequently selected are shown in table 12.

After developing and fixing, line spacings were measured to 0.05 mm. on an illuminated vernier scale and the relative intensities of the lines estimated, defining the most dense line as having an intensity of 100.

Cell edges of the sphalerite were calculated by computer, utilising two successive programmes. Data presented to the computer for calculation using the first programme (DPOW) included:

(a) For each corresponding pair of lines a number 1, 2, or 3 depending on whether the lines were part of a doublet (e.g. $K_{\alpha_1}$ and $K_{\alpha_2}$) in which case the numbers 1 and 2 were assigned to $K_{\alpha_1}$ and $K_{\alpha_2}$ respectively. If one single reflection only occurred, the number 3 was assigned to the line.

(b) The "left" and "right" measurements of the distances of corresponding pairs of lines from an arbitary zero point, determined by the vernier rule. Front reflection and back reflection lines were paired separately.

(c) A figure representing the relative intensity of each pair of lines, determined as described previously.

The print - out from the computer included:

(a) The sum of each pair of "left" and "right" measurements, from an inspection of which any errors in measurement could be determined.

(b) The computed 2θ angle corresponding to each particular reflection.

(c) The square of the sine of the angle.

(d) The crystal d - spacing in angstroms corresponding to the 2θ angle calculated.

(e) A figure representing the sum of the squares of the hkl intercepts for each reflection, from which possible hkl combinations can be deduced.

(f) A preliminary value for the length of the cell edge in angstroms using each pair of lines in turn in the calculations.

In order to determine an accurate value for the cell edge, a second programme (NELRIL) was required. The 2θ value and the corresponding cell edge for each pair of lines reflecting above $80^{o}$ (2θ) were presented to the computer as data. The function of this latter programme was, by using a plot of the apparent values of A against $\frac{1}{2}$ ($\cos^2\theta$ / sin θ + $\cos^2\theta$ / θ), (the Nelson - Riley Extrapolation Function), and extrapolating linearly to zero value of this function, to obtain an accurate value for the true cell edge A.

The values obtained by means of the above procedure are shown in table 13.

It has been amply demonstrated that a precise determination of the cell edge of sphalerite provides a sensitive measure of composition (Skinner, 1961). The cell edges of both Mn- and Cd- bearing sphalerites change linearly with composition. Kullerud (1953) first suggested and demonstrated that the effects of Fe, Mn, and Cd on the cell edge of sphalerite were additive.

Barton and Skinner (1967) have shown that the cell edges of most natural sphalerites may be expressed by the function $a = 5.4093 + 0.000456U + 0.00424V + 0.00202W - 0.000700X + 0.002592Y - 0.003Z$, where "a" is the cell edge in Å and U, V, W, X, Y and Z are respectively the FeS, CdS, MnS, CoS, ZnSe and ZnO contents in mole percent. Each of these constituents has been shown to have measureable effects on the sphalerite lattice. It was intended, by means of the above

procedure, to measure the cell edge of certain zones, determine the Fe and Mn content of the crystal by electron microprobe analysis, and to determine the possible general level of concentration of additional impurities immeasurable by means of the electron microprobe, by substitution in the above formula.

It is seen that CoS and ZnO have negative effects on the cell edge. Neither of these phases is expected to be present, however, and thus only those having positive effects are considered.

Although the cell size was found to increase with intensity of colour of the sphalerite and thus with Fe content, the samples selected obviously did not cover the whole range of concentration as, even if other elements are not present, the largest cell edge determined corresponds to only 6.3 mole % FeS, below the maximum determined from electron microprobe analysis. It is difficult then, particularly as small fluctuations in Fe content have a large effect on the cell edge, and other elements are expected to be present in such small amounts, to relate the results to concentrations of these other elements. It is also possible, but unlikely, that those elements producing negative effects on the cell edge are present.

It was also hoped by this method to detect and identify wurtzite if present, as its identification by other means is extremely difficult. Its presence, however, was not demonstrated.

TABLE 12

## OPERATING CONDITIONS FOR POWDER PHOTOGRAPHY

| | |
|---|---|
| Camera: | Debye-Scherrer |
| Diameter: | 11.460 cm. |
| Radiation: | $CoK_{\alpha}$ |
| Filter: | Fe |
| Film: | Ilford 35 x 355 mm. |
| Collimator: | Fine (Coarse for mineral identification) |
| Exposure Time: | 6 hrs. (3 hrs." " " ) |
| M.A.: | 60 |
| K.V.: | 25 |

TABLE 13

RESULTS OF CELL EDGE DETERMINATIONS

| SAMPLE | CELL EDGE (Å) |
|---|---|
| Light | 5.4097 ± 0.0003 |
| Med. | 5.4110 ± 0.0005 |
| Med. - Dark | 5.4117 ± 0.0007 |
| Dark | 5.4122 ± 0.0010 |

## 1.13 STAINING TECHNIQUES

To elucidate the textural relationships among the various carbonates in the total section, and to enable more precise differentiation of the carbonate minerals from quartz and the remainder of the rock, staining techniques were employed.

The procedure followed was that outlined by Warne (1962). The method involved first treating the specimen with dilute HCl to provide a rough surface which is then lightly washed with water and allowed to dry. A dilute, slightly acidified solution of Alizarin Red S is spread on the surface, permitted to react for a period of 5 mins., and then lightly removed by washing. As a result of this step calcite is plainly differentiated from quartz by its red stain. Other effects are that ankerite and strontianite are stained purple, and siderite and dolomite remain unaffected. Further differentiation and identification was obtained by inverting each slab of sample in a boiling mixture of 50/50 Alizarin Red S and 30% sodium hydroxide solution for a period of 5 mins.. The result of this step is that siderite is stained dark brown, ankerite deep purple, strontianite and calcite are not affected, and high-Mg calcite and dolomite are stained purple. Additional tests were carried out but no other carbonates were identified. The procedure followed and the results produced are shown diagramatically in Fig.23.

Such tests were applied to only one side of the V - shaped slab split from the borehole so as to allow for comparision of the treated portion with the original material.

A control on the tests described was afforded by removing portions of material producing a particular colour, and confirming the identification by x-ray diffraction techniques. The tests were also applied to independent specimens of the pure minerals considered likely to be present. It was found that several shades of colours produced were different from those described by Warne, but by applying the above control on the technique, these were easily applied to the correct mineral species.

Fresh solutions were made up each day as it was found that the stain produced did depend to a large extent on the freshness of the solution and the relative proportions of the various components of the solutions. Slight variations in the colour of the stain produced are also no doubt due to subtle variations in the compositions of the individual carbonate species, but due to the difficulty in controlling the other sources of variation to a sufficient degree, these could not be used as indicators of the detailed compositional variations in particular carbonates.

It was found that in the host rock, as expected, the carbonate present is almost exclusively calcite as had been shown by x-ray diffraction. The main forte of the method in this case lay in the determination of the textural relationships of the calcite with the associated material, and the ease with which it could be differentiated from quartz.

Those carbonates which were identified in the wallrock are calcite, siderite, dolomite and ankerite. A tentative identification of strontianite was not confirmed by x-ray diffraction techniques.

Following the second stage of treatment of the samples it was found that quartz and fluorite were sharply differentiated, a white stain being produced on quartz and a bright pink stain on fluorite. This latter effect was particularly useful in distinguishing between very small disseminated quartz and fluorite grains in the wallrock, in the vicinity of mineralisation.

After staining, all samples were scrutinised under a binocular microscope, the finer details being resolved more clearly by covering the surface with a thin film of water.

In order to distinguish between calcite and dolomite in the polished sections, the staining method recommended by Rodgers (1940) was used. This involves immersion of the surface of the specimen in a molar solution of $Cu(NO_3)_2$ for a period of 6 hours at room temperature, following which it is placed, without washing, in ammonia solution for several seconds, washed and dried. As a result of this treatment, the calcite is stained a deep blue. Dolomite is attacked slightly, but does not acquire a stain.

It was found that, as was suggested by the electron microprobe analyses, the carbonate present is predominantly dolomite (and ankerite) with rare grains of calcite.

FIG. 23. STAINING SCHEME FOR CARBONATES.

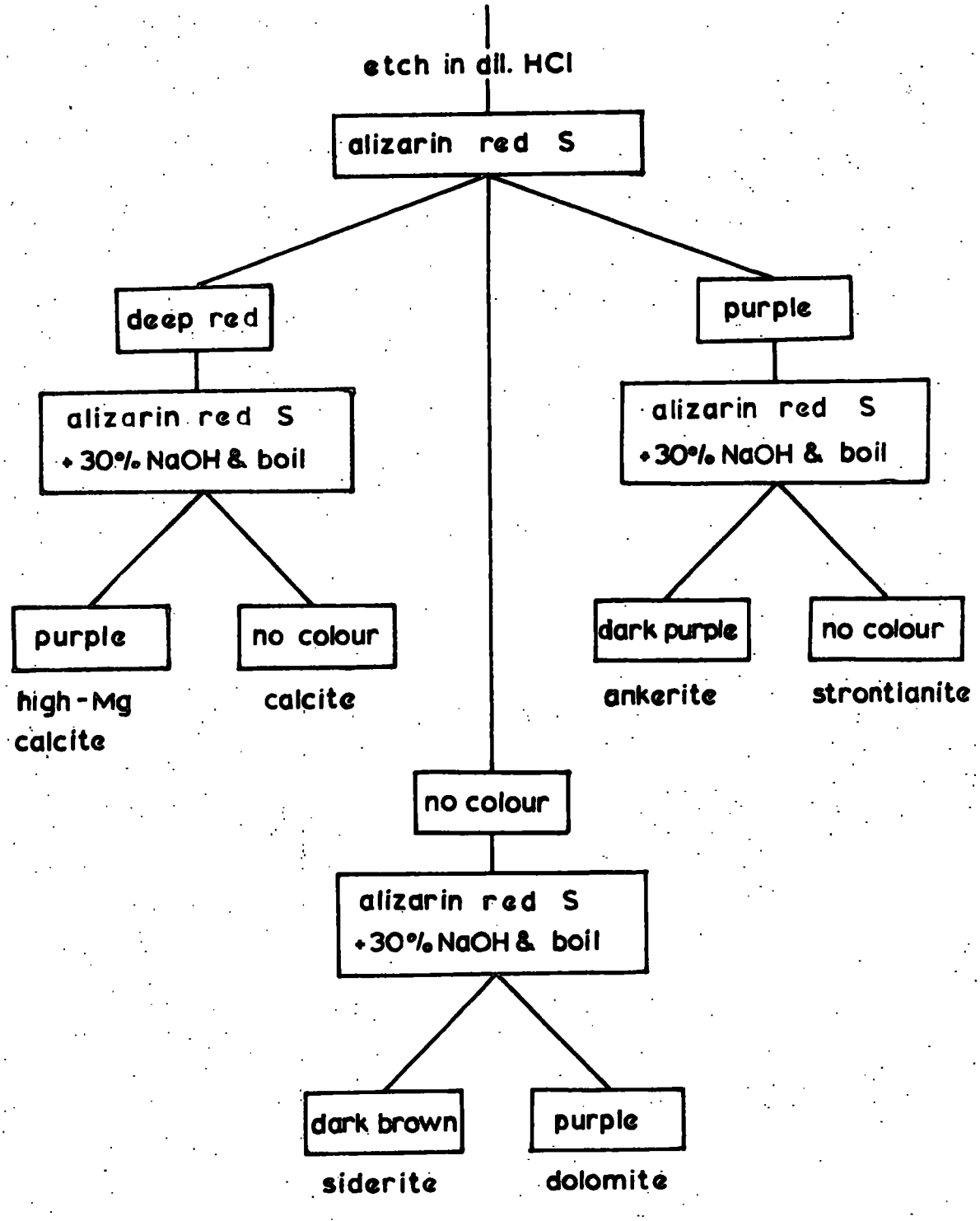

## 1.14 COMPUTING

All computing was carried out on the NUMAC IBM / 360/77 machine using both Fortran and PL/1 languages.

The programmes employed, their functions, and the languages used, are summarised below. Additional details such as data requirements and the form of the print - out appearing after computation are supplied in the relevant sections. TRATIO (1): Calculation of peak minus background / background ratios from raw count data for XRF trace element determinations.

Language: PL/1, Programmer: R.C.O. Gill, modified by J.L. Knight.

TRATIO (2): Calculation of absolute concentrations of trace elements after insertion of the calibration factor calculated from the results of TRATIO (1), substitution of interference factors and contamination corrections. In this programme, the limits of applicability of the results, defined by the plotted calibration curve and the calculated detection limits may be presented to the computer, and where these limits are exceeded, the value is omitted from the print-out.

Language: PL/1. Programmer: R.C.O. Gill.

COMPARE: Comparison of two sets of results obtained from two successive runs during the analysis of trace elements in order to identify and correct for machine instabilities or spurious pulses, and to determine the possible gravity of the effect of these on other determinations. Where one value differed from a corresponding value by more than the tolerance limit (five times the standard deviation) these values were indicated in the print-out.

If the tolerance limit was not exceeded, both values were added. A new set of cards containing the corrected counts were then punched.

Language: PL/1. Programmer: R.C.O. Gill.

TIMDATA: Correction of apparent elemental concentrations determined on the electron probe for atomic number effects, fluorescence and absorption factors to give true elemental concentrations. If so desired, elemental concentrations can be converted to oxides and their sum determined.

Language: Fortran. Programmer: A. Peckett (adapted from Sweatman and Long, 1969).

DPOW: Calculation of 2θ, N and A (as described in section 1.12) from vernier measurements and intensity data taken from powder photographs.

Language: PL/1. Programmer: A. Hall.

NELRIL: Application of the Nelson - Riley Extrapolation Function in the calculation of an accurate value for the cell edge of sphalerite from information returned from the previous programme.

Language PL/1. Programmer: A. Hall.

PKBG: Simple subtraction of background from peak counts from the XRF analysis of manganese.

Language: PL/1. Programmer: D. Stevenson.

TAPE: Subtraction of background from peak counts on all major elements from XRF analysis with the exception of Mn. The results of PKBG are then combined with these to comprise part of the data presented to the following programme.

Language: PL/1. Programmer: G. Fitton.

XRFMOD: Computation of normalised total major element oxide percentages from peak minus background count data obtained from PKBG and TAPE, taking into account standard calibration data and all mass absorption effects, using the method recommended by Holland and Bindle (1966).

Language: PL/1. Programmer: M. Reeves.

## 1.15 PHOTOGRAPHY

For photomicrographs of polished and thin sections a Zeiss Ultraphot was used. When high magnification of small portions was required, the instrument was set to automatic exposure, setting 6 (transmitted light) or 8 (reflected light), with various objectives (3.2, 16 and 25) and values of the optovar (1.25, 1.6 and 2.0) and using FP4, 35 mm. panchromatic film. For low magnifications, possible only for thin sections, plate photography was used. The exposure time required for each section was found by trial and error.

Photographs of cathode ray tube displays of electron microprobe scanning and raster images were taken with a polaroid camera. Exposure times varied from several seconds for the scanning images up to 8 mins. for the rasters.

Where applicable, individual details are in cluded in the captions to the various photographs as they appear in the text.

# CHAPTER 2

# DISCUSSION

## 2.1 SULPHIDES

### 2.1.1. Sphalerite.

Sphalerite is the most abundant sulphide mineral and has been shown to be the earliest mineral in the paragenetic sequence. The principal modes of occurrence are as disseminations in the wallrock grading into massive colloform sphalerite, as discussed by Barton et al (1963) and Roedder (1968).

Sphalerite distribution throughout the section is irregular and depends predominantly on the location and size of pre-existing fractures and cavities which the depositing fluids have invaded. In the host rock, sphalerite is present only in small amounts within narrow (0.5 mm.), fracture-filling, calcite veinlets. In the wallrock it has penetrated the walls of all accessible cavities and lines of weakness provided by stylolitic seams. Colloform sphalerite is deposited on the walls of most open-spaces and around breccia fragments. Where this is not apparently so, banded remnant fragments suggest that the bulk of the sphalerite has been replaced by later fluorite or quartz. The cavities are of variable shape, size and distribution.

Zinc sulphide has been shown to exist in three polymorphic forms:- $\alpha$ ZnS, $\beta$ ZnS, and $\gamma$ ZnS (Buck and Strock, 1955). Isometric $\beta$ Zns (sphalerite) occurs in the present case.

The FeS content of the sphalerite ranges from 1.63% to 18.63%. A strong correlation could be discerned between the colour banding and Fe content and between cell size and colour of the sphalerite.

Although it has been shown that cell size can be affected to a certain degree by Mn substitution, the level of concentration of this element is insignificant in comparison with that of Fe, and thus its effect is considered to be negligible. Interpretations which can be made from these facts concern fluctuations in certain environmental parameters, e.g. sulphur fugacity (Barton and Toulmin, 1966), during deposition, and the possible determination of temperatures of deposition of the sphalerite. The difficulties in actually quantifying the former are outlined by the above authors. The latter possibility is considered in more detail in section 2.5.

2.1.2. Galena.

Galena ranks second in abundance among the sulphides and occurs in the mineralised section in two distinct generations. The first is closely associated with the sphalerite and its distribution is controlled, like the sphalerite by the location of solution channelways. It does not penetrate the wallrock for distances of more than 1 cm.. The later generation is visible in the hand specimen at a depth of 691'6" where the galena lines fractures in open-space filling fluorite and quartz. At depths up to 700' it is deposited in most cavity-filling situations and is localised around the walls of the cavities. It is present in relatively large amounts in a narrow (2 cm. width) veinlet penetrating argillaceous material above the silicified zone at a depth of 686'10". This vein contains no sphalerite and was apparently opened at an advanced stage in the mineralising process.

Marshall and Joensuu (1961) note the effect of temperature on the control of crystal habits of galena. At higher temperatures cubes are replaced by higher-order polygons of combinations of more than one habit. They conclude that the cubic habit of galena is favoured by low temperature, implying reversible crystal growth and a low rate of nucleation. A low rate of nucleation is consistent with the fact that cubic crystals tend to be large while octahedral crystals are generally smaller. In the present situation all galena crystals are of cubic habit, further supporting the conclusion that the mineralisation in general was deposited at relatively low temperatures.

### 2.1.3. Chalcopyrite

Chalcopyrite is visible in the hand specimen only at a depth of 691'6" where it projects into a cavity from a quartz base (see section 1.1.) Other occurences are as microscopic exsolution bodies within sphalerite and as isolated grains closely associated with the sphalerite. It is not certain whether the chalcopyrite disseminated in the wallrock gangue minerals is of primary depositional origin or whether the disseminations are residuals from the replacement of sphalerite. The former interpretation appears more likely as the "pisolitic" sphalerite does not appear to have been replaced to any large extent.

2.1.4. Pyrite

Pyrite occurs in two modes - as original diagenetic material and as epigenetic hydrothermal pyrite. The former is present most obviously in the host rock in which it is irregularly distributed in large (up to 3 cm. in length) elongate masses and smaller euhedral grains. The masses are usually closely related to, and often completely pseudomorph, fossil relics. In cases where this is not apparently so, the longest dimension of the aggregate always parallels the bedding. No fracture-filling relationships were noted. It is likely, therefore, that the host rock pyrite is of diagenetic origin, the distribution and form of which has been modified by heat effects from the intruding Whin Sill. This interpretation does not conform with that of Dunham et al (1965) who imply that the pyrite is hydrothermal in origin. Some of the wallrock pyrite is probably remnant diagenetic material.

The hydrothermal pyrite is limited in distribution to the wallrock and is intimately related to the other sulphides, particularly sphalerite, with which it appears to be contemporaneous. It is distinguished from original pyrite by its fine grain size and its close relationship to the pattern of distribution of the sphalerite. Both the original and introduced pyrite are only present in significant amounts to a depth of approximately 692'6".

## 2.2. NON-SULPHIDE MINERALS

### 2.2.1. Carbonates

From an examination of thin sections, coupled with the results of XRD investigations and staining tests, the unaltered limestone was found to consist almost entirely of calcite with a little organic matter, quartz and feldspar. There are, however, more argillaceous bands, the nature and extent of which are discussed in section 2.4, in which calcite is accompanied by significant amounts of quartz and clay minerals in varying proportions.

The first occurrence of mineralisation is at a depth of 686'10" where a 2 cm. width vein occurs. The argillaceous limestone above and below this contact is not obviously altered but analytical results suggest that dolomite is present in small amounts. The lack of core from 687'3" to 688'3", at which latter depth all the limestone is silicified, precludes the possibility of investigating the nature of the transition zone between the altered and unaltered wallrock.

In the mineralised zone the original limestone host rock is completely replaced by $SiO_2$ and other epigenetic minerals, as shown by thin section, XRF, and staining procedures. $CO_2$ has been detected in most analyses, but this is attributed to the occurrence of epigenetic carbonates.

The replaced limestone is in general lighter in colour than the host rock. Fossil relics are clearly visible throughout as these are pseudomorphed by $SiO_2$.

Other carbonates identified are found only in the altered wallrock within the mineralised zone, with the exception of ankerite which also occurs as vein-filling material.

The most abundant carbonate in the wallrock is ankerite, the bulk of which appears to be a late-stage product of the hydrothermal processes, occurring mainly as a cavity lining or as single crystals projecting into cavities. From 691' to 691'3" the ankerite occurs as irregular stringers in the wallrock. It also occurs in an earlier generation as small disseminations together with dolomite, as noted in section 1.1.

Siderite was detected in the wallrock by staining techniques at depths of 688'9" and 690'. In both cases the siderite is disseminated in localised portions of the wallrock, access for the depositing solutions being provided by carbon-rich bands.

Dolomite was identified by means of the electron probe in most of the sections examined and during XRD investigations. It could not be discerned in the hand specimen and thus its mode of distribution throughout the section could not be determined.

## 2.2.2. Fluorite

Fluorite is the most abundant mineral in the section and occurs in two generations, the first being identified as replacement blebs in the wallrock generally not penetrating for distances of more than 1 cm. from cavity walls. This form could be examined in all polished sections and its broader distribution determined as a result of staining techniques. The second generation is predominantly of cavity-filling type but also replaces earlier sphalerite to a certain extent.

The fluorite in this case is always of cubic habit and green in colour, a combination in disagreement with the results of Twenhofel (1947), who, in a study on the crystallisation temperatures of successive zones of a single fluorite crystal, found a correlation between crystal habit and colour, crystal habit changing from octahedral (green colour) to cubic (violet) with decreasing temperature. This author also suggested that the habit of fluorite crystal growth may be related to temperature of crystallisation, the cubic habit developing at approximately 170$^{o}$C. Different conditions of deposition have also been postulated for the different colours and habits of fluorite by Drugman (1932), who also suggested that the different habits may be due to different temperatures of deposition in the decreasing order: octahedrons, dohecahedrons and the cube, with various transitions between these habits. The fact that fluorite is cubic throughout the section thus supports the results of fluid inclusion studies which suggest that the mineral was deposited at relatively low temperatures.

### 2.2.3. Quartz

Quartz was identified in XRD traces of material from both the wallrock and the host rock, the former being hydrothermal in origin and the latter sedimentary. In the host rock the proportions of quartz fluctuate down the borehole (section 2.4). The wallrock, however, consists predominantly of introduced cryptocrystalline quartz which has replaced all original constituents of the limestone but feldspar and carbon. Remnant fossils are pseudomorphed by the quartz.

Quartz also occurs in an open-space filling mode in the generation deposited after the second generation of fluorite. This fluorite/quartz association occurs in all mineralised portions of the section. Cavities are not completely filled and euhedral hexagonal quartz crystals project into these.

### 2.2.4. Feldspar

Orthoclase feldspar occurs in all thin sections and polished sections cut from both wallrock and host rock material, identification being confirmed by XRD and electron probe techniques.

It was deduced that the feldspar is authigenic in origin from the facts that it occurs throughout the otherwise-unaltered limestone host rock, the distribution in the wallrock samples is similar to that in the host rock, and textural relationships indicate that the mineral was present prior to the deposition of all other minerals in the assemblage. Also feldspar is known to occur in similar rocks in the general area but remote from the influence of hydrothermal activity.

As noted by Goldsmith (1967), authigenic feldspars are relatively common and tend to be rather pure K or Na end-members. Electron probe results are in agreement with this observation as all the feldspars in the section were found to be highly deficient in Na.

## 2.2.5. Graphite

Organic material occurs throughout the host rock and wallrock in approximately constant proportions. In the host rock the material is irregularly distributed and normally occurs in bands roughly paralleling the bedding as revealed in thin sections. Stylolitic seams have developed in several locations. In the silicified wallrock the organic material appears not to have been removed to any extent during the hydrothermal activity but has been mechanically forced to the boundaries of the calcite - replacing quartz grains to form a regular network. This again does not conform with the interpretation of Dunham et al (1965) who suggest that the limestone had previously been recrystallised by the thermal effect of the Whin Sill causing elimination of the carbon to the calcite grain boundaries with subsequent silicification preserving the shape of these grains.

Graphite flakes were identified in polished sections cut from both the altered wallrock and unaltered host rock. In the former case these are often enclosed within sphalerite, the earliest mineral in the paragenetic sequence.

From the above considerations it is suggested that the graphite is produced by recrystallisation of organic material by the thermal effect of the Whin Sill, prior to the onset of hydrothermal activity.

## 2.3. TRACE ELEMENT DISTRIBUTION

Having prepared pellets for major element XRF analyses, these were used also for the determination of certain trace elements. The choice of the actual elements determined was in general governed by the current availability of the machine. Thus it was only possible to determine the following 9 elements, which can be divided into four groups:

(a) Cu, Ni, Zn - elements related to the heavy metal content of the mineralisation.

(b) Y - a common rare earth trace constituent of fluorite in these veins.

(c) Ba, Sr, Rb - large cations, common trace constituents of carbonate minerals.

(d) Zr, Nb - trace elements available in the XRF programme, but with no obvious expected distribution.

The results of the analyses are plotted in figs. 24 to 26.

Group (a). Zn - In fig. 24 only the analyses from the host rock are shown as the wallrock contains Zn in the form of sphalerite in amounts in excess of the range covered by the standards.

The distribution is seen to be irregular, but broadly there is a decrease in concentration of a direction away from the vein. It is difficult to attach any significance to the higher peaks, as in several hand specimens, narrow, sphalerite - containing veinlets were noted. Although an attempt was made to exclude these from the sample it is possible that contamination may have taken place.

Turekian and Wedephol (1961) cite the average geochemical abundance of Zn in shales and carbonates as 95 ppm and 20 ppm respectively. The concentrations in most cases are in excess of these.

Cu, Ni - These elements are present in low concentrations and are relatively uniformly distributed except for a slight increase in the argillaceous bands for both elements, and an increase in several wallrock samples for Cu. The low level of concentration of Ni in the wallrock supports the contention that the wallrock material was originally carbonate rich.

The average geochemical abundance of Cu in shales and carbonates is given as 45 ppm and 4 ppm, and of Ni in shales and carbonates - 68 ppm and 20 ppm respectively.

(b) Y - concentrations of Y higher than the general level are seen to be present in the argillaceous bands, with no other apparent pattern. It is unlikely, therefore, that the Y distribution is related to the mineralising processes except in sample X46 in which Y is concentrated far above the general level. Average geochemical abundance in shales and carbonates 26 ppm and 30 ppm respectively.

(c) Sr - this element shows high concentrations in carbonate - rich areas and decreases markedly in the argillaceous bands in the host rock. It may therefore be deduced that the Sr distribution is the result of original sedimentary depositional conditions and is incorporated in the structure of the carbonate minerals.

Average geochemical abundance of Sr in shales and carbonates - 300 ppm and 610 ppm respectively.

Ba, Rb - Both elements vary sympathetically with each other and antipathetically with Sr. Concentrations in the wallrock are low. The possible relationship of this pattern to the mineralisation cannot be deduced. Average geochemical abundance in shales and carbonates - Ba, 580 ppm and 10 ppm, and Rb, 140 ppm and 3 ppm respectively.

(d) Zr , Nb - Concentrations are highest in the argillaceous bands and both elements are depleted in the wallrock. The distribution of these elements is considered to be unrelated to the mineralising processes.

Average geochemical abundance of Zr in shales and carbonates 160 ppm and 19 ppm respectively.

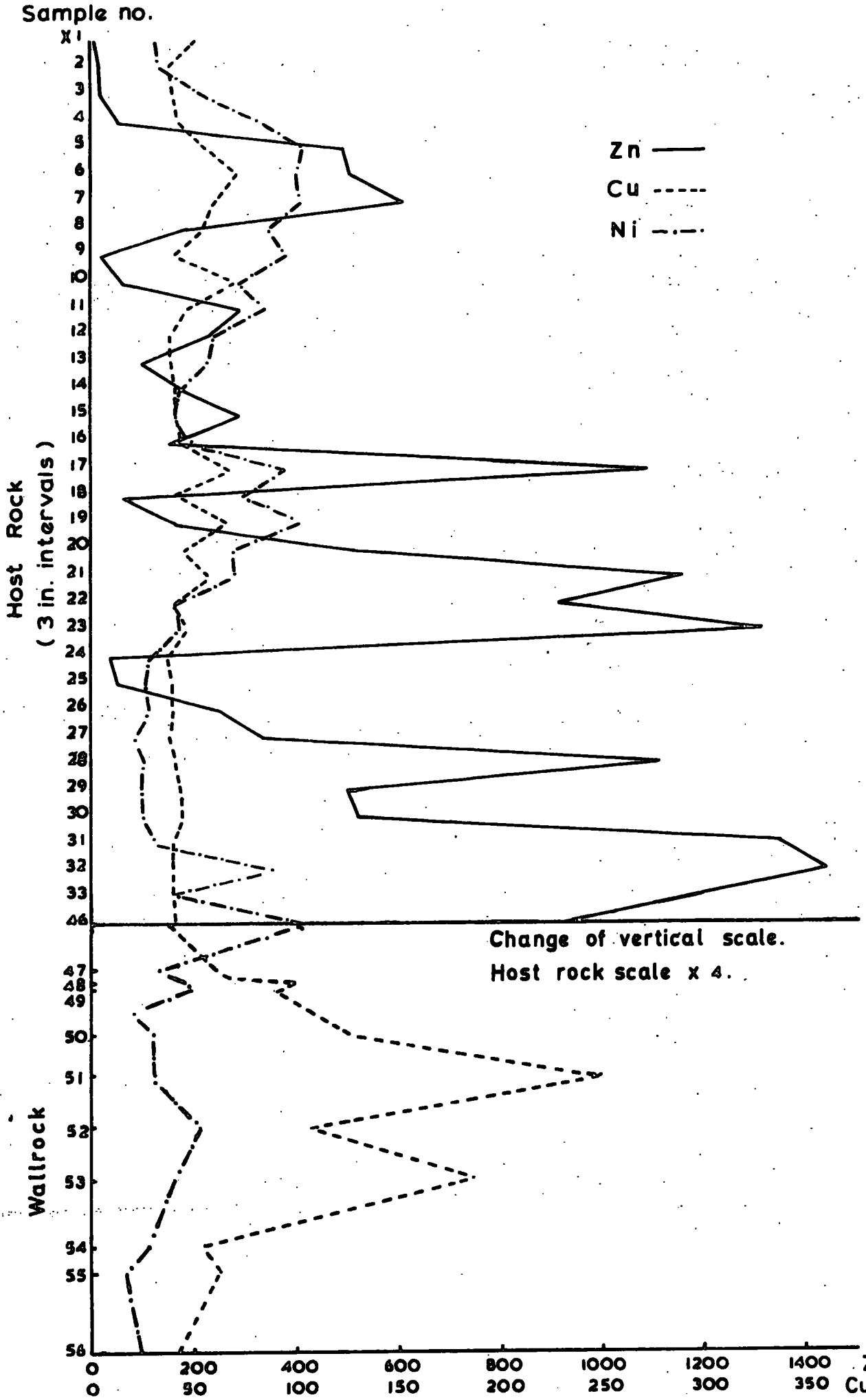


FIG. 24. VARIATION OF Zn, Cu, AND Ni WITH DEPTH.

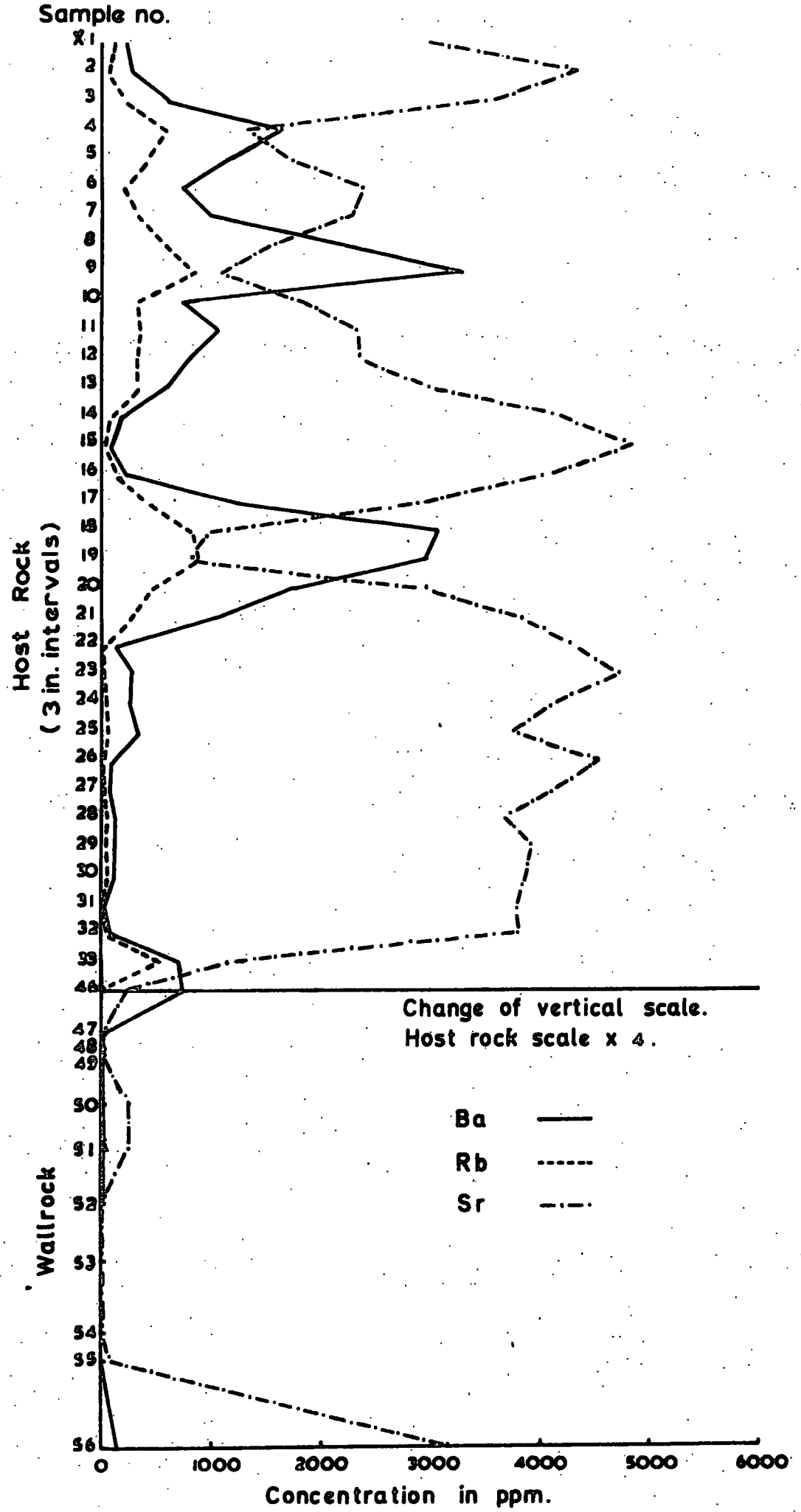


FIG. 25. VARIATION OF Ba, Rb, AND Sr WITH DEPTH.

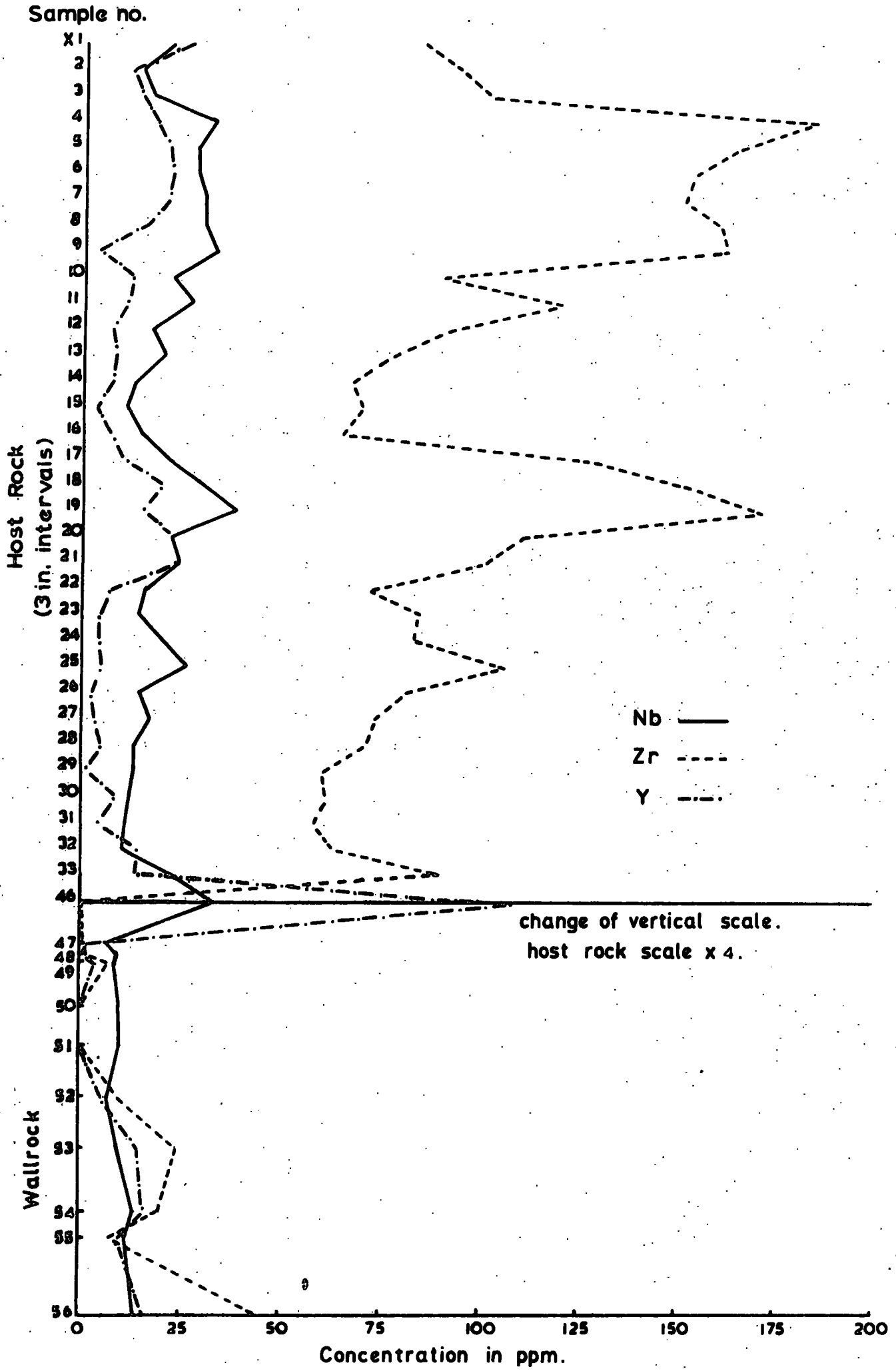


FIG. 26. VARIATION OF Nb, Zr, AND Y WITH DEPTH.

## 2.4 MAJOR ELEMENT DISTRIBUTION

From x-ray diffraction studies it has been shown that the major mineralogy of the apparently relatively fresh host rock remains practically constant in kind, but variable in proportions in each of the 3-inch sections examined. Evidence points to lack of alteration by hydrothermal activity in this region, and thus, barring the presence of minor phases undetactable by x-ray diffraction and later obliteration of altered phases, the mineralogical distribution determined by x-ray diffraction is assumed to represent the pre-mineralisation nature of the limestone.

$SiO_2$. The $SiO_2$ is present throughout the section but is particularly abundant in three sections in the host rock, from samples X3 to X14, X16 to X21 and in sample X33. In the wallrock $SiO_2$ is extremely high, having replaced most other components.

The $SiO_2$ distribution shows a distinct positive correlation with $Al_2O_3$, $Na_2O$, $K_2O$, $TiO_2$ and $H_2O^+$, a slight negative correlation with $Fe_2O_3$, MgO, and S, and a strong negative correlation with CaO and $CO_2$. No correlation is apparent between $SiO_2$ and MnO, $P_2O_5$, C or $H_2O^-$.

X-ray diffraction results suggest that a large amount of the $SiO_2$ is present in the form of quartz, but a certain percentage also is contained in clay minerals and orthoclase feldspar. This is demonstrated by the high degree of correlation with the silicate mineral component oxides.

$Al_2O_3$

It is apparent from XRD results and from the degree of correlation with other relevant oxides that the $Al_2O_3$ is present predominantly in the clay minerals and orthoclase feldspar.

In the host rock, $Al_2O_3$ varies in sympathy with $SiO_2$ and reflects the relative proportions of silicates in a particular sample.

Concentrations in the wallrock are low and are predominantly due to the presence of orthoclase feldspar.

$\underline{K_2O}$

$K_2O$ also shows the same correlation relationships to the other components as does silica.

This oxide is contained in the silicates - predominantly orthoclase, but also no doubt is present in montmorillonite and illite to some degree.

As $K_2O$ concentrations are at a consistent low level in the carbonate - rich portions of the host rock and in the wallrock, and as orthoclase feldspar has not been affected during the mineralising period, it may be inferred that the wallrock consisted initially of similar carbonate-rich material.

$\underline{Na_2O}$

In the host rock, $Na_2O$ increases in the argillaceous bands above the low level of the carbonates, reflecting its presence in the clay minerals. It occurs also in small amounts in the feldspar.

The relatively high concentrations indicated in the wallrock are largely unexplained but may be due in part to the brine content of fluid inclusions which have been noted in the wallrock quartz.

$\underline{Fe_2O_3}$

The Fe is partitioned among the carbonates, sulphides and silicates. The actual proportions to be assigned to each of these phases vary down the section, as a result of fluctuations in the

proportions of dolomite, siderite, ankerite, pyrite, sphalerite and certain silicates.

The level of total $Fe_2O_3$ concentration fluctuates markedly down the section with no apparent pattern in the distribution.

MgO

The MgO reflects only variations in composition and proportions of the carbonates and clay minerals. In the host rock carbonates, MgO may occur in small amounts of dolomite, but it has been noted by Runnels (1970) that the calcite secreted by organisms contains an appreciable percentage of magnesium in isomorphous substitution for calcium, and an appreciable amount is probably present in this form.

In the wallrock, MgO concentration is lower, maintaining the same positive correlation with $Fe_2O_3$. In this situation dolomite and ankerite are the likely host minerals.

MnO

The MnO concentration in the host rock is too low to enable any significance to be attached to the results or to detect any possible fluctuations.

In the wallrock, however, MnO is present in concentrations up to 1.5%, the fluctuations correlating positively with the $Fe_2O_3$ and MnO variations. As was suggested by the results of the electron microprobe this probably reflects variations in the carbonate content of the sample. There is a slight degree of correlation between the MnO and the CaO and $CO_2$ variations in the wallrock, supporting this interpretation.

CaO

The direct positive correlation of CaO with $CO_2$, the results of the x-ray diffraction analysis, and the staining tests, show that the CaO occurs predominantly as a component of calcite, although it may be present in small amounts in clays.

In the wallrock, the CaO concentration is comparatively low. Here it is mainly contained in carbonates - ankerite and dolomite. The positive correlation with $CO_2$ variation is not as strong as in the host rock, reflecting the variation in major element composition of the carbonates.

$TiO_2$.

$TiO_2$ increases markedly in the argillaceous portions of the wallrock, and remains at a general low level in the carbonate-rich areas and in the wallrock.

$P_2O_5$.

In the host rock $P_2O_5$ shows a slight general increase in the lower argillaceous horizon.

The wallrock is markedly deficient in this component.

S.

S concentration in the wallrock is due to the inclusion of galena and sphalerite in the samples, in addition to pyrite, and is not shown in the graph.

In two samples in the host rock, the calculated S concentrations are extremely high. As the true concentration is outside the range of the standards, at best it can only be stated that S is high in these two samples.

C.

C distribution is highly irregular, the general level of concentration remaining fairly consistent in both the wallrock and the host rock.

$CO_2$.

In the host rock, $CO_2$ correlates positively with CaO.

In the wallrock, however, the $CO_2$ correlates with $Fe_2O_3$, MgO and MnO demonstrating the abrupt change in composition of the carbonates in this region, and providing further support for the suggestion of the hydrothermal origin of these carbonates.

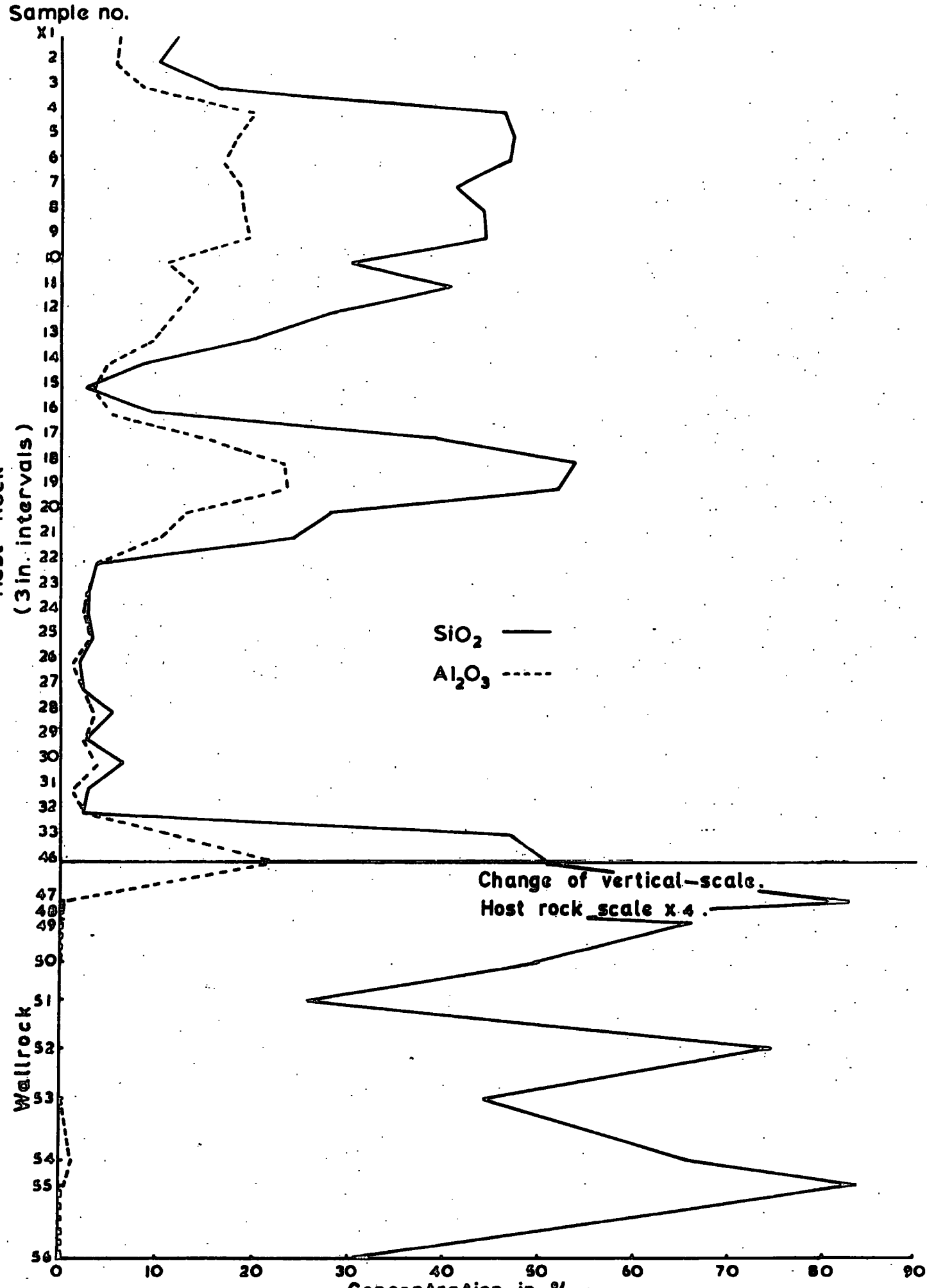


FIG. 27. VARIATION OF $SiO_2$ AND $Al_2O_3$ WITH DEPTH.

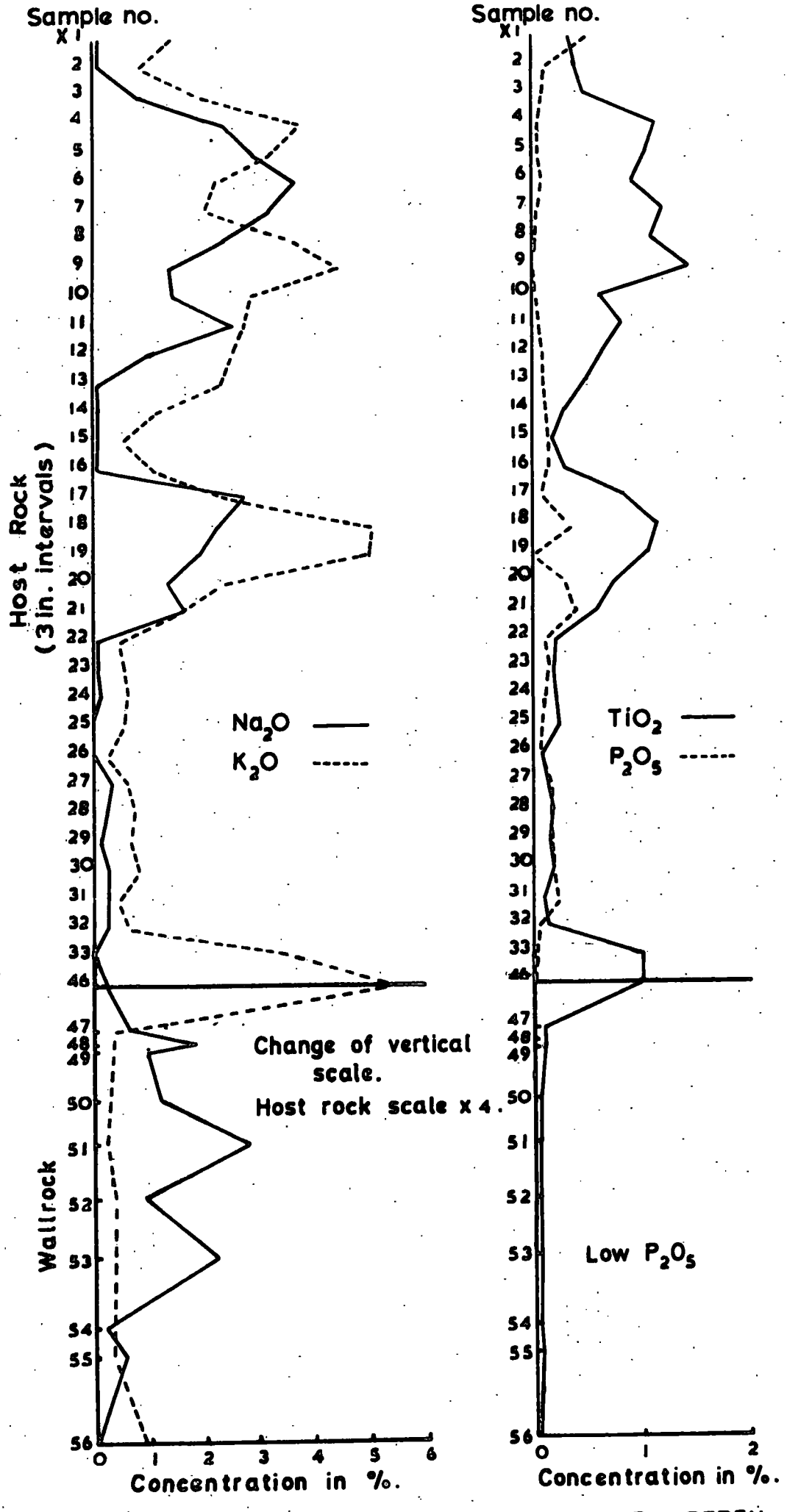


FIG. 28. VARIATION OF $Na_2O$ AND $K_2O$ WITH DEPTH.

FIG. 29. VARIATION OF $TiO_2$ AND $P_2O_5$ WITH DEPTH.

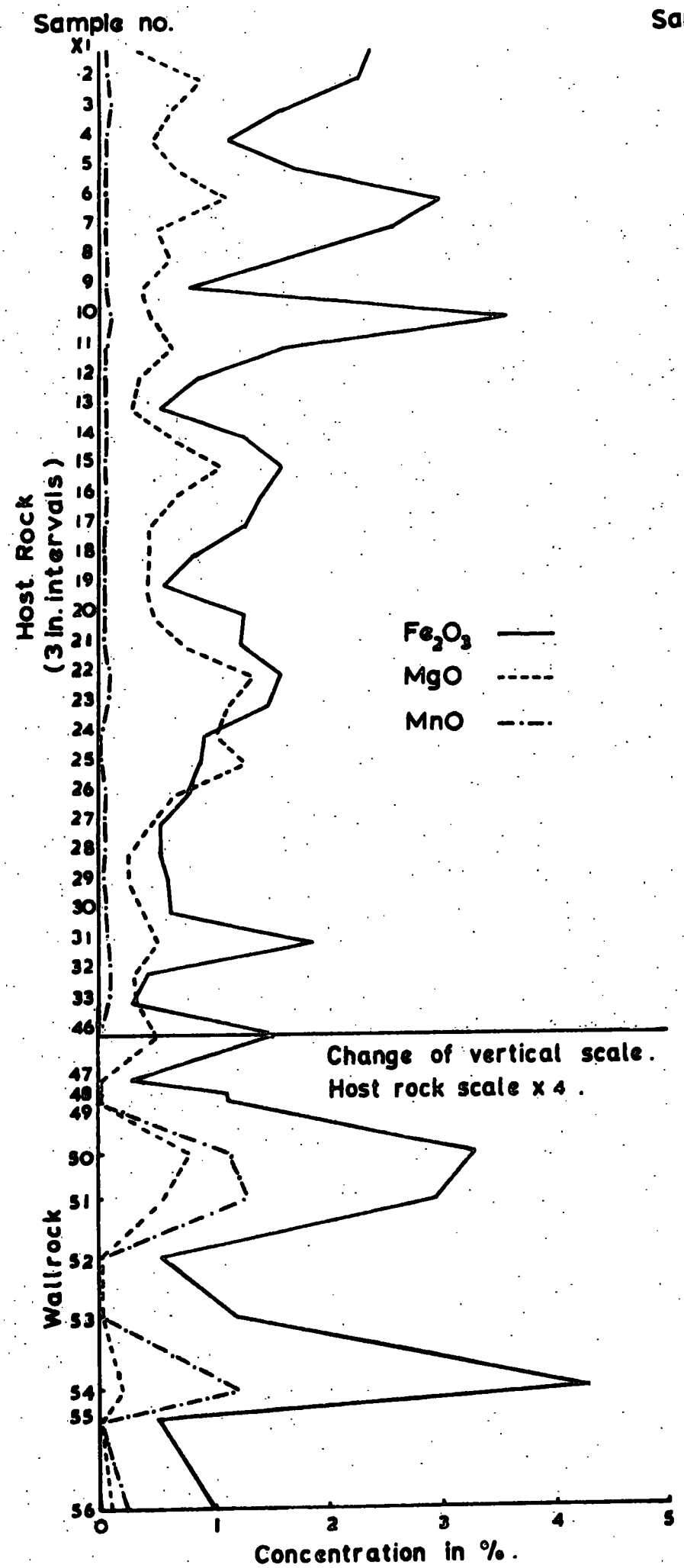


FIG. 30. VARIATION OF $Fe_2O_3$, MgO, AND MnO WITH DEPTH.

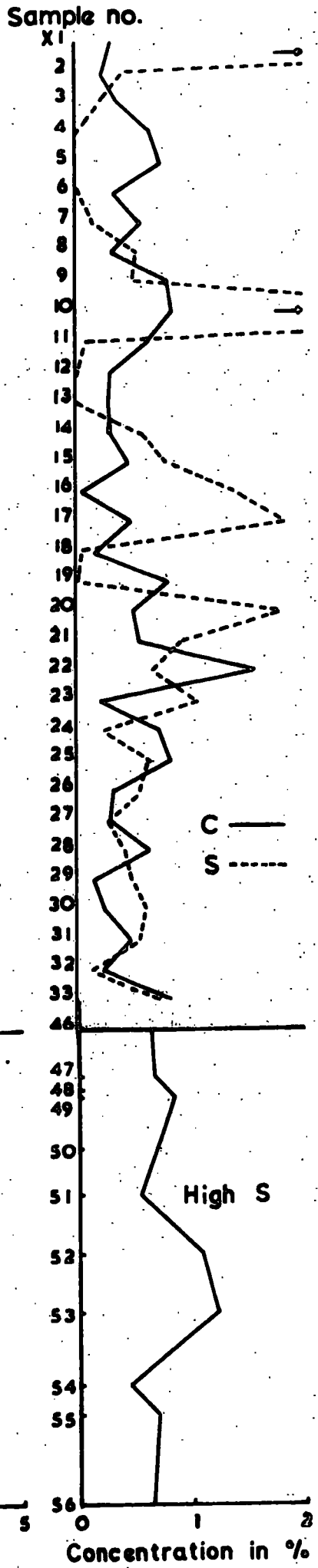


FIG. 31. VARIATION OF C AND S WITH DEPTH.

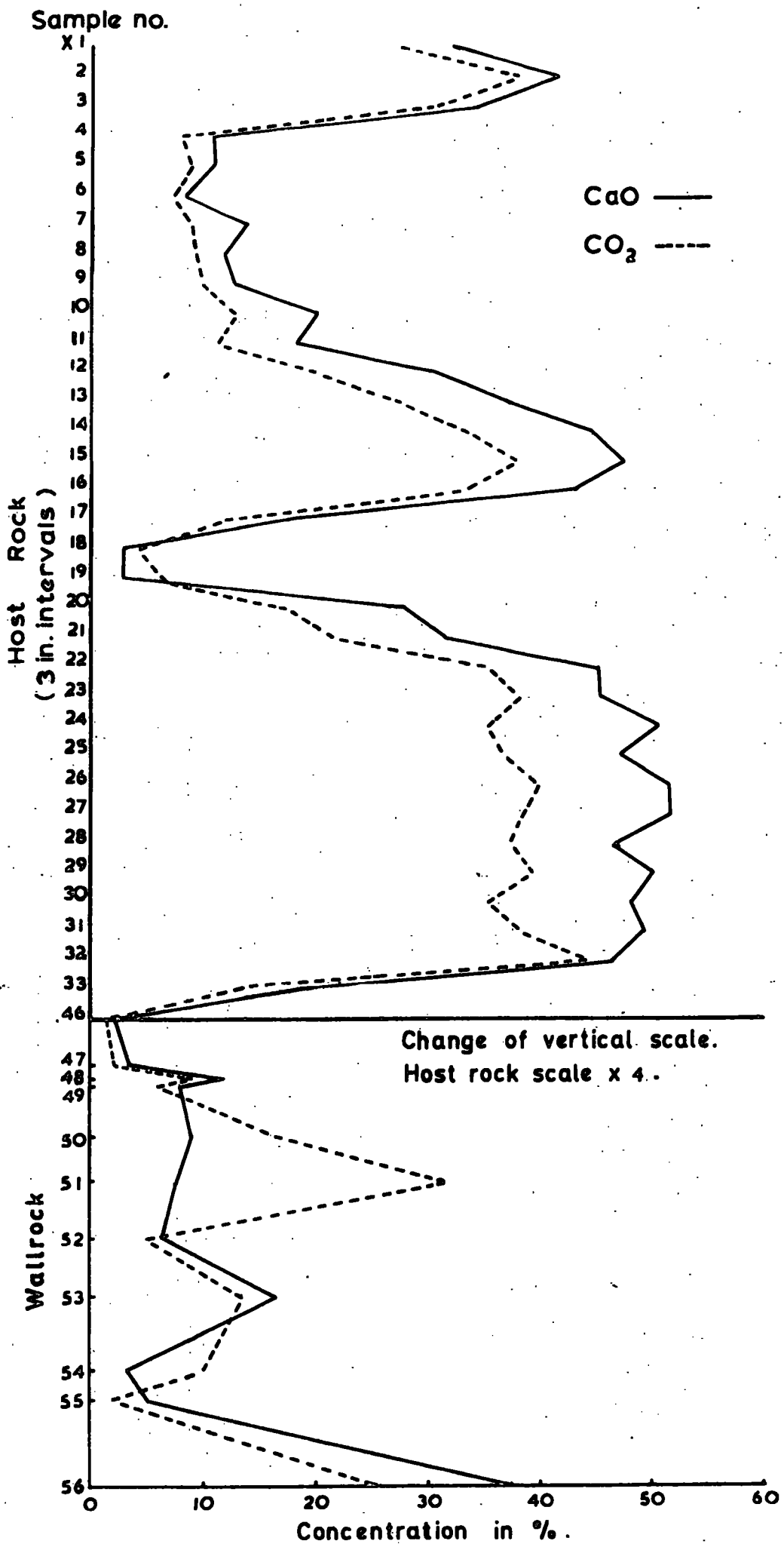


FIG. 32. VARIATION OF CaO AND $CO_2$ WITH DEPTH.

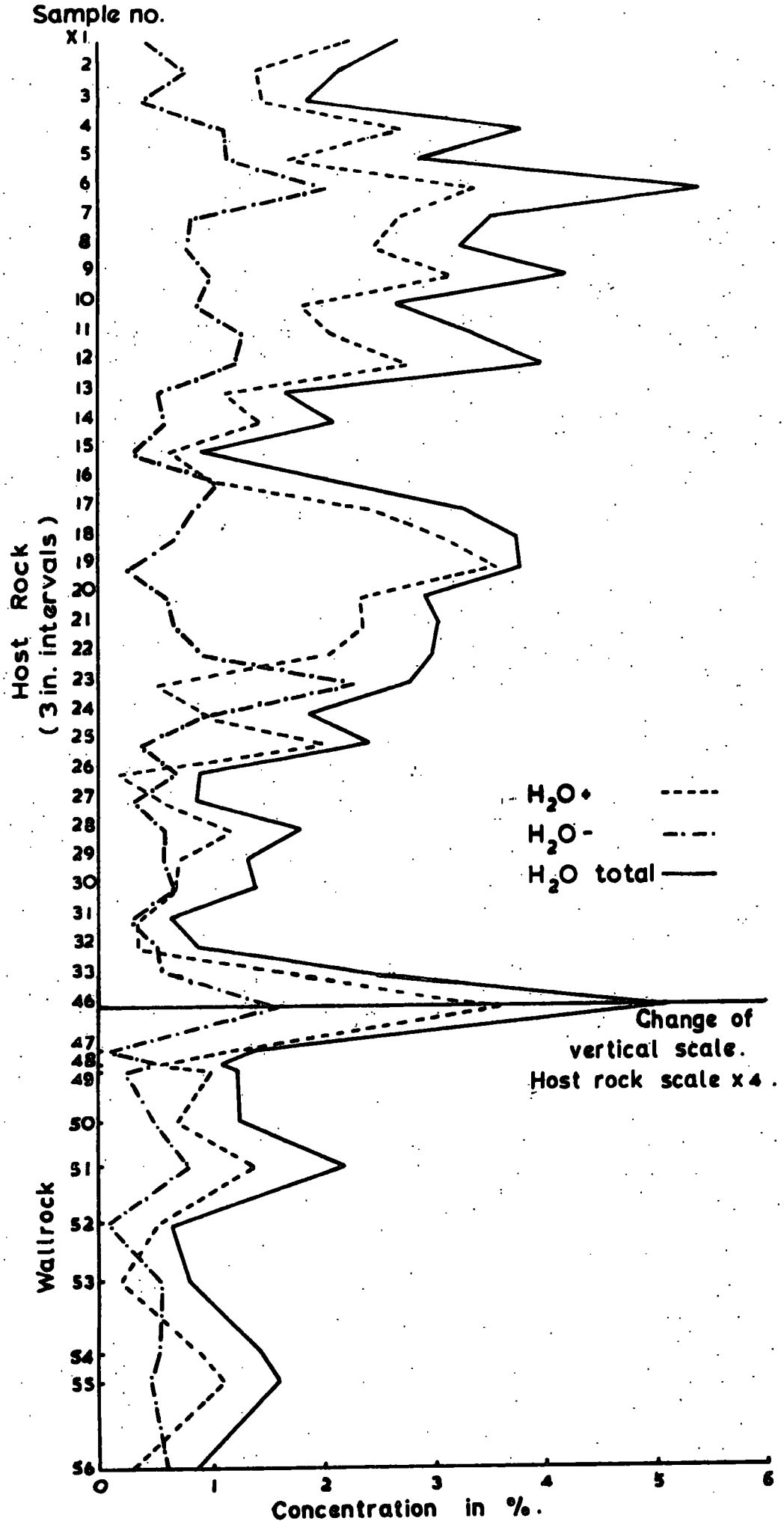


FIG. 33. VARIATION OF $H_2O+$, $H_2O-$, AND TOTAL $H_2O$ WITH DEPTH.

## 2.5 GEOTHERMOMETRY

To date no completely reliable geothermometers have been established but several of those with the greatest potential were considered in the determination of depositional temperatures at various stages. These are:

(a) Trace element fractionation between coexisting sulphides.

(b) The cell edge of sphalerite.

(c) The iron content of sphalerite.

(d) Fluid inclusion homogenisation temperatures.

(a) The study of trace element fractionation between coexisting phases in equilibrium as a potential geothermometer has been suggested by various workers. Attempts made by these workers to apply the geothermometer have, however, not been successful, perhaps due to the difficulties inherent in actually proving the equilibrium relationships existing between the minerals in question. To date most attention has been directed towards determining the fractionation of Se between galena, chalcopyrite, and sphalerite, and Cd and Mn between galena and sphalerite.

In the present study, although equilibrium between the various coexisting phases could not be proven, an attempt was made to apply the geothermometer as far as present states of knowledge would permit. As has been discussed, however, in section 1.8 it was found that within the limits of the analytical methods used it was not possible to detect the small concentrations of elements other than Mn, this element being detected only in sphalerite, in small amounts, and with limited accuracy.

(b) The results of the determination of the cell edge of sphalerite by powder photographic techniques are presented in table 13. Curves connecting the length of the cell edge of sphalerite with iron content have been determined, as have the corresponding plots of cell edge versus temperature of deposition. For the reason that the cell edge is affected by indeterminate amounts by substitution of elements other than Fe, and for reasons outlined in (c), this method could not be applied.

(c) The potential of the iron content of sphalerite as a geothermometer has been discussed by many workers, notably Kullerud (1953), Barton and Kullerud (1957), Einaudi (1968), Skinner (1959), Toulmin (1960), Arnold et al (1962), Fryklund and Fletcher (1956) and Rose (1961). However, Boorman (1967) found, by extending the sphalerite solvus to the pyrrhotite hexagonal/monoclinic inversion temperature, that there is a FeS composition maximum at 550°C with a constant drop to at least 303°C, (fig. 34) differing from the postulated extrapolation of Barton and Toulmin (1967). Boorman deduced that the sphalerite geothermometer is not valid below 550°C. This opinion is corroborated by the results obtained on the electron probe. Even the minimum temperatures determined from the postulated curves of Sims and Barton (1961) are in many instances far in excess of those expected from all other lines of geological reasoning. It is concluded that the iron content of sphalerite is invalid as a geothermometer as applied to the present case. The results suggest also that the experimentally determined curve of Boorman may continue vertically to even lower temperatures.

(d) This method could in theory be employed to determine the depositional temperatures of sphalerite, carbonates, quartz and fluorite. It was, however, found to be suitable only for application to the fluorite. The actual procedure and the results obtained have been discussed in section 1.11. The results indicated that the second generation of fluorite was deposited at a maximum temperature of approx. 150°C., with evidence of the trapping of later cooler solutions.

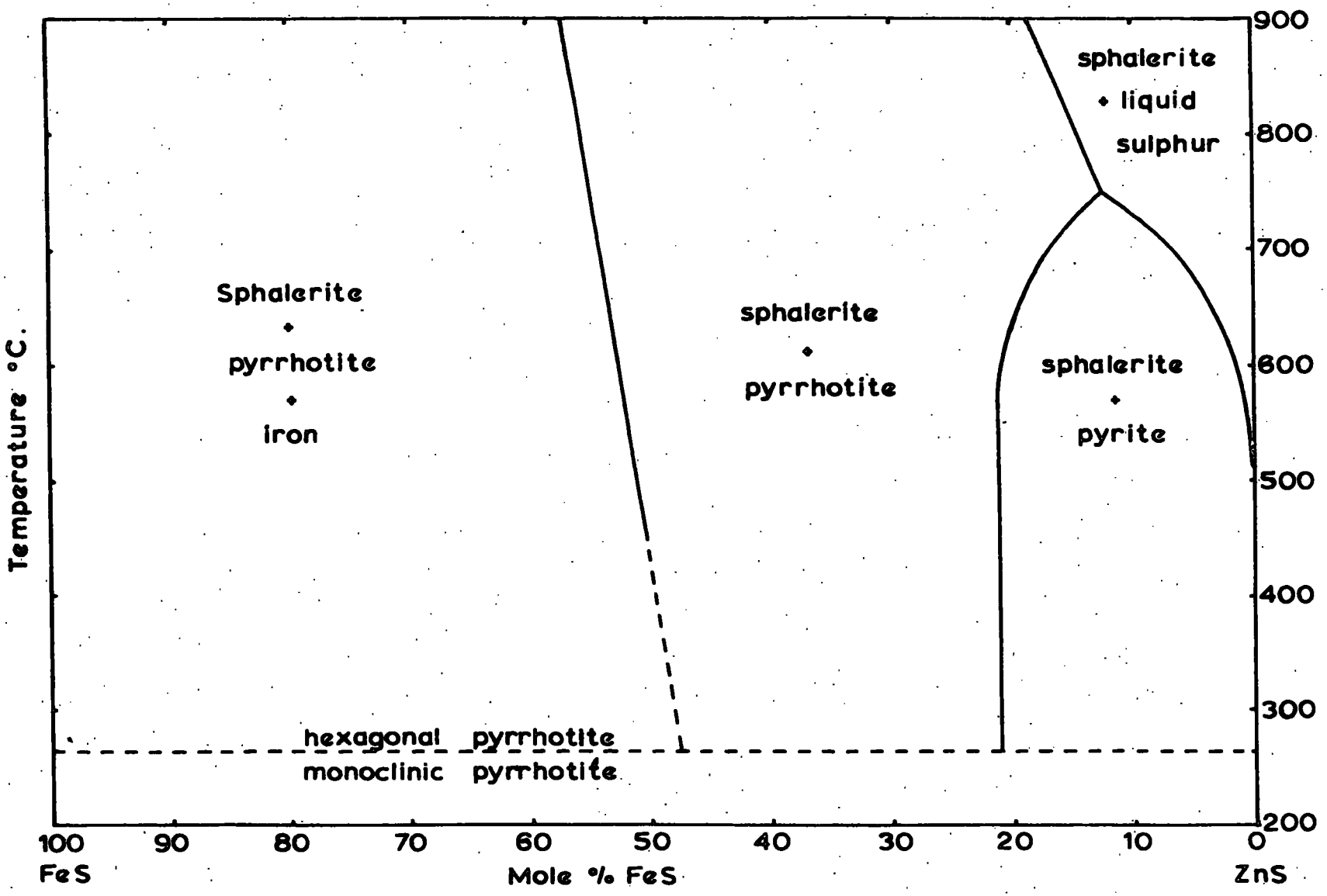


FIG. 34. The composition of sphalerite in equilibrium with iron and iron sulphide phases. (After Boorman, 1967).

## 2.6. ATTITUDE OF MINERALISATION

It is difficult to determine from the available information the actual attitude and form of the main body of the mineralisation intersected by the borehole. Several possibilities exist:

1) the borehole intersects a single dipping vein within which are included a variety of sizes of breccia fragments.

2) A horizontal, flat-like body is intersected, including a number of breccia fragments.

3) The form is of two or more dipping veins with minor offshoots and some small breccia fragments.

4) Each of the mineralised portions are minor projections from a main vein system which is not intersected by the borehole.

Evidence presented previously for the lack of an alteration or trace element aureole around the mineralisation is possibly due to the presence of a highly argillaceous band which occurs at the top of the mineralised zone, since all lower limestone sections show penetration of mineralisation.

Mineralisation may be emplaced either by cavity filling in, or replacement guided by, pre-existing fractures, but a suggestion by Phillips (1972) of a mechanism of hydraulic fracturing as a means of extension of vein conduits and as a cause of brecciation may apply to the present case. By this mechanism faults are extended by hydraulic fracturing on the accumulation of a body of hydrothermal fluid on the fault zone under pressures greater than the pore water pressure. The abrupt drop in pressure of the solution when fracturing occurs causes the bursting apart of the rock, thus producing an angular breccia.

## 2.7. PHYSICAL CHEMISTRY

Several aspects of the physiochemical nature of the hydrothermal fluid at various stages may be deduced from a consideration of the minerals deposited from the fluid.

Studies which are relevant to the present situation with regard to sphalerite have been carried out by Laudise et al (1965), Barton and Skinner (1967), Stevenson and Jeffery (1964), Roedder (1968), Barton and Toulmin (1966), Mookherjee (1962), Dickson et al (1962), and particularly Barnes and Kullerud (1961) who, from a series of experiments and thermodynamic calculations, make several deductions concerning the nature of the ore depositing fluid, and in particular that of a solution depositing sphalerite. From constructed phase diagrams it is deduced that the lack of native sulphur in hydrothermal deposits suggests a neutral to alkaline ore solution. Fig. 35 shows the common range of acidity and oxidation state of sphalerite-depositing ore solutions at $250^{o}C$ and $(\Sigma S) = 0.1m$. In this case, the association of sphalerite with pyrite fixes $P_{S_2}$ above the pyrite/pyrrhotite curve. An upper limit has been fixed by the deduction that in most ore deposits the $P_{S_2}$ does not exceed that permitting the stable coexistence of covellite and digenite. The shaded area gives a region within which the $P_{S_2}$ commonly lies. Additional boundaries are imposed by the fact that no barite is deposited. Changes in the assumed value of $\Sigma S$ affect the position and shape of the shaded area. It is concluded that sphalerite is transported in reduced, neutral to alkaline ore solutions where $HS^{-}$ is probably the predominant sulphur-containing ion. It has been shown by Barnes (1965) that limestone

should be replaced by sphalerite at decreasing temperatures from a consideration of the equilibrium conditions existing between calcium carbonate and the zinc complex $Zn(HS)_3^-$, a probable means of transport of Zn in hydrothermal solutions.

Pyrite has a wide stability field with respect to most geochemical variables and thus significant limits cannot be placed on a pyrite-depositing solution. As its deposition appears to be associated with that of sphalerite, any limits imposed for this mineral may also be applied to pyrite. The stability relations of pyrite with respect to other iron compounds are outlined by Garrels and Christ (1965). Other suggestions with bearing on the development of pyrite or marcasite have been put forward by Barton and Toulmin (op. cit), Goldsmith (1967), Krauskopf (1967), Meyer and Hemley (1967), and Allen et al (1912).

Very little work has been carried out on the nature of a chalcopyrite-depositing solution but significant limits probably could not be imposed as the mineral occurs in a wide variety of situations.

The nature of a galena-depositing solution has been discussed by many workers but satisfactory agreement has not as yet been attained.

Broad limits on the activities of various components of the solution may be placed using the method of Barton (1957).

Considering a case in which both fluorite and calcite are deposited simultaneously and in equilibrium with a hydrothermal fluid, the ratio of the activities of the relevant anions in solution may be determined from the following relations

$$CaF_2 \rightleftharpoons Ca^{2+} + 2F^- \qquad K_{CaF_2} = a_{Ca^{2+}} \cdot a^2_{F^-} = 10^{-9.77}$$

$$CaCO_3 \rightleftharpoons Ca^{2+} + CO_3^- \qquad K_{CaCO_3} = a_{Ca^{2+}} \cdot a_{CO_3^-} = 10^{-8.33}$$

(activity product constants, K , from Latimer, 1952).

Therefore, $$\frac{a^2_{F^-}}{a_{CO_3^-}} = \frac{10^{-9.77}}{10^{-8.33}} = 10^{-1.44}.$$

From this relation it may be deduced that when calcite and fluorite are deposited in equilibrium, the ratio of the activity of the fluoride ions to carbonate ion activity is $10^{-1.44}$. At ratios in excess of this, fluorite is deposited, and below this, calcite.

The calculations are based on thermodynamic values in aqueous systems at 25°C and 1 atm.. It has been shown that the effect of pressure on ionic equilibria is negligible, but the values must be extrapolated to temperatures in the vicinity of 150°C in the present case to become tenable. The variation of the relevant anionic ratios with temperature according to the van't Hoff equation, $d \ln T/d T = \Delta H / RT^2$ (where K is the activity product constant, $\Delta H$ is the change in heat content, R is the gas constant and T the absolute temperature) is not great but because the temperature of deposition of each of the minerals is not accurately known, only the values for 25° and 1 atmosphere are given.

Restrictions may be placed on the fugacity of $H_2S$ during sulphide deposition using the relationship:

$$P.H_2S = 10^{-6.0} \ ( a\ S^- / a^2\ OH^- ).$$

The $a\ S^- / a\ CO_3^-$ ratio has been converted to a ratio of the thermodynamic partial pressures (fugacities) of $H_2S$ and $CO_2$, and the relationship determined as

$$P\ H_2S / P\ CO_2 = 10^{3.8}\ a\ S^- / a\ CO_3^-.$$

These relationships are invoked to produce the values given in table 14 as a summary of the broad limits to be imposed at particular stages.

As quartz is deposited in a wide variety of situations, little can be deduced concerning the chemistry of the depositing medium. The behaviour of quartz in the hydrothermal environment has been discussed by Kennedy (1950) and Holland (1967).

The deposition of fluorite depends on a variety of physical and chemical aspects of the transporting medium as has been discussed by Holland (op. cit.) and thus only the anionic ratios discussed provide meaningful limits. The significance of the colour of fluorite has been considered by Dunham (1952) and Goldberg (1963), among other workers.

Other contributions concerning the deposition of the non-sulphide minerals have been made by Barton et al (1963), Barton and Skinner (1967), Goldsmith et al (1962), Goldsmith (op. cit.), Rosenberg and Holland (1964), Ellis (1963), Holland et al (1964), Ames (1961), and Garrels and Dreyer (1952).

Apparent lack of alteration of the host rock away from the silicified portions precludes any possibility of delimiting the geochemical environment by a consideration of alteration patterns produced at certain stages as attempted by Meyer and Hemley (1967) and Ellis and Mahon (1967).

All figures logarithms of actual values

Carbonate figures apply to calcite.

| Minerals Deposited | Sphalerite/ pyrite | galena | Fluorite/ carbonate | quartz | fluorite | quartz | galena | pyrite/ marcasite | chalco- pyrite | sphalerite/ quartz | carbonate |
|---|---|---|---|---|---|---|---|---|---|---|---|
| $aS_2^-/aCO_3^-$ | $>-19.6$ | | | | | | | $>-19.6$ | | | |
| $aS^-/aCO_3^-$ | $>-15.5$ | $>-15.3$ | $<5.3$ | | | | $>-15.3$ | | | $>-15.5$ | $<5.3$ |
| $aS^-/a^2OH^-$ | $>-4.1$ | $>-13.8$ | | | | | $>-13.8$ | | | | |
| $aS_2^-/a^2OH^-$ | $>-10.8$ | | | | | | | $>-10.8$ | | | |
| $aS_2^-/aS^-$ | $>-11.9$ | | | | | | | $>-11.9$ | | | |
| $aCO_3^-/a^2OH^-$ | | | $>2.7$ | | | | | | | | $>2.7$ |
| $aS^-/OH^-$ | | $>-11.8$ | | | | | $>-11.8$ | | | | |
| $aS^-/a^2Cl^-$ | | $>-23.4$ | | | | | $>-23.4$ | | | | |
| $a^2F^-/aCO_3^-$ | | | $\sim -1.44$ | | $>-1.44$ | | | | | | $<-1.44$ |
| $aCO_3^-/aSO_4^-$ | | | $>-3.9$ | | | | | | | | $>-3.9$ |
| $PCO_2$ | | | $>-7.1$ | | | | | | | | $>-7.1$ |
| $PH_2S$ | $>-10.1$ | $>-17.8$ | | | | | $>-17.8$ | | | | |
| $PH_2S/PCO_2$ | $>-11.7$ | $>-11.5$ | $<9.1$ | | | | $>-11.5$ | | | $>-11.7$ | $<9.1$ |
| $PO_2$ | $<-37, >-45$ | | | | | | | | | $<-37, >-45$ | |
| $PS_2$ | $<-9, >-15$ | $<-15, >-38$ | $<-15, >-38$ | | | | | | | $<-9, >-15$ | |
| pH | 6 to 7 | 5 to 12 | 5 to 12 | | | | | | | 6 to 7 | |
| Na/K | | | | | $\sim 7$ | $\sim 11$ | | | | | |

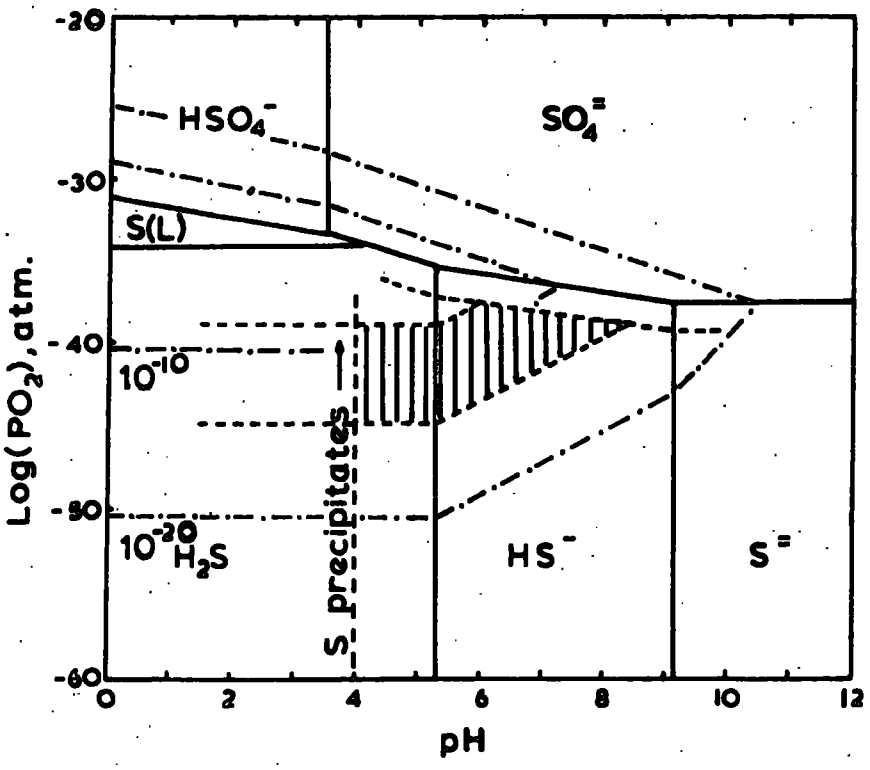


FIG. 35. The common range of acidity and oxidation state of sphalerite-depositing ore solutions at ($\Sigma$ S) = 0·1 m and 250 °C. (After Barnes and Kullerud, 1967).

Contours of $P_{S_2}$ in atmospheres -·-·-·-

## SUMMARY

The salient points brought out during the preceding study are summarised in the following:

1. The paragenetic sequence of deposition of the hydrothermal mineralisation is: sphalerite/pyrite, galena, fluorite/carbonate, quartz, fluorite, quartz, galena, pyrite/marcasite, chalcopyrite, sphalerite/quartz, carbonate.

2. Hydrothermal influence extends into the wallrock for relatively minor distances, probably not more than 50 cms., during the silification of relatively pure calcite limestone.

3. Argillaceous bands in the limestone provide effective barriers to the penetration of hydrothermal fluids.

4. Epigenetic sulphide mineralisation penetrates the wallrock for relatively insignificant distances - in most cases not more than 1 cm.

5. Fluorite mineralisation penetrates the wallrock for distances up to 1 cm. in disseminated form but in general is deposited in open cavities without actual replacement of the wallrock. This observation may have bearing on the interpretation of the many reported "replacement flats" in the Northern Pennine Orefield.

6. The mineralisation was probably deposited at fairly low temperatures - in the vicinity of 150°C.

7. The study confirms the non-validity of the iron content of sphalerite as a geothermometer, at least at low temperatures.

8. Very little information may be obtained from a study of the trace element distribution in the host rock.

9. Disseminated sphalerite in the wallrock occurs in the form of 1 mm. diameter, concentrically colour-banded spheroids. The colour-banding is caused by fluctuations in the iron content of individual bands.

10. Individual carbonate masses investigated by means of the electron probe vary widely in composition on a micron scale, although the grains appear optically homogeneous.

APPENDIX

TABLE 1 RESULTS OF MAJOR ELEMENT ANALYSES

| Sample No. | $SiO_2$ | $Al_2O_3$ | $Fe_2O_3$ | MgO | CaO | $Na_2O$ | $K_2O$ | $TiO_2$ | MnO | $P_2O_5$ | S | C | $CO_2$ | $H_2O$ |
|---|---|---|---|---|---|---|---|---|---|---|---|---|---|---|
| X1 | 12.03 | 6.13 | 4.79 | 0.65 | 31.74 | 0.10 | 1.43 | 0.32 | 0.17 | 0.47 | 10.98 | 0.30 | 28.24 | 2.65 |
| X2 | 10.24 | 5.82 | 4.53 | 1.75 | 41.45 | 0.09 | 0.84 | 0.37 | 0.20 | 0.12 | 0.41 | 0.23 | 31.79 | 2.16 |
| X3 | 16.28 | 8.99 | 3.19 | 1.28 | 34.07 | 0.78 | 1.82 | 0.48 | 0.22 | 0.07 | 0.22 | 0.36 | 30.40 | 1.84 |
| X4 | 46.40 | 20.14 | 2.27 | 0.96 | 10.64 | 2.35 | 3.73 | 1.10 | 0.18 | 0.05 | n.d. | 0.66 | 7.74 | 3.82 |
| X5 | 47.34 | 18.53 | 3.48 | 1.36 | 10.09 | 2.87 | 3.25 | 1.02 | 0.18 | 0.05 | n.d. | 0.74 | 8.65 | 2.87 |
| X6 | 46.82 | 17.07 | 5.99 | 2.26 | 8.02 | 3.63 | 2.23 | 0.91 | 0.18 | 0.09 | n.d. | 0.33 | 7.27 | 5.36 |
| X7 | 41.45 | 18.83 | 5.07 | 1.07 | 13.73 | 3.18 | 2.02 | 1.18 | 0.18 | 0.05 | 0.16 | 0.57 | 8.98 | 3.53 |
| X8 | 44.25 | 19.19 | 3.18 | 1.25 | 11.88 | 2.38 | 3.52 | 1.07 | 0.17 | 0.04 | 0.54 | 0.31 | 9.29 | 3.26 |
| X9 | 44.33 | 19.67 | 1.59 | 0.78 | 12.54 | 1.39 | 4.41 | 1.41 | 0.16 | 0.02 | 0.50 | 0.81 | 9.87 | 3.53 |
| X10 | 30.24 | 11.10 | 7.19 | 0.91 | 19.98 | 1.47 | 2.87 | 0.61 | 0.22 | 0.04 | 8.92 | 0.85 | 12.92 | 2.68 |
| X11 | 40.88 | 14.23 | 3.21 | 1.30 | 18.03 | 2.54 | 2.74 | 0.80 | 0.19 | 0.06 | 0.08 | 0.65 | 11.13 | 3.36 |
| X12 | 28.35 | 12.04 | 1.71 | 0.75 | 30.34 | 1.03 | 2.55 | 0.62 | 0.18 | 0.10 | n.d. | 0.32 | 19.97 | 3.98 |
| X13 | 20.40 | 9.97 | 1.10 | 0.60 | 36.00 | 0.09 | 2.31 | 0.49 | 0.15 | 0.10 | n.d. | 0.28 | 27.27 | 1.64 |
| X14 | 8.82 | 5.20 | 2.53 | 1.26 | 44.28 | 0.10 | 1.14 | 0.27 | 0.18 | 0.12 | 0.58 | 0.30 | 33.15 | 2.06 |
| X15 | 2.86 | 3.52 | 3.18 | 2.14 | 47.25 | 0.10 | 0.53 | 0.17 | 0.16 | 0.14 | 0.79 | 0.46 | 37.84 | 0.91 |
| X16 | 9.48 | 5.52 | 2.82 | 1.32 | 42.58 | 0.09 | 1.02 | 0.27 | 0.18 | 0.14 | 1.38 | 0.02 | 33.15 | 2.03 |
| X17 | 39.23 | 15.30 | 2.54 | 0.90 | 18.29 | 2.73 | 2.45 | 0.84 | 0.13 | 0.09 | 1.85 | 0.47 | 11.91 | 3.27 |
| X18 | 53.91 | 23.41 | 1.66 | 0.92 | 2.90 | 2.28 | 5.09 | 1.12 | 0.12 | 0.33 | 0.04 | 0.17 | 4.28 | 3.77 |
| X19 | 52.14 | 23.55 | 1.17 | 0.88 | 2.61 | 1.90 | 4.99 | 1.04 | 0.12 | n.d. | n.d. | 0.80 | 6.10 | 4.82 |
| X20 | 28.13 | 13.17 | 2.59 | 0.98 | 27.64 | 1.34 | 2.31 | 0.72 | 0.13 | 0.30 | 1.77 | 0.50 | 17.48 | 2.94 |
| X21 | 24.30 | 10.40 | 2.50 | 1.43 | 31.05 | 1.66 | 1.55 | 0.56 | 0.12 | 0.38 | 0.91 | 0.54 | 21.55 | 3.05 |

| | $SiO_2$ | $Al_2O_3$ | $Fe_2O_3$ | MgO | CaO | $Na_2O$ | $K_2O$ | $TiO_2$ | MnO | $P_2O_5$ | S | C | $CO_2$ | $H_2O$ |
|---|---|---|---|---|---|---|---|---|---|---|---|---|---|---|
| X22 | 3.65 | 3.68 | 3.17 | 2.66 | 45.19 | 0.10 | 0.48 | 0.20 | 0.21 | 0.11 | 0.66 | 1.57 | 35.31 | 2.97 |
| X23 | 3.14 | 3.11 | 2.96 | 2.27 | 45.34 | 0.10 | 0.56 | 0.16 | 0.19 | 0.15 | 1.03 | 0.20 | 38.13 | 2.80 |
| X24 | 3.16 | 2.96 | 1.85 | 2.07 | 50.53 | 0.11 | 0.63 | 0.20 | 0.09 | 0.12 | 0.24 | 0.73 | 35.42 | 1.86 |
| X25 | 3.63 | 3.31 | 1.79 | 2.57 | 47.04 | n.d. | 0.53 | 0.23 | 0.08 | 0.08 | 0.64 | 0.82 | 36.88 | 2.40 |
| X26 | 2.11 | 1.51 | 1.54 | 1.32 | 51.45 | n.d. | 0.29 | 0.06 | 0.13 | 0.07 | 0.56 | 0.34 | 39.72 | 0.9 |
| X27 | 2.48 | 2.55 | 1.10 | 0.88 | 51.79 | 0.31 | 0.63 | 0.13 | 0.12 | 0.16 | 0.27 | 0.30 | 38.40 | 0.88 |
| X28 | 5.74 | 3.97 | 1.06 | 0.59 | 46.91 | 0.22 | 0.77 | 0.17 | 0.14 | 0.17 | 0.41 | 0.64 | 37.38 | 1.83 |
| X29 | 3.00 | 2.80 | 1.21 | 0.54 | 50.22 | 0.11 | 0.68 | 0.15 | 0.12 | 0.15 | 0.48 | 0.14 | 39.09 | 1.31 |
| X30 | 6.72 | 4.15 | 1.27 | 0.79 | 48.07 | 0.29 | 0.80 | 0.18 | 0.15 | 0.17 | 0.60 | 0.23 | 35.17 | 1.36 |
| X31 | 3.29 | 1.53 | 3.72 | 1.00 | 49.40 | 0.26 | 0.48 | 0.10 | 0.18 | 0.19 | 0.55 | 0.47 | 38.18 | 0.65 |
| X32 | 2.58 | 2.75 | 0.86 | 0.65 | 46.32 | 0.22 | 0.66 | 0.13 | 0.22 | 0.24 | 0.14 | 0.24 | 44.10 | 0.90 |
| X33 | 48.13 | 12.77 | 0.60 | 0.67 | 17.31 | n.d. | 3.63 | 0.97 | 0.24 | 0.05 | 0.72 | 0.81 | 11.59 | 2.51 |
| X46 | 50.77 | 21.25 | 3.19 | 1.01 | 2.24 | 0.26 | 5.97 | 0.95 | 0.04 | n.d. | 6.64 | 0.65 | 1.76 | 5.28 |
| X47 | 82.65 | 0.70 | 0.68 | 0.08 | 3.37 | 0.69 | 0.49 | 0.07 | 0.04 | n.d. | 6.50 | 0.67 | 2.65 | 1.43 |
| X48 | 51.63 | 0.34 | 2.28 | 0.09 | 11.93 | 1.98 | 0.47 | 0.07 | 0.13 | n.d. | 16.88 | 0.78 | 9.38 | 1.12 |
| X49 | 66.01 | 0.53 | 2.22 | 0.14 | 8.03 | 1.10 | 0.42 | 0.10 | 0.09 | 0.01 | 12.89 | 0.88 | 6.31 | 1.27 |
| X50 | 49.41 | 0.21 | 6.55 | 2.22 | 8.80 | 1.27 | 0.35 | 0.04 | 1.60 | n.d. | 10.77 | 0.70 | 16.62 | 1.27 |
| X51 | 28.47 | n.d. | 5.84 | 2.62 | 7.56 | 2.85 | 0.30 | 0.03 | 1.17 | n.d. | 16.84 | 0.52 | 31.73 | 2.19 |
| X52 | 74.36 | 0.18 | 1.09 | 0.07 | 6.42 | 0.96 | 0.40 | 0.05 | 0.03 | n.d. | 9.70 | 1.06 | 5.05 | 0.63 |
| X53 | 44.33 | 0.17 | 2.37 | 0.10 | 16.85 | 2.27 | 0.38 | 0.06 | 0.04 | 0.03 | 18.18 | 1.20 | 13.24 | 0.80 |

| | $SiO_2$ | $Al_2O_3$ | $Fe_2O_3$ | MgO | CaO | $Na_2O$ | $K_2O$ | $TiO_2$ | MnO | $P_2O_5$ | S | C | $CO_2$ | $H_2O$ |
|---|---|---|---|---|---|---|---|---|---|---|---|---|---|---|
| X54 | 65.89 | 1.42 | 8.60 | 0.38 | 3.15 | 0.20 | 0.17 | 0.04 | 2.43 | 0.02 | 18.18 | 0.47 | 10.24 | 1.46 |
| X55 | 83.93 | 0.52 | 0.96 | 0.10 | 5.10 | 0.51 | 0.38 | 0.06 | 0.03 | 0.01 | 5.53 | 0.70 | 2.12 | 0.60 |
| X56 | 30.56 | 0.46 | 1.94 | 0.20 | 39.40 | 0.08 | 0.39 | 0.04 | 0.43 | 0.09 | 4.99 | 0.68 | 27.25 | 0.78 |

n.d. - not detected.

Appendix

TABLE 2 RESULTS OF TRACE ELEMENT ANALYSES (in ppm)

| SAMPLE No. | Zn | Cu | Ni | Ba | Nb | Zr | Y | Sr | Rb |
|---|---|---|---|---|---|---|---|---|---|
| X1 | 9 | 50 | 32 | 224 | 22 | 85 | 27 | 2980 | 118 |
| X2 | 19 | 38 | 34 | 276 | 14 | 94 | 12 | 4332 | 66 |
| X3 | 21 | 41 | 54 | 599 | 17 | 102 | 14 | 3608 | 209 |
| X4 | 55 | 44 | 84 | 1644 | 32 | 184 | 18 | 1310 | 581 |
| X5 | 495 | 56 | 103 | 1166 | 28 | 164 | 19 | 1676 | 431 |
| X6 | 510 | 71 | 101 | 722 | 28 | 153 | 22 | 2372 | 227 |
| X7 | 611 | 60 | 102 | 996 | 30 | 151 | 21 | 2295 | 315 |
| X8 | 185 | 55 | 87 | 2146 | 30 | 160 | 15 | 1559 | 563 |
| X9 | 19 | 40 | 95 | 3297 | 33 | 162 | n.d. | 1082 | 843 |
| X10 | 58 | 70 | 72 | 721 | 22 | 90 | 12 | 1834 | 330 |
| X11 | 287 | 47 | 85 | 1054 | 27 | 120 | 11 | 2315 | 346 |
| X12 | 220 | 38 | 60 | 782 | 17 | 91 | 7 | 2349 | 317 |
| X13 | 101 | 38 | 57 | 564 | 20 | 77 | 8 | 2973 | 317 |
| X14 | 173 | 41 | 43 | 166 | 13 | 67 | 7 | 4171 | 81 |
| X15 | 292 | 41 | 39 | 88 | 11 | 70 | n.d. | 4840 | 22 |

| | Zn | Cu | Ni | Ba | Nb | Zr | Y | Sr | Rb |
|---|---|---|---|---|---|---|---|---|---|
| X16 | 147 | 45 | 47 | 224 | 14 | 65 | 7 | 4114 | 135 |
| X17 | 1092 | 67 | 94 | 1209 | 21 | 127 | 10 | 2919 | 435 |
| X18 | 61 | 41 | 73 | 3053 | 30 | 152 | 20 | 995 | 804 |
| X19 | 162 | 65 | 102 | 2945 | 38 | 171 | 15 | 779 | 866 |
| X20 | 516 | 45 | 68 | 1728 | 22 | 110 | 23 | 2940 | 450 |
| X21 | 1159 | 57 | 70 | 1049 | 24 | 101 | 23 | 3773 | 260 |
| X22 | 908 | 39 | 42 | 122 | 16 | 72 | 7 | 4312 | 28 |
| X23 | 1315 | 46 | 43 | 270 | 14 | 84 | 4 | 4729 | 43 |
| X24 | 35 | 37 | 29 | 258 | 20 | 83 | 4 | 4117 | 52 |
| X25 | 50 | 39 | 31 | 313 | 26 | 106 | 5 | 3739 | 62 |
| X26 | 246 | 39 | 28 | 98 | 14 | 81 | n.d. | 4540 | 20 |
| X27 | 333 | 37 | 21 | 78 | 17 | 73 | n.d. | 4130 | 34 |
| X28 | 1114 | 41 | 25 | 106 | 13 | 71 | 5 | 3672 | 61 |
| X29 | 494 | 43 | 25 | 107 | 13 | 60 | n.d. | 3909 | 52 |
| X30 | 513 | 45 | 25 | 115 | 12 | 61 | 8 | 3845 | 58 |
| X31 | 1345 | 40 | 32 | 42 | 11 | 58 | 4 | 3789 | 25 |
| X32 | 1433 | 40 | 89 | 91 | 10 | 63 | 14 | 3805 | 59 |

| | Zn | Cu | Ni | Ba | Nb | Zr | Y | Sr | Rb |
|---|---|---|---|---|---|---|---|---|---|
| X33 | 1170 | 39 | 33 | 634 | 22 | 89 | 13 | 1160 | 524 |
| X46 | high | 42 | 101 | 739 | 32 | 108 | n.d. | 171 | 765 |
| X47 | " | 58 | 33 | 16 | 7 | n.d. | n.d. | 40 | 22 |
| X48 | " | 98 | 43 | n.d. | 9 | n.d. | n.d. | 31 | 16 |
| X49 | " | 85 | 47 | n.d. | 9 | 7 | n.d. | 43 | 22 |
| X50 | " | 124 | 29 | n.d. | 10 | n.d. | n.d. | 228 | 15 |
| X51 | " | 246 | 30 | n.d. | 11 | n.d. | n.d. | 235 | 4 |
| X52 | " | 106 | 51 | n.d. | 8 | 10 | 7 | 19 | n.d. |
| X53 | " | 184 | 44 | n.d. | 10 | 24 | 15 | 32 | n.d. |
| X54 | " | 56 | 26 | 12 | 14 | 20 | 16 | 23 | n.d. |
| X55 | " | 62 | 19 | 41 | 12 | 8 | 10 | 56 | 18 |
| X56 | " | 40 | 23 | 126 | 14 | 44 | 16 | 3297 | 23 |
| Detection Limits | | | | | | | | | |
| | 2 | 4 | 2 | 6 | 5 | 4 | 4 | 5 | 4 |

n.d. - not detected.

## BIBLIOGRAPHY

The following publications were consulted although not all are mentioned in the text.


ADLER, I., 1963, Electron Probe Analysis of Minerals: Symposium on X-ray and Electron Probe Analysis. ASTM Special Technical Publication No. 349, p. 183.

AKINCI, O.T., 1970, The Effect of Iron Substitution on the Cell Size, Reflectivity and Colour of Sphalerite: unpublished M.Sc. Thesis, University of Durham.

ALLEN, C.A., CRENSHAW, J.L., JOHNSTON, J. and LARSEN, E.S., 1912, The mineral sulphides of iron: Am.Jour.Sci., v.33, p.169.

AMES, L.L. Jr., 1961, The metasomatic replacement of limestone by alkaline fluoride bearing solutions: Econ. Geol., v.56, p.730.

1961 Anion metasomatic replacement reactions: Econ. Geol., v.56, p.521?

1961 Cation metasomatic replacement reactions: Econ. Geol., v.56, p.1017.

ANDERMANN, G. and KEMP, G.W. 1958, Scattered x-rays as internal standards in x-ray emission spectroscopy: Anal Chem., v.30, p. 1306.

ANGINO, E.E. and BILLINGS, G.K., 1967, Atomic Absorption Spectrometry in Geology: Elsevier Publishing Co.

ARNOLD, R.G., COLEMAN, R.G. and FRYKLUND, V.C., 1962, Temperature of crystallisation of pyrrhotite and sphalerite from the Highland - Surprise mine, Coeur D'Alene District, Idaho: Econ. Geol., v.57, p.1163.

BAILEY, S.W. and CAMERON, E.N., 1951, Temperatures of mineral formation in the bottom - run lead - zinc deposits of the upper Mississippi Valley, as indicated by liquid inclusions: Econ. Geol., v.46, p.626.

BARNES, H.L., 1965, Environmental limitations to mechanisms of ore transport: Symposium, Problems of Postmagmatic Ore Deposition, Prague, 2, p.316.

_____ and KULLERUD, G., 1961, Equilibria in sulphur - containing aqueous solutions, in the system Fe - S - O, and their correlation during ore deposition: Econ. Geol., v.56, p. 648.

BARTON P.B., Jr., 1957, Some limitations on the possible composition of the ore - forming fluid: Econ Geol., v.52, p.333.

1957, Preliminary report on the system FeS - ZnS - S and implications regarding the use of the sphalerite geothermometer: Bull. Geol. Soc Am. (No. 12, pt. 2), p. 1699.

_____, BETHKE P.M. and TOULMIN P. III, 1963, Equilibrium in ore deposits: Mineral.Soc.Am., Spec. paper 1, p.171.

_____, _____ 1967 Sulphide mineral stabilities: Geochemistry of Hydrothermal Ore Deposits, Ed.Barnes, H.L. : Holt, Reinhart and Winston, Inc., p. 236.

_____, TOULMIN P. III 1966, Phase relations involving sphalerite in the Fe - Zn - S system: Econ. Geol., v.61, p. 815.

BETHKE, M.P., and BARTON P.B. Jr., 1971, Distribution of some minor elements between coexisting sulphide minerals: Econ. Geol., v.66, p. 140.

BILLINGS, G.K., 1965, Light scattering in trace element analysis by atomic absorption: Atomic Absorption Newsletter, Perkin-Elmer Corp., 4, p.357.

BOORMAN, R.S., 1967, Subsolidus studies in the ZnS - FeS - $FeS_2$ system: Econ Geol. v. 62, p.614.

BRETT, R., 1964, Experimental data from the system Cu - Fe - S and their bearing on exsolution textures in ores: Econ. Geol., v.59, p. 1241.

BUCK, D.C. and STROCK, L.W., 1955. Trimorphism in zinc sulphide: Amer. Mineral, v.40, p.192.

BUERGER, N.W. and BUERGER, M.J., 1934, Crystallographic relations between cubanite segregation plates, chalcopyrite matrix and secondary chalcopyrite twins: Amer. Mineral., v.19, p.289.

BUERGER, N.W., 1934, The unmixing of chalcopyrite from sphalerite: Amer. Mineral., v.19, p.525.

COATS, A.W. and REDFERN, J.P., 1963, Thermogravimetric analysis - a review: The Analyst, v.88, p.906.

COOPER, J.A., 1963, The flame photometric determination of K in geological materials used for potassium - Ar dating: Geochim. et Cosmochim. Acta, v.27, p.525.

CURTIS, C.D., 1969, Trace element distribution in some British Carboniferous sediments: Geochim. et Cosmochim. Acta, v.33, p.519.

DEAN. J.A., 1960, Flame Photometry: McGraw-Hill Book Co.

DICKSON, F.W., SHIELDS, L.D. and KENNEDY, G.C., 1962, A method for the determination of equilibrium sulphur pressures of metal sulphide reactions: Econ. Geol., v.57, p.1021.

DRUGMAN, J., 1932, Different habits of fluorite crystals: Mineral. Mag., v.23, p.137.

DUNHAM, K.C., 1948, Geology of the Northern Pennine Orefields: Mem. Geol. Surv., U.K., 357 p.

_____, 1952 Fluorspar: Spec. Ref. Miner. Resources, G.B., v.4, (4th ed.)

_____, DUNHAM A.C. HODGE, B.L. and JOHNSON, G.A.L., 1965, Granite beneath Visean sediments with mineralisation at Rookhope, Northern Pennines: Q.Jl.Geol.Soc.Lond., v.121, p.383.

EINAUDI, M.T., 1968, Sphalerite - pyrrhotite - pyrite equilibria - a re-evaluation: Econ. Geol., v.63, p.832.

ELLIS, A.J. and MAHON W.A.J., 1967, Natural hydrothermal systems and experimental hot water/rock interactions (part II): Geochim. et Cosmochim. Acta, v.31, p.519.

FITTON, J.G. and GILL, R.C.O., 1970, The oxidation of ferrous iron in rocks during mechanical grinding: Geochim. et Cosmochim. Acta, v.34, p. 518.

FREAS, D,G., 1961, Temperatures of mineralisation by liquid inclusions, Cave-in-Rock fluorspar district, Illinois: Econ. Geol., v.56, p.542.

GARN, P.D., 1965, Thermoanalytical Methods of Investigation: Academic Press.

GARRELS, R.M. and CHRIST, C.L., 1965, Solutions, Minerals and Equilibria: Harper and Row, New York.

_____, DREYER R.M., 1952, Mechanism of limestone replacement at low temperatures and pressures: Geol. Soc. America Bull., v.63, p. 325.

GIBBONS, G.S., 1967, Optical anisotropy in pyrite: Amer. Mineral., v.52, p.359.

GILL, J.E., 1969, Experimental deformation and annealing of sulphides and interpretation of ore textures: Econ. Geol., v. 64, p.500.

GOLDBERG, I.S., 1963, Colour of fluorite from the Takob Deposit: Geokhimya, no. 11, p.1057.

GOLDSMITH, J.R., 1967, Metastability and hangovers in crystals: Geochim. et Cosmochim. Acta, v.31, p.913.

GROVES, A.W., 1951, Silicate Analysis: Allen and Unwin, London, 2nd ed., 334 p.

HALL, W.E. and FRIEDMAN I., 1963, Composition of fluid inclusions, Cave-in-Rock fluorite district, Illinois, and Upper Mississippi Valley lead-zinc district: Econ.Geol. v.58, p.886.

HEINRICH, K.F.J., 1966, The Electron Microprobe: Eds. T.D. McKinley, K.F.J. Heinrich and D.B. Wittry, John Wiley, p.296.

HEMLEY, J.J., 1959, Some mineralogical equilibria in the system $K_2O - Al_2O_3 - SiO_2 - H_2O$: Am. J. Sci., v.257, p.241.

_____, JONES W.R., 1964, Chemical aspects of hydrothermal alteration with emphasis on hydrogen metasomatism: Econ. Geol., v.59, p.538.

HOLLAND, J.G. and BRINDLE, D.W., 1966, A self-consistent mass absorption correction for silicate analysis by x-ray fluorescence: Spectrochemica Acta, v.22, p.2083.

HOLLAND, H.D., 1967, Gangue minerals in hydrothermal deposits: Geochemistry of Hydrothermal Ore Deposits, Ed.Barnes; Holt, Reinhart and Winston, Inc., p. 382.

JOHNSON, G.A.L., 1972, personal communication.

HOLLAND, H.J. and MUNOZ, J.L., 1964, The coprecipitation of cations with $CaCO_3$-11. The coprecipitation of $Sr^{2+}$ with calcite between 90°C and 100°C: Geochim. et Cosmochim. Acta, v.28, p. 1287.

KAYE, M.J., DUNHAM, A.C. and HIRST, D.M., 1968, A comparison of two methods of quantitative mineralogical analysis of sedimentary rocks: Jour. Sedimentary Petrology, v.38, p.675.

KERN, R. and WEISBROD, A., 1967, Thermodynamics for Geologists: Translated Freeman, Cooper and Co., San Fransisco.

KRAUSKOPF, K.B., 1967, Introduction to Geochemistry: McGraw-Hill Book Co.

KULLERUD, G., 1953, The FeS - ZnS system, a geological thermometer: Norsk. Geol. Tidsskr., v.32, p. 61.

KUTINA, J. and SEDLACKOVA, J., 1961, The role of replacement in the origin of some cockade textures: Econ. Geol., v.56, p.149.

LATIMER, W.M., 1952, The oxidation states of the elements and their potentials in aqueous solution: New York, Prentice-Hall.

LAUDISE, R.A., KOLB, E.D. and De NEUFVILLE, J.P., 1965, Hydrothermal solubility and growth of sphalerite: Amer. Mineral., v.50, p.382.

MacKENZIE, R.C. and MITCHELL, B.D., 1962, Differential Thermal Analysis - a Review: The Analyst, v.87, p.420.

MARSHALL, C.E. 1962, Reactions of feldspars and micas with aqueous solutions: Econ. Geol., v.57, p.1219.

MARSHALL, R.R. and JOENSUU, O., 1961, Crystal Habit and trace element content of some galenas: Econ. Geol., v.56, p.758.

MEYER, C. and HEMLEY, J.J., 1967, Wall rock alteration: Geochemistry of Hydrothermal Ore Deposits, Ed. H.L. Barnes: Holt, Reinhart and Winston, Inc., p.166.

MILLER, J.D., 1969, Fluid inclusion temperature measurements in the East Tintic District: Econ. Geol., v.64, p.109.

MOOK HERJEE, A., 1962, Certain aspects of the geochemistry of cadmium: Geochim. et Cosmochim. Acta, v.26, p.351.

PENFIELD, S.L.,1894, On some methods for the determination of water: Am. J. Sci., v.189, p.30.

PHILLIPS, W.J., 1972, Hydraulic fracturing and Mineralization: Jl. Geol. Soc., v.128, p.337.

PLATTE, J.A. and MARCY, V.M., 1965, Atomic absorption spectrophotometry as a tool for the water chemist: At. Absorption Newsletter, Perkin-Elmer Corp., v.4, p.289.

POLUEKTOV, N.S., NIKONOVA, M.P. and VITKIN, R.A., Flame photometric determination of sodium and potassium in silicate minerals: Zhuv.Anal.Khim., v.13, p.48.

RAMDOHR, P., 1969, The ore minerals and their intergrowths: Pergamon Press, London.

RODGERS, J., 1940, Distinction between calcite and dolomite on polished surfaces: Am.Jour .Sci., v. 238, p. 788.

ROEDDER, E., 1960, Studies of primary fluid inclusions in sphalerite crystals from the OH vein, Creede, Colorado: Econ. Geol., v. 55, p. 1335.

_____, 1967 Fluid inclusions as samples of ore fluids: Geochemistry of Hydrothermal Ore Deposits, Ed. H.L. Barnes: Holt, Reinhart and Winston, Inc., p. 515.

_____, 1968 Non-colloidal origin of colloform textures: Econ. Geol., v. 63, p. 451.

_____, and DWORNIK E.J., 1968, Sphalerite colour banding - lack of correlation with iron content, Pine Point, North-West Territories, Canada: Amer. Mineral., v. 53, p. 1523.

ROSE, A.W., 1961, The iron content of sphalerite from the Central District, New Mexico and the Bingham District, Utah: Econ. Geol., v.56, p. 1363.

ROSENBERG, P.E. and HOLLAND, H.D., 1964, Calcite/dolomite stability relations in solutions at elevated temperatures: Science, v. 145, p. 700.

RUNNELS, D.D., 1970, Errors in x-ray analysis of carbonates due to solid solution variation in composition of component minerals: Jour. Sed. Pet., v. 40, p. 1158.

SALOTTI, C.A., HEINRICH, E.W. and GIARDINI, A.A., 1971, Abiotic carbon and the formation of graphite deposits: Econ. Geol., v.66, p. 929.

SAWKINS, F.J., DUNHAM, A.C. and HIRST, D.M., 1964, Iron-deficient low temperature pyrrhotite: Nature, v. 204, p. 175.

SAWKINS, F.J., 1966, Ore deposition in the North Pennine Orefield, in the light of fluid inclusion studies: Econ Geol., v. 61, p. 385.

SCHMIDT, R.A., 1962, Temperatures of mineral formation in the Miami-Pitcher district as indicated by liquid inclusions: Econ. Geol., v.57, p. 1.

SIMS, P.K. and BARTON, P.B. Jr., 1961, Some aspects of the geochemistry of sphalerite, Central City district, Colorado: Econ. Geol., v.56, p. 1.211.

SKINNER, B.J., 1959, Effect of manganese on the sphalerite geothermometer (abs.): Geol. Soc. America Bull., v.70, p.1676.

_____, 1961 Unit cell edges of natural and synthetic sphalerites: Amer. Mineral., v. 46, p. 1399.

_____, 1959 BARTON, P.B. Jr. and KULLERUD, G., 1959, Effect of FeS on the unit cell edge of sphalerite. A revision: Econ.Geol., v.54, p.1040.

SNELL, F.D. and SNELL, C.T., 1936, Colorimetric Methods of Analysis. vol. 1 - Inorganic: Chapman and Hall, Ltd., London.

SMITH, F.W., 1972, Personal communication.

STANTON, R.L. and GORMAN, H., 1968, A phenomenological study of grain boundary migration in some common sulphides: Econ. Geol., v.63, p.907.

SWEATMAN, T.R. and LONG, J.V.P., 1969, Quantitative electron-probe analysis of rock-forming minerals: Jour.Pet., v.10, p. 332.

TOULMIN, P., III, 1960, Effect of Cu on sphalerite phase equilibria - a preliminary report (abst.): Geol. Soc. Amer. Bull., v. 71, p. 1993.

_____, and CLARK S.P. Jr., 1967, Thermal aspects of ore formation: Geochemistry of Hydrothermal Ore Deposits, Ed. H.L. Barnes: Holt, Reinhart and Winston, Inc., p. 437.

TUREKIAN, KK. and WEDEPOHL, K.H., 1961, Distribution of the elements in some major units of the earth's crust: Geol. Soc. America Bull., v.72, p.175.

TWENHOFEL, W.S., 1947, The temperature of crystallisation of a fluorite crystal from Luna County, New Mexico: Econ. Geol., v.42, p. 78.

WARNE, S. ST. J., 1962, A quick field or laboratory staining scheme for the differentiation of the major carbonate minerals: Jour. Sed. Pet., v. 32, p. 29.

WAUGH, W.N. and HILL, E.H., 1960, Determination of carbon dioxide and other volatiles in pyritic limestones by loss on ignition: Jour. Sed. Pet., v.30, p.144.

WILLIAMS, K.L., 1965, Determination of the iron content of sphalerite: Econ. Geol., v.60, p.1740.

_____, 1967 Electron probe microanalysis of sphalerite: Amer. Mineral., v. 52, p. 475.

WITTRY, D.B., 1963, Methods of quantitative electron probe analysis: Symposium on x-ray and electron probe analysis, ASTM Special Technical Publication no. 349, p. 128.